HARTREE-FOCK-SLATER WAVE FUNCTIONS AND STERNHEIMER SHIELDING-ANTISHIELDING FACTORS IN ATOMS AND IONS

A Thesis Submitted
in Partial Fulfilment of the Requirements
for the Degree of

DOCTOR OF PHILOSOPHY

By

KALIDAS SEN

to the

DEPARTMENT OF CHEMISTRY

INDIAN INSTITUTE OF TECHNOLOGY KANPUR

AUGUST, 1976

DEPARTMENT OF CHEMISTRY

INDIAN INSTITUTE OF TECHNOLOGY KANPUR, INDIA

CERTIFICATE I

This is to certify that Mr. K. D. Sen has satisfactorily completed all the courses required for the Ph.D. degree programme. These courses include:

Chm 500	Mathematics for Chemists I
Chm 501	Advanced Organic Chemistry I
Chm 521	Chemical Binding
Chm 523	Chemical Thermodynamics
Chm 541	Advanced Inorganic Chemistry I
Chm 624	Valence Bond and Molecular Orbital Theories
Chm 628	Quantum Chemistry I
Chm 629	Quantum Chemistry II
Chm 630	Ligand Field Theory
Chm 800	General Seminar
Chm 801	Graduate Seminar
Chm 900	Research

Mr. K. D. Sen was admitted to the candidacy of the Ph.D. degree in September 1970 after he successfully completed the written and oral qualifying examinations.

A. Chakravorty

(A. Chakravorty)
Professor & Head
Department of Chemistry

19/8/76

D. Devaprabhakara

(D. Devaprabhakara)
Convener
Departmental Post-graduate Committee
Department of Chemistry

CERTIFICATE II

Certified that the work contained in this thesis "HARTREE-FOCK-SLATER WAVE FUNCTIONS AND STERNHEIMER SHIELDING-ANTISHIELDING FACTORS IN ATOMS AND ION" has been carried out by Mr. K. D. Sen under my supervision and the same has not been submitted elsewhere for a degree.

P. T. Narasimhan

(P. T. Narasimhan)
Thesis Supervisor

STATEMENT

I hereby declare that the matter embodied in this thesis is the result of investigations carried out by me in the Department of Chemistry, Indian Institute of Technology, Kanpur, India under the supervision of Professor P. T. Narasimhan.

In keeping with the general practice of reporting scientific observations, due acknowledgement has been made wherever the work described is based on the findings of other investigators.

K. d. Sen

(K. D. Sen)

ACKNOWLEDGEMENTS

It has been my good fortune and a rare privilege to work under the supervision of Professor P. T. Narasimhan, with whom my relations have been mainly personal rather than just professional.

In the context of this thesis I am grateful

to Professor P. T. Narasimhan, who suggested the problems and extended timely guidance and encouragement throughout the course of this work.

to Dr. K. M. S. Saxena, my senior colleague, and Dr. B. K. Rao, Department of Physics, Rourkela Engineering College, Orissa for their help in the initial stages of this work.

to my teachers, Professor R. S. Vaidya and Dr. K. K. Ahuja of the Department of Chemistry, S. N. Government P.G. College, Khandwa, M.P.

to Dr. R. M. Sternheimer, Brookhaven National Laboratory, New York, U.S.A., whose original work on the core polarization effects continues to be a constant source of inspiration to me. His kind interest in this work and his promptness in answering many of my queries have helped immensely the progress of this work.

to Professor T. P. Das, Department of Physics, State University of New York at Albany, U.S.A., for several fruitful discussions during his two short visits to I.I.T. Kanpur.

to Professor C. N. R. Rao, Professor M. V. George, Professor Animesh Chakravorty and Professor P. T. Manoharan for their interest in my career.

to Mrs. P. T. Narasimhan for her parental interest in my welfare.

to my colleagues, Drs. S. Aravamudhan, J. Subramanian, M. S. Gopinathan, D. N. Nanda, K. V. Raman, R. Jagannathan, and Messrs. V. H. Subramanian, P. P. Thankachan, S. R. Gadre, Chandrakumar, S. Shanker, B. L. Tembe, Ramchandran, Sunderajan, Balkrishnan and Devarajan for creating a lively atmosphere in the laboratory.

to Nihal Ahmad for efficient typing of the manuscript in a short time.

to K. K. Bajpai, Anil, Ram Singh and Bishambhar for their help in the office of the department of chemistry, IITK.

to the operators of the Computer Centre, for the generous help, without which this work would have been incomplete.

to the Council of Scientific and Industrial Research, New Delhi, for providing the financial support in the form of a Junior Research Fellowship and subsequently a Senior Research Fellowship in the initial stages of this work.

CONTENTS

CHAPTER I

Electric Multipole Polarization in Atoms and Ions: Theoretical Methods and Experimental Evidences for Sternheimer Polarization Effects

I.1 Introduction

The study of polarization of electron-distribution in atoms in presence of a perturbing electric or magnetic field still continues to be one of the most important research areas, although the early experimental measurements of electric dipole polarizabilities[1,2] in terms of dielectric constants for the noble gas systems were carried out in the twenties. The lowest nonlinear contribution to the induced electric dipole moment in helium has now been measured[3] using laser sources to produce strong fields in optical Kerr-effect studies. The theoretical studies[4] on one-electron systems in presence of external fields were undertaken immediately after the formulation of new quantum mechanics. For the treatment of multielectron atomic systems - where exact results cannot be obtained due to limitations in theory - several approximate methods[5] with varying degrees of accuracy have been put forward.

The perturbing field can be internal, e.g. originating from the valence electrons, the electric quadrupole and hexadecapole moment of the nucleus and/or external electric field. This is the basis of Sternheimer's pioneering work on the magnetic dipole,[6] nuclear electric quadrupole[7] and hexadecapole[8] polarizations commonly known as Sternheimer shielding-anti-shielding factors. Their knowledge becomes essential in interpreting the experimental data on hyperfine interactions

which have largely become available during recent years via γ-resonance, magnetic-resonance and perturbed angular-correlation studies. In fact, the shielding-antishielding factors represent our lack of knowledge of accurate electronic wave functions. In this thesis we shall be concerned with the Sternheimer shielding-antishielding factors in a variety of atoms and ions that are of importance both from the theoretical and experimental points of view.

The different approximate methods used to calculate the shielding-antishielding factors are similar to those used for the calculation of polarizabilities and in this chapter we shall review these methods together, after presenting the general definition of static multipole-polarizabilities and shielding factors. As always, the accuracy of a given theoretical method will be judged from its ability to interpret the experimental observations. The dipole shielding factor for an N-electron atomic system is a known quantity given by[9] N/Z, where Z is the atomic number and this provides an independent means of assessing the accuracy of the approximate method used.

I.2 Multipole Polarizabilities and Shielding Factors

Consider the physical situation in which a distant point charge q is located at R a.u. from the nucleus of a non-degenerate N-electron atom, along the Z axis. The perturbation

of interest to us here can be expressed as a symmetric sum of one electron operators. The perturbing potential (in a.u.) can be expressed in terms of the electron coordinates with respect to the nucleus as:

$$V_L = - \lambda \sum_{i=1}^{N} {}^{L}_{i} P_L (\cos \theta_i), \qquad (I.1)$$

where L varies from 1 to ∞ and $\lambda = q/R^{L+1}$. The total wave function for the atom under the influence of V_L can be written to the first order in λ :

$$\Phi = \Phi^{o} + \Phi^{1} \qquad (I.2)$$

The 2^L-pole polarizability is defined as $(-1)^L L!$ times the ratio of the induced 2^L-pole moment to the Lth-order gradient of V_L and is given by

$$\alpha_L = -2 < \Phi^{1} | \sum_{i=1}^{N} r_i^L P_L (\cos \theta_i) | \Phi^{o} > \qquad (I.3)$$

The 2^L-pole shielding factor is given by the ratio of the change in Lth-order electric field gradient at the nucleus due to the electron distribution to the Lth-order gradient due to external charge alone. This is given by

$$\gamma_L = 2 < \Phi^{1} | \sum_{i=1}^{N} (P_L(\cos \theta_i)/r_i^{L+1}) | \Phi^{o} > \qquad (I.4)$$

The polarizability largely depends on the outer parts of the wave function, whereas the shielding-antishielding factors

largely depend on the description of the wave function near the nucleus. The 2^L-pole polarization of the spherical electron distribution can be given a physical interpretation in terms of angular and radial distortions. The angular distortion leads to a shielding effect (positive) and significantly contributes to the polarizability. The radial distortion produces an antishielding (negative) effect and contributes to polarizability much less significantly. Thus the total shielding can be either positive (shielding) or negative (antishielding) depending upon the relative magnitudes of the angular and radial contributions.

The static dipole, quadrupole and hexadecapole polarizabilities will be denoted hereafter as α_d, α_q and α_h respectively (vide eqn. I.3) and the associated Sternheimer shielding-antishielding factors due to distant point charges be denoted as β_∞, γ_∞ and η_∞ respectively (vide eqn. I.4). The shielding-antishielding factors corresponding to the valence shells at the nuclear site for quadrupole[7a] and hexadecapole[8d] cases will be denoted by R and R_H respectively. The shielding factor corresponding to the quadrupole term in the crystalline electric field[10-12] A_2^o, at the valence electron site and the atomic quadrupole moment[13] will be respectively given by σ_2 and R .

The various interactions of the nucleus with the surrounding charges are always measured in terms of the product of a nuclear and electronic property. In the present thesis we

shall be concerned primarily with the nuclear quadrupole and hexadecapole interactions. The nuclear quadrupole interaction is generally measured in terms of the coupling constant e^2qQ, where eq is the total electric field gradient at the nuclear site due to the surrounding charges and eQ is the nuclear quadrupole moment.

Using a predetermined value of eQ by means of some independent experiment eq can be extracted from the e^2qQ data on a given system and the available knowledge of the electronic structure of the system can be put to test. For this purpose the total field gradient is generally expressed as

$$q = (1 - \gamma_\infty)\, q_{lat} + (1 - R)\, q_{val} \qquad (I.5)$$

where q_{lat} and q_{val} give the field gradients due to the distant charges and valence electrons respectively and $-\gamma_\infty q_{lat}$ and $-Rq_{val}$ represent the field gradients induced in the core electrons due to q_{lat} and q_{val}, respectively. For the accurate calculation of q in solids therefore it is essential to have reliable theoretical values of γ_∞ and R. Values of q_{lat} and q_{val} can be evaluated from the point-multipole model and the valence-electron wave functions. The quadrupolar polarizability α_q is useful in the accurate calculations of q_{lat} based on point-ionic model, where the lattice potential V at the ionic site A is modified due to the induced quadrupole moment $Q_{xy} = \alpha_q \frac{\partial^2 V}{\partial x \partial y}$.

The more fundamental quantity Q, the nuclear quadrupole moment, is most conveniently derived from the quadrupole coupling constants measured from the hfs studies on isolated atoms. The calculated field gradient q_{val} in this case is corrected for the Sternheimer effect according to

$$q = (1-R)\, q_{val} \qquad (I.6)$$

Thus the uncertainties in eQ and eq obtained from experiments to a large extent depend on the reliability of $(1 - \gamma_\infty)$ and (1-R) values.

The fourth-order gradient m_{16} of the electrostatic potential at the nucleus can be expressed as,

$$m_{16} = (1 - \eta_\infty) m_{16\ ion} + (1 - R_H)\, m_{16\ val} \qquad (I.7)$$

where $-\eta_\infty\, m_{16\ ion}$ and $-R_H m_{16\ val}$ represent the Sternheimer polarization effects in the core electrons arising from the distant ions and the valence electrons respectively. It is important to note here that values of $(1 - \eta_\infty)$ are of the order of 10^3 and can drastically change the fourth-order gradient, $m_{16\ ion}$ due to distant ions. The $m_{16\ val}$ arises from the d and f valence electrons. Using a predetermined value of H, the nuclear hexadecapole moment, and the calculated value of $(1 - \eta_\infty) m_{16\ ion}$, it is possible to extract $m_{16\ val}$ from the measured hexadecapole coupling constant $e^4 m_{16} H$. It is then possible to obtain

experimentally information regarding d and f electron distributions in terms of an extremely sensitive fourth derivative term $^{m}_{16\ val}$.

Similar to the quadrupole moment case, the nuclear hexadecapole moments derived from the experimental data on isolated atoms have to be corrected for the Sternheimer polarization effect $(1 - R_H)$. Thus, accurate calculations of $(1 - \eta_\infty)$ and $(1 - R_H)$ are highly desirable since experimental data on hexadecapole coupling constants are now becoming available.

The quadrupolar part of the static crystalline electric field at the valence site is shielded due to the Sternheimer polarization of the core electrons according to

$$A_2^{o'} = (1 - \sigma_2)\, A_2^o \qquad (I.8)$$

and it is necessary to interpret the experimental measurements involving $A_2^{o'}$, e.g. in the study of the temperature dependence of Mossbauer quadrupole splittings, nuclear alignment experiments etc. The shielding factors, σ_{nl}, to the external crystalline field at the core electron sites can lead to detectable core level splittings in photoelectron spectra of heavier atoms. It is therefore essential to calculate σ_2 and σ_{nl} to interpret such data.

The atomic quadrupole moment Θ_p due to the aspherical np-electron density distribution can itself act as the source

of perturbation and induce a quadrupole moment within the electronic shells in the atom, which can change the value of Θ_p according to

$$\Theta = (1 - R_\Theta) \Theta_p \qquad (I.9)$$

Depending upon the atomic system under consideration R_Θ can be $\rightarrow 1$ in which case the observed atomic quadrupole moment will have a sign opposite to that predicted by the shielding uncorrected value of Θ_p. Therefore, it is of interest to calculate R_Θ for various atomic systems.

Although we shall be dealing mainly with the quantities γ_∞, R, σ_2, η_∞, and R_Θ in this thesis, the methods for calculations of these and other polarizabilities and shieldings have much in common and hence we shall outline the general theoretical procedures that have been employed so far in the calculation of polarizabilities and shielding-antishielding factors. In the next section (I.3) we give a review of various approximate methods available for the calculation of polarizabilities and shielding-antishielding factors.

I.3 Approximate Methods for the Calculation of Polarizabilities and Shielding-Antishielding Factors

The various approximate methods available for the calculation of polarizabilities and shielding-antishielding factors can be broadly classified into the following categories:

(A) Statistical Methods [Gombas (1944), Sternheimer (1950)].

(B) Coupled Hartree-Fock (CHF) Methods for Closed Shells [Dalgarno (1959), Kaneko (1959), Watson and Freeman (1963), Cohen and Roothaan (1964), and Lahiri and Mukherji (1966)].

(C) Uncoupled Hartree(UCH) and Uncoupled Hartree-Fock (UCHF) Methods for Closed Shells [Sternheimer (1954), Das and Bersohn (1956), Dalgarno (1959), Karplus and Kolker (1963), Yoshimine and Hurst (1964), Langhoff, Karplus, and Hurst (1966), Duff and Das (1968), Sadlej (1971) and others].

(D) Perturbed Uncoupled Hartree-Fock (PUCHF) Methods Hirschfelder and co-workers (1966), Musher (1967), Epstein and Johnson (1967), Sadlej (1971, 1973), Stewart (1975) .

(E) CHF Methods for Open Shell Systems [Mukherji (1975), Stewart (1975)].

(F) Methods Including Electron Correlation Effects Explicitly [Donath (1961), Kelly (1964), Das (1968), Nesbet (1970), Krauss (1972), Sims (1973), Lindgren (1975)].

I.3.A Statistical Methods

Gombas[14] has developed a statistical procedure for calculating α_d and has obtained satisfactory results for

heavy atoms. Sternheimer[7a,9,15] has employed the Thomas-Fermi scheme to evaluate the electric field at the nucleus. Due to incorrect behaviour at large r this model is inadequate particularly for polarizability calculations. In the case of the Thomas-Fermi-Dirac model, Sternheimer found that the induced field is far too large for lighter atoms. This method has been extensively used to obtain theoretical estimates of the total angular contributions to the multipole shielding-antishielding factors.

I.3.B Coupled Hartree-Fock Method for Closed-Shells

We shall first consider the 'closed-shell' N-electron atomic systems which can be satisfactorily represented by a single determinant (SD) wave function within the Hartree-Fock (HF) model. The coupled Hartree-Fock (CHF) method is actually a generalization of the HF idea which seems variationally the SD solution of lowest energy in a self-consistent manner either by using a perturbation expansion and obtaining the first order corrections to the unperturbed HF orbitals, or by directly solving the problem in presence of a finite perturbation without using the expansion. In the former method, known as coupled Hartree-Fock perturbation (CHFP) method, the second order properties can be calculated in two ways. One can solve the appropriate inhomogeneous differential equations or alternatively extremize the corresponding energy functional. This

latter method will be called the coupled Hartree-Fock perturbation variation (CHFPV) method.

Peng[16] and Allen[17] have discussed earlier the HF model for atomic systems in presence of a static external field. Langhoff, Karplus and Hurst[18] (LKH) have presented an instructive analysis of the various coupled and uncoupled methods in use. We shall present here and in the next section the methods denoted as a, b, c, and d in the paper of LKH and identify various approximate methods in use to calculate multipole polarizabilities and shielding-antishielding factors. In what follows, we shall present a general outline of the CHF procedure.[5]

Denoting the one-electron Fock operator and the external perturbation as $h(1)$ and $h^1(1)$ respectively, the problem reduces to solving the following coupled equations:

$$\{h(1) + \lambda\, h^1(1) - \varepsilon_i\}\ \chi_i(1) = 0,\ i = 1, 2, 3, \ldots N \qquad (I.10)$$

where spin orbitals, χ, obey the orthonormality criterion

$$\langle \chi_i | \chi_j \rangle = \delta_{ij}, \quad i,j = 1, 2, \ldots N \qquad (I.11)$$

$$\text{and } h(1) = -\tfrac{1}{2}\nabla_1^2 - \left(\frac{Z}{r_1}\right) + \sum_{j=1}^{N} \langle \chi_j |\ r_{12}^{-1}\,(1 - P_{12}) \,|\, \chi_j \rangle \qquad (I.12)$$

Here P_{12} is the permutation operator for electron 1 and 2. Expanding χ_i as

$$\chi_i = \chi_i^o + \chi_i^1 + \ldots \qquad (I.13)$$

$$\varepsilon_i = \varepsilon_i^o + \varepsilon_i^1 + \ldots \qquad (I.14)$$

and substituting in eq (I.10), the differential equations up to first order in λ are obtained as,

$$\{ h^o(1) - \varepsilon_i \} \chi_i^o (1) = 0 \qquad (I.15)$$

$$\{ h^o(1) - \varepsilon_i^o \} \chi_i^1 (1) + \{ h^1(1) - \varepsilon_i^1 \} \chi_i^o (1)$$

$$+ \sum_{j=1}^{N} \{ \langle \chi_j^1 | r_{12}^{-1} (1 - P_{12}) | \chi_j^o \rangle$$

$$+ \langle \chi_j^o | r_{12}^{-1} (1 - P_{12}) | \chi_j^1 \rangle \} \chi_i^o(1) = 0 \qquad (I.16)$$

where $h^o(1)$ is the zeroth-order Fock operator:

$$h^o(1) = -\tfrac{1}{2} \nabla_1^2 - \left(\frac{Z}{r_1}\right) + \sum_{j=1}^{N} \langle \chi_j^o | r_{12}^{-1}(1-P_{12}) | \chi_j^o \rangle \qquad (I.17)$$

Eq. (I.16) defines the coupled Hartree-Fock perturbation procedure 'a' of LKH paper and has been used by Dalgarno,[19a,d] Kaneko,[19b,20] and Langhoff, Karplus and Hurst[18] to calculate α_d, β_∞ , α_q and γ_∞ for two-, three- and four-electron sequences and α_d for Ne, Mg, and A[20]. Dalgarno and Kaneko have solved the differential equation (I.11) while Langhoff et al.[18] have used the variational method based on product approximation for the perturbed function, viz., $\chi^1 = f\ \chi^o$.

Watson and Freeman[21] have used a finite perturbation method within the unrestricted Hartree-Fock (UHF) scheme and

solved the equations corresponding to (I.5) to calculate quadrupole shielding-antishielding factors for heavier ions such as Cl^-, Br^-, I^-. These authors have shown that within the UHF approximation, relaxation of Nesbet's symmetry and equivalence restriction[22] yields the angular and radial contributions to γ_∞ (and R) respectively. Relaxing the symmetry condition, however, poses computational problems particularly for large systems and in the WF method the angular estimates have to be based on less accurate uncoupled methods. Cohen and Roothaan[23] have solved eq. (I.5) within the Hartree-Fock-Roothaan model with the finite perturbation and have obtained α_d for the members of two-, four- and ten-electron sequences. One of the drawbacks of the finite perturbation methods is that the HF calculations have to be carried through to a high degree of self-consistency in order to efficiently retain the effects of a small part of the Hamiltonian. This inherent error becomes magnified as the perturbation becomes smaller and smaller.

Lahiri and Mukherji[24] have proposed a fully-coupled restricted Hartree-Fock-Roothaan perturbation-variation method and have calculated α_d, β_∞, α_q and γ_∞ values for He, Li, Be, Ne and A isoelectronic sequences. This is the most economic CHF method which gives β_∞ values close to the theoretical limit of N/Z. This indicates that the variational form used for the first-order wave function is sufficiently flexible.

Before closing this section on CHF methods the following remarks on some of the procedures described here are in order. In the method 'a' of LKH the use of the product-approximation forces the perturbed wave functions to have the same nodes and a similar exponential decay as the unperturbed wave functions. Kaneko's procedure, due to its numerical character, accords a full variation to the perturbed wave function but it demands heavy computational effort. In Lahiri and Mukherji's method the choice of an accurate variational function as a sum of Slater type orbitals (STO's) becomes complicated for systems beyond argon; hence calculations beyond argon series have not been attempted with this method.

I.3.C Uncoupled Hartree (UCH) and Uncoupled Hartree-Fock (UCHF) Methods for Closed-Shells

The various uncoupled methods in use are the result of compromises between accuracy and computational labour. With the assumption that the coupling terms in eq. (I.11) do not contribute significantly to the total second order energy and therefore to second order properties such as polarizabilities and shielding factors, it has been the practice in uncoupled methods to completely neglect them. These methods can be best described as semi-empirical methods since they do not conform to any well defined physical model.

I.3.C(i) Uncoupled Hartree Methods

Our understanding of the polarization of closed shells is largely due to Sternheimer[6-9,11,13,15] and the uncoupled perturbation-numerical method formulated by him. This method can be very briefly described as an uncoupled Hartree method (UCH) which uses Hartree or Hartree-Fock wave functions for the unperturbed state with a local approximation[6,7c] to the effective potential in the first-order perturbed inhomogeneous Schrodinger equation. We shall discuss this method in greater detail in Chapter II. Khubchandani, Sharma and Das[25] have shown that the inclusion of exchange among the perturbed wave functions in the Sternheimer method significantly increases γ_∞ (in magnitude) for K^+ and Cl^- but α_q values are not affected as much. This method rectifies the inconsistencies arising due to the use of HF wave functions in the UCH method. Ray, Lee, Das and Sternheimer[26] have extended the perturbation-numerical (differential equation) approach to incorporate intra-shell and inter-shell coupling effects which are ignored in the uncoupled formalism.

Das and Bersohn[27] (DB) have formulated the variational equivalent of Sternheimer's method. Dalgarno[19a] has shown that for the lighter atoms and ions the small discrepancies between the perturbation-numerical and variational methods can be ascribed to the different representations used by the two

authors for the unperturbed wave functions. Wilkner[28] and Burns[29] have adopted the variational method of DB to obtain the multipole polarizabilities and shielding factors for heavier ions. We shall show in the subsequent chapters that for heavier ions the variational method underestimates the antishielding effect. The variational procedure of DB requires that the trial first-order perturbed wave functions are orthogonal to the associated unperturbed wave functions. The apparent difficulties concerning such an orthogonality requirement have been discussed by Ingalls.[30]

I.3.C(ii) Uncoupled Hartree-Fock Methods

Dalgarno[5,31] has proposed the uncoupled Hartree-Fock (UCHF) method in which both the unperturbed and perturbed wavefunctions satisfy the Pauli principle. Dalgarno and McNamee[31b] have solved the appropriate differential equations to calculate α_d, β_∞ , α_q and γ_∞ for Be. Yoshimine and Hurst,[32] and Langhoff and Hurst[33] have used a variational version of Dalgarno's UCHF method[31] to calculate multipole polarizabilities and shielding-antishielding factors for a large number of atoms and ions. In this method the energy functional is extremized without subjecting the trial perturbed wave functions to any orthogonality constraints. Karplus and Kolker[34] have proposed a similar method in connection with the calculation of electric and magnetic susceptibilities of small molecules. There is,

however, an important difference between the methods of Karplus and Kolker[34] and those of Dalgarno[31] which has been first pointed out by LKH.[18] In the following we shall present LKH methods b, c and d as obtained from method a (see sec. I.2.B(ii)) and bring out this difference.

Cancelling the self-potential term (j=i) in $h^{o}(1)$ in eq. (I.17) with (j=i) term of the explicit sum in eq. (I.16) and neglecting all the terms involving first order functions χ_j^1, other than the one being considered, equations are obtained for LKH[18] UCHF method 'b':

$$\{ h_i^o(1) - \varepsilon_i^o \} \chi_i^1(1) + \{h^1(1) - \varepsilon_i^1\} \chi_i^o(1) = 0 \qquad (I.18)$$

$h_i^o(1)$ is now a modified Fock operator in the sense that under independent variation of spin orbitals only χ_i^o is an eigenfunction of h_i^o. It should be noted that in the closed-shell version of eq. (I.18), χ_i^o is not an eigenfunction of the zeroth-order Fock type operator which replaces h^o. Owing to the cancellation of the self-interaction term, the perturbation in method 'b' is obtained in presence of N-1 electrons only.

Neglecting completely the summation terms in eq. (I.16) the equations corresponding to LKH method 'c' are obtained as,

$$\{h^o(1) - \varepsilon_i^o \} \chi_i^1(1) + \{ h^1(1) - \varepsilon_i^1 \} \chi_i^o(1) = 0 \qquad (I.19)$$

where h^o is the zeroth-order Fock operator. Eq. (I.19) is

equivalent to Dalgarno's[5,31] UCHF method. It can be seen that due to the self-interaction term in h^o the perturbed wave functions are obtained in presence of an inappropriate core potential due to N electrons. This method provides an upper bound to the CHF second order energy.

Substituting for $h^o(1)$, the Temkin[35] operator $g_i^o(1)$ in eq. (I.18) or (I.19) LKH have defined their UCHF method d as,

$$\{ g_i^o(1) - \varepsilon_i^o \} \chi_i^1(1) + \{h^1(1) - \epsilon_i^1\} \chi_i^o(1) = 0, \qquad (I.20)$$

where $g_i^o(1) = -\frac{1}{2} \nabla_i^2 - (\frac{Z}{r_i}) + \sum_{j=1}^{N} (\langle \chi_j^o | r_{12}^{-1} | \chi_j^o \rangle -$

$$\frac{\langle \chi_j^o | r_{12}^{-1} | \chi_i^o \rangle}{\chi_i^o} \chi_j^o \qquad (I.21)$$

The variational method of Karplus and Kolker[34] is similar to LKH method 'd'. Therefore in the Karplus-Kolker method the perturbation is obtained in presence of (N-1) electrons as against the core potential due to N electrons in Dalgarno's UCHF method. Duff and Das[36] have formulated the counterparts of LKH methods 'a' and 'b' wherein the orthogonality restriction on perturbed one-electron wave function is relaxed. The counterpart of method b has a computational advantage over the original method due to simplifications achieved in the orthonormalization process. Sadlej[37a] has modified Karplus-Kolker method by including intra-orbital contribution of the non-local part of the HF potential and self-consistency respectively. His

calculations of α_d for two-, four- and ten-electron systems are in good agreement with the CHF results. In a subsequent paper Sadlej[37b] has omitted the nonorthogonality contributions and has obtained improved results for α_d and β_∞ for ten-electron atomic systems.

The more approximate uncoupled Hartree perturbation variation method of Pople and Schofield[38] has been applied to calculate α_d for all neutral atoms. Adelman and Szabo[39] have described the Coulomb-approximation method to calculate α_d and β_∞ and have obtained good agreement with the experimental α_d values for monovalent ground and excited S-state atoms. The β_∞ values differ significantly from N/Z. Ahlberg and Goscinski[40] have calculated α_d and β_∞ using a local linear-response method for singlet ground state atoms up to Z = 36 and obtained excellent agreement with the experimental α_d and theoretical β_∞ values. These authors have observed that the full Slater exchange[41] rather than the optimized counterpart yields more accurate results.

I.3.D Perturbed Uncoupled Hartree-Fock (PUCHF) Methods for Closed-Shells

Tuan, Epstein and Hirschfelder[42] (TEH) have shown that starting with Dalgarno UCHF wave functions at the zeroth-order, the first order correlation correction to the UCHF second order energy can be obtained without solving any new equations.

According to these authors, the first order correction to the second order property can be obtained from

$$\langle\Omega\rangle_1 = \tfrac{1}{2} \sum_{i=1}^{N} \sum_{j=1}^{N} \{ \langle x_i^1 \, x_j^1 | \frac{1}{r_{12}} | x_i^o \, x_j^o \rangle +$$

$$\langle x_i^o \, x_j^o | \frac{1}{r_{12}} | x_i^1 \, x_j^1 \rangle + 2 \langle x_i^1 \, x_j^o | \frac{1}{r_{12}} | x_i^o \, x_j^1 \rangle$$

$$- \langle x_i^1 \, x_j^1 | \frac{1}{r_{12}} | x_j^o \, x_i^o \rangle - \langle x_i^o \, x_j^o | \frac{1}{r_{12}} | x_j^1 \, x_i^1 \rangle -$$

$$\langle x_i^1 \, x_j^o | \frac{1}{r_{12}} | x_j^1 \, x_i^o \rangle \} \qquad \text{(I.22)}$$

where

$$\langle x_i^m \, x_j^n | \frac{1}{r_{12}} | x_k^o \, x_l^p \rangle$$

$$= \iint x_i^{m*}(1) \, x_j^{n*}(2) \, \frac{1}{r_{12}} \, x_k^o(1) \, x_l^p(2) \, d\tau_1 d\tau_2 \qquad \text{(I.23)}$$

and the superscripts o and 1 refer to the unperturbed and the first order perturbed wave functions respectively.

Musher[43] has given a more rigorous treatment for such corrections and has shown that the UCHF result is equivalent to the first term in the double-perturbation theory expansion and the CHF result differs from first two terms of the general expansion only by higher order terms. He has also shown that when perturbation theory is applied to improve upon CHF method the resulting solution offers no additional advantage. Epstein and Johnson[44] have carried out such perturbed uncoupled

Hartree-Fock (PUCHF) calculations of α_d and α_q for H, Li, Be isoelectronic series and have found that except for the near-neutral atomic systems these results are in satisfactory agreement with the CHF results. In a diagrammatic double-perturbation analysis Caves and Karplus[45] have shown that the first-order correlation correction to the second order UCHF energy coincides with the first iterative solution in the CHF theory. Schulman and Musher[46] improved the situation by proposing a geometrical approximation on empirical grounds. These authors have shown that the hydrogen atom dipole polarizability α_d can be obtained from the double perturbation expansion based on a Hartree-Fock potential, H_o, by approximating the perturbation series by a geometrical series according to,

$$\alpha_d^{geom} = \alpha_d^o \{ 1 - (\alpha_d^1/\alpha_d^o) \}^{-1} \qquad (I.24)$$

where α_d^o corresponds to H_o and α_d^1 is the first-order correlation correction to α_d^o.

Amos,[47] Tuan,[48] Sadlej and Jaszunski[49] and Jamieson and Gafarian[50] have independently given theoretical justifications for the GA method. Tuan and Davidz[51] have performed PUCHF calculations of α_d and β_∞ for two-, three- and four-electron systems with varying amount of self-interaction terms in the effective Hamiltonian and have shown that an optimum self-interaction term along with the GA can be a good substitute for the CHF calculations of the second-order properties. Sadlej[52]

has generalized the PUCHF method of TEH for the approximate SCF unperturbed orbitals. Stewart[53] has applied GA to Dalgarno UCHF by using the uncoupled differential equation (rather than using the appropriate functional method as in Saldej's GA to Karplus-Kolker method) and obtained α_d and α_q in excellent agreement with CHF results. In the PUCHF calculations of polarizability the computer time required is one-fifth of that required for CHF calculations. The first-order correlation corrections to the shielding factors which are bilinear in the perturbation parameter require twice the computer effort as compared to the polarizability calculation. Litt[54] has introduced an effective-field method which is equivalent to GA for the polarizability calculations if the zeroth-order approximation is chosen to be Sternheimer approximation. The GA methods of Sadlej and Stevens seem to be worth pursuing for heavier systems.

I.3.E Coupled HF Methods for Open-Shells

Mukherji and coworkers[55] have extended the CHF perturbation-variation method to calculate multipole polarizabilities and shielding factors for open-shell atoms. This method neglects the core rearrangement and core polarization effects but includes all the first-order correlation and parts of higher order correlation effects. The core rearrangement effects have been recently included by these workers.[55b] Stewart[56]

has solved the numerical version of CHFPV method of Mukherji and coworkers and has obtained good agreement with the latter calculations and the experimental result for α_d of $A^+(^2P)$.

I.3.F Methods Including Electron Correlation Effects Explicitly

For accurate calculations of second-order properties it becomes necessary to go beyond Sternheimer polarization and include two-particle interaction in an explicit manner.

Donath[57] has adopted a variational approach including configuration interaction to calculate α_d for Ne. Similar calculations[58] of other first row atoms have been performed. In the case of larger number of valence electrons a balanced treatment of the unperturbed and perturbed wave functions cannot be guaranteed since the multiconfigurational structure has to be ascribed to the perturbed wave function in the lowest approximation. Indeed such methods have produced low values for the dipole polarizabilities of C, N and Ne. For the cases with smaller number of valence electrons the variational configuration interaction method is certainly the most powerful one.

Sitter and Hurst[59] have used CHF method using an extended polarization basis to compute α_d of Ne. Stevens, Billingsley and Krauss[60] used a coupled multiconfiguration self-consistent field (CMCSCF) method to calculate α_d for the first row atoms to within $\pm$5% in accuracy.

Meyer and coworkers[61] have performed the most accurate calculations of α_d for the first row atoms ($\sim$2% accuracy) using pair natural-orbital configuration-interaction (PNO-CI) and coupled electron pair approximation with pair natural-orbitals (CEPA-PNO). Ahlrichs and coworkers[62] have reported a computationally improved version of these methods to calculate correlation energy in Ne and smaller molecular systems. These methods have not been applied so far to the calculation of shielding factors.

Kelly[63] first applied the linked-cluster many-body perturbation theory (LCMBPT) expansion method of Brueckner and Goldstone[64] to atomic systems and obtained α_d, β_∞ , α_q and γ_∞ for Be including correlation contributions up to second order. Similar MBPT calculations[65] of Li, C, O, Ne have also been carried out. Doran[66] calculated multipole polarizabilities and shielding factors for Ne, A, Kr and Xe. Ray, Lee and Das[67] have calculated γ_∞ for Fe^{3+}, Rb^+ and Cs^+ using LCMBPT method. Similar calculation of R has been first reported by Lyons, Pu and Das[68] for Li(^{2}P). These authors have noted that the effect of second-order correlation correction to R is a small positive contribution with respect to the first-order correlation correction. Accurate calculations of Nesbet[69] using variational Bethe-Goldstone approach have suggested that the two-particle correlation corrections give rise to near cancellation of the

single-particle correlation effect. Hameed and Foley[70] have applied the perturbation method to second order within RHF scheme and obtained an agreement with Nesbets' calculations to within 2%. This is probably due to the limited number of configurations which Hameed and Foley used to construct the first-order wave functions. Garpman, Lindgren, Lindgren and Morrison[71] have formulated an elegant effective-operator form of LCMBPT method and applied it to calculate ab initio, the hyperfine interaction in Li(np) and Na(np) sequences. Instead of generating a complete set of excited states as in Kelly's approach the first- and second-order corrections to the HF value are obtained by solving inhomogeneous one- and two-particle equations. Their value of $R(^2P\ Li)$ is in excellent agreement with Nesbets' calculation. Das and coworkers[72] have recently shown that the discrepancy in their earlier calculation on $Li(^2P)$ is a result of neglecting some diagrams corresponding to two-particle (1s-2p) correlation. The calculations of R with similar accuracy have been reported[73] for the first row atoms, alkali metals and Fe^{2+} ion.[72] These calculations are in reasonably good agreement with the corresponding calculations based on Sternheimer[74] method. One remarkable advantage of the Brueckner-Goldstone approach lies in its transparency which makes it suitable to physically evaluate[65b] the numerical results at various levels of approximation. The convergence of the perturbation series seems to depend considerably on the

particular system and this leads to practical difficulties in carrying out all the calculations with the same accuracy. The electron pair approaches,[61,62,69] on the other hand, include three-particle correlation effects which become important beyond nitrogen. Such calculations are formidable even with present day computers.

It is evident from the survey of theoretical methods presented above that not many detailed calculations of γ_∞, R, σ_2, η_∞ and R_θ have been carried out using reasonably accurate uncoupled methods. There is, therefore, a need to undertake a project involving extensive calculations of these Sternheimer shielding-antishielding factors in a consistent manner. Such calculations will be equally important for both experimentalists and theoreticians. An attempt has been made in this thesis to make some contribution in this direction.

In the next section (I.4) we shall review the experimental evidences that support the viewpoint that the shielding-antishielding phenomena play an important role in the study of quadrupolar and hexadecapolar interactions.

I.4 Experimental Evidences for Sternheimer Factors

As mentioned earlier in this thesis, we are interested in the quantities γ_∞, R, σ_2, η_∞, and R_θ. So we shall confine our attention in this section to the quadrupole and hexadecapole interactions.

In the earlier literature, the importance of Sternheimer polarization effect corresponding to the electric quadrupole interaction has been recognised mainly through nuclear magnetic resonance (NMR) and nuclear quadrupole resonance (NQR).[75] Later, other methods such as Mössbauer effect, time differential perturbed angular correlation (TDPAC), low temperature colorimetry and atomic hyperfine structure studies have also emphasized the role of Sternheimer effects. In the following we shall present a survey of these experimental evidences for Sternheimer polarizations.

I.4.A Quadrupolar Interactions and $(1 - \gamma_\infty)$

Sternheimer[7g] estimated the effective antishielding factors for ^{81}Br, ^{35}Cl, ^{35}Cl and ^{127}I in the polar molecules of KBr, NaCl, KCl, and KI, respectively from the available quadrupole coupling constants derived from molecular beam electric resonance studies[76] and the known[77] Ω values and concluded for the first time that the experimental results give support to the calculated antishielding factors.

I.4.A(i) Magnetic resonance studies

Pound[78] has shown that the perturbing nuclear quadrupole interaction in noncubic ionic solids can split and/or shift the high field[79] NMR line in the cases of ^{7}Li, ^{23}Na, and ^{27}Al. The spin lattice relaxation time (T_1) of these lines were also

shown to be affected by such interactions. Bersohn[80a] and Volkoff[80b,c] have given perturbation expressions to extract the quadrupole coupling tensor components from the NMR spectrum of noncubic single crystals. Several theoretical models such as acoustic ionic-model of Van Kranendonk,[81] charge-transfer covalency model of Yoshida and Moriya[82a] and overlap-covalency model of Kondo and Yamashita[82b] have been proposed to explain the quadrupolar relaxation time T_1.

Van Kranendonk[81] has estimated the combined effect of covalency and $(1 - \gamma_\infty)$ to be $> 10^3$ from ^{127}I NMR relaxation time measurements in KI. Kawamura, Otsuka and Ishiwatari[83] have observed striking reduction in intensity of the satellite lines of ^{23}Na in NaCl crystal when small amounts of NaBr are added. In such mixed-crystal experiments the field-gradient results from the size differences in solute and solvent ions. From the second-order shift of the central line at 10% of solute concentration, Kawamura et al. have estimated $(1 - \gamma_\infty) \sim 9$ for Na^+. Otsuka and Kawamura[84] have similarly studied the second-order shift of ^{79}Br and ^{81}Br resonance lines in KBr-NaBr system and concluded that $(1 - \gamma_\infty) \sim 40$ for Br^-. Bersohn[85] has interpreted the quadrupole coupling constants available from NMR data on ^{23}Na, ^{27}Al, ^{63}Cu and ^{65}Cu nuclei in ionic solids using the point-charge model and has found that the abandonment of the factor $(1 - \gamma_\infty)$ representing the polarization effect removes all agreement with experiment.

Wikner and Das[28] have shown that the ratio of field gradients obtained by Kiddle and Proctor[86] for ^{87}Rb and ^{133}Cs NMR in tutton salts can be explained by considering the theoretical ratio of $(1 - \gamma_\infty)$ for Rb^+ and Cs^+ ions. Valiev[87] has obtained reasonable results for $(1 - \gamma_\infty)^2$ from the NMR line-width studies on Al^{3+} and Ga^{3+} in solution. Wikner, Blumberg, and Hahn[88] have included the effects of induced dipole moments due to optical modes into Van Kranedonk[81] model and have assumed the theoretical value of $(1 - \gamma_\infty)$ for Na^+ to estimate $(1 - \gamma_\infty)$ for Cl^- as 20 from the ratio of spin-lattice relaxation times for the two nuclei. From the temperature dependence of the quadrupole coupling for Al^{3+} in $C(NH_2)_3\ Al(SO_4)_3.6H_2O$ and Al^{3+} and Ga^{3+} in isomorphous ionic solids, Burns[89] has obtained good agreement with experiment on including theoretical $(1 - \gamma_\infty)$ for Al^{3+} and Ga^{3+}. Burns and Wikner[29c] have concluded that the experimentally estimated values of $(1 - \gamma_\infty)$ for positive ions are in reasonably good agreement with the theoretical values but the empirical γ_∞ values for negative ions are 3-5 times smaller than the calculated values. Das and Dick[90] have criticized these estimates for the negative ions on the basis that the empirical values for the negative ions have been derived in a crude fashion. Thus, the empirical estimate of γ_∞ for Br^- by Otsuka and Kawamura[84] has been derived from a simple compression theory which leads to erroneous estimates of the the displacements of the lattice points and also neglects the

polarization contribution of the nearest-neighbour ions which are important. Das and Dick[90] have included these contributions in interpreting the results on NaCl-Br, NaBr-Cl and KBr-Na and have observed that the NMR data can be satisfactorily explained on the basis of theoretically calculated values of γ_∞ for Na^+ and Br^-.

Wilson and Blume[91] have measured the quadrupolar shifts of NMR lines of the off-centre Li^+ and Cu^+ impurity ions in KCl and have noted that the ratios of first- and second-order effects obtained in the two cases can be explained by assuming the theoretical values of $(1 - \gamma_\infty)$. Raymond[92] has used the point-multipole model and obtained the best fit value of γ_∞ -4.9 to explain 34 independent field gradient components extracted from ^{27}Al NMR in three Al_2SiO_5 polymorphs. Sharma[93] has used the overlap model along with the Sternheimer shielding-antishielding factors and obtained the nuclear quadrupole moment for ^{27}Al from the NMR data[78] on Al_2O_3. His value of $Q(^{27}Al)$ = 0.148 b is in excellent agreement with the atomic beam result[94] of 0.149b.

There are innumerable examples from pure quadrupole resonance experiments[95] which have led to the determination of nuclear quadrupole interactions in solids. These have also provided evidences in favour of shielding-antishielding effects. Hewitt[96] has estimated $(1 - \gamma_\infty) = 16$ for Nb^{5+} from the NQR data

on ^{93}Nb in $KNbO_3$ which compares well with the theoretical estimate of 15. Barnes, Segal and Jones[97] have shown that using the empirically estimated values of γ_∞ for Cl^-, Br^- and I^- as -10, -35 and -45 respectively, the NQR data on a series of solid layer-type metal halides can be explained if a small increase in the value of s-hybridization due to covalency is assumed. Rao and Narasimhamurthy[98a] using a point charge model with induced dipole-moments found that $\gamma_\infty = -75$ for Cl^- is necessary to fit the NQR data on $CuCl_2.2H_2O$. Narath[99] has used a point-charge model and observed that $\gamma_\infty = -27$ for Cl^- gives a reasonable agreement with the NQR data on $CoCl_2.2H_2O$. The value of $(1 - \gamma_\infty)$ estimated by Rao and Narasimhamurthy for Cl^- appears to be too high. In fact, a later calculation on $CuCl_2.2H_2O$ including charges and effective dipole moments by Raj and Amirthalingam[98b] favours a value of $\gamma_\infty = -27.4$ for Cl^-. Liu[100] has reported the best fit value of ionicity and γ_∞ for Cl^- as 0.911 and -31 respectively to explain the NQR and NMR data on $CoCl_2.2H_2O$. Applying a soft sphere model to explain the experimental ^{35}Cl NQR data on $GdCl_3$ and a series of alkali-metal-hexachlorostanates, Current[101] has estimated $\gamma_\infty \sim -30$ for Cl^-.

The quadrupole coupling constant for ^{121}Sb and ^{123}Sb in antimony metal have been measured by means of NQR[102] and low temperature calorimetry[103] methods. Krusius and Picket[104] have obtained the extra-ionic contribution to the field gradient by subtracting the ionic field gradient corrected for antishielding

and assuming[105] $Q(^{121}Sb) = 0.5$ b. Their value of 560×10^{15} V/cm^2 compares well with the conduction electron contribution calculated by Hygh and Das.[106]

The quadrupolar relaxation time in liquid metals and III-V alloys have been measured.[107] From such experiments Haldar[108] has estimated γ_∞ values for Ga^{3+} and In^{3+} close to -10.5 and -24.9 respectively. He has observed that the theoretical value for Hg^{2+} calculated by Rao and Murthy[109] is too low by a factor of 2 or more. Kerlin and Clark[110] have found that in liquid GaSb the alloying can significantly enhance $(1 - \gamma_\infty)$ value for Sb over Ga due to an increase in negative charge on Sb.

From electron nuclear double resonance (ENDOR) studies on F-centres in KCl crystal, Feuchtwan[111] has estimated that the theoretical $(1 - \gamma_\infty)$ for Cl^- is probably too large by a factor of 2 or more. Zimmerman and Valentin[112] have made ENDOR studies on uniaxial stress-induced quadrupole splitting for Eu^{2+} doped in BaF_2, SiF_2, CaF_2 and CdF_2. Using the theoretical values of γ_∞ for Eu^{2+} these authors have obtained reasonably good agreement with the experiment.

I.4.A(ii) Electric Field Gradients and Acoustic Effects in Magnetic Resonance

Kaslter[113] and Al'tshuler[114] have independently predicted the possibility of observing saturation effects in NMR by inducing

the fluctuating field gradient by means of ultrasonics. The coupling between small elastic strain and electric field gradient can be represented[115] by a fourth-order tensor and in Voigt notation two independent tensor components $S_{11}-S_{12}$ and S_{44} are sufficient for the calculation of quadrupolar transition probabilities for a cubic crystal. In one method, the S components can be determined by studying the quadrupolar broadening of NMR lines due to an applied static uniaxial stress[115] or due to the presence of internal strains from a known concentration of dislocation[116] or impurity atoms[117] in a crystal. In the second method[118] ultrasound of known distribution of elastic strain amplitudes at Larmor or twice the Larmor frequency is applied and the transition between the nuclear spin levels induced by the time-varying electric field gradients at nuclear sites are studied from the decrease in intensity (saturation) of NMR absorption in a pulse or cw NMR experiment. In the more accurate method of nuclear acoustic resonance (NAR),[119] the resonant acoustic absorption by a spin system is directly measured as an additional attenuation. In NAR the elastic strain magnitudes do not enter into the determination of S components for certain directions of acoustic wave propagation and polarization in a cubic crystal. The accuracy of these three methods is estimated to be $\pm$15%, a factor of 2, and $\pm$6% respectively.

Otsuka[116] has estimated $(1 - \gamma_\infty) \sim 50$ for I^- from reduction in intensity of I^{127} resonance due to dislocations in KI. His

estimate is however based on the choice of $(1 - \gamma_\infty) \sim 40$ for Br^-. Fukai[117] has expressed the gradient elastic tensors for ^{23}Na, ^{35}Cl, ^{81}Br and ^{127}I in a series of alkali halide solid-solutions in terms of antishielding factor, nearest-neighbour overlap integrals and degree of covalency. He has found that the theoretical γ_∞ for the ions lead to S_{11}/S_{44} for Na^+, Br^- and I^- in fair agreement with the experimental data. A better agreement results by assuming a reduction of 10%, 40%, 50% in the theoretical γ_∞ values. Due to the lack of availability of good atomic wave functions the overlap integrals were calculated in an approximate manner. Marsh and Cassabella[120] have included second nearest neighbour overlap effects and obtained satisfactory agreement with the measured S components in uniaxially strained sodium halides using free ionic γ_∞ for Na^+ and contracted for Cl^- and Br^-. The nonlocal terms in the overlap effects were neglected by Fukai[117] and Marsh and Casabella.[120] Ikenbery and Das[121] have calculated the electric field gradient by including these terms in the overlap model and have observed that an increase in γ_∞ for positive ions and a substantial decrease in γ_∞ for negative ions would give a tolerable agreement with the experimental results without invoking any charge-transfer covalency.

The predictions of Kastler[113] and Al'tshuler[114] regarding spin-phonon coupling has been realized in a pulsed NMR ultrasonic-saturation experiment on $NaClO_3$ crystal by Procter and coworkers.[122] Jennings, Tantilla and Krauss[123] have compared the

relative saturation behaviour of ^{127}I and ^{23}Na resonances. Assuming the theoretical value of γ_∞ for Na^+ they have estimated $(1 - \gamma_\infty) \sim 50$ for I^-. Taylor and Bloembergen[118] have measured S components in NaCl single crystal by ultrasonic-saturation method and estimated $(1 - \gamma_\infty) \sim 5$ and 9 for Na^+ and Cl^- respectively. This experimental value for $(1 - \gamma_\infty)$ for Cl^- appears to be very low. Antokolskii, Sarnatskii and Shutilov[124] have studied ^7Li in LiF by ultrasonic-saturation and derived $\gamma_\infty = 0.5 \pm 0.3$ for Li^+. Anderson and Karra[125] in a similar study have derived $\gamma_\infty = 4.4 \pm 0.4$ for Li^+. The reason for this discrepancy in the two measurements is not clear to us. Kanashiro[126] has explained the experimental values of S components in alkali bromides by including overlap effects and assuming the free ionic γ_∞ values. Kanashiro, Ohno and Satoh[127] have studied ferroelectric $NaNO_2$ by ultrasonic-saturation of ^{23}Na resonance and found that a point multipole model coupled with the theoretical γ_∞ for Na^+ gives reasonable agreement with the experiments.

Bolef and Menes[119] have studied ^{81}Br and ^{127}I in KBr and KI single crystals respectively by NAR and estimated $(1 - \gamma_\infty)$ for Br^- and I^- to be 26 and 38 respectively. Sundfors[128] has carried out similar measurements on III-V semiconductors and Sundfors and Tsui[129] have analysed their data on S_{11} to derive $(1 - \gamma_\infty)$ for Al, Ga, In, As and Sb as 16, 45-59, 95-108, 79-82 and 85-104 respectively. Sundfors, Wang, Bolef, Fedders and

and Westlake[130] have studied ^{181}Ta NAR in a hydrogen-free pure Ta single crystal and obtained the effective $(1 - \gamma_\infty)$ to be 10 times the theoretical value.

I.4.A(iii) Electric Field Gradients from Mössbauer and TDPAC Studies

The quadrupole splittings obtained from Mössbauer effect studies on ^{57m}Fe in solids have been generally interpreted on the basis of eq. (I.5). The agreements obtained via eq. (I.5) with the experimental data can be regarded as indirect evidences in favour of Sternheimer shielding-antishielding effects. The Mössbauer data on ferric compounds have been interpreted[131] on the basis of ionic model. In the case of ferrous compounds,[132] on the other hand, the valence contribution is dominating. Such interpretations have led to a range[133] of values (0.1-0.4b) of nuclear quadrupole moment Q for ^{57m}Fe. Including the effects due to overlap and Sternheimer shielding-antishielding factors, Sharma[134] has resolved this ferric-ferrous anomaly to obtain $Q(^{57m}Fe) = 0.18 \pm 0.02$ b and has satisfactorily explained the Mössbauer data on several rare earth garnets.

Bhide and Hegde[135] have compared the efg at Sc^{3+} and Fe^{3+} sites, as determined by γ-γ directional correlation of ^{44}Sc and ^{57m}Fe Mössbauer effect studies in $PbTiO_3$, respectively. Assuming the theoretical value of γ_∞ for Fe^{3+} these authors have estimated $\gamma_\infty = -19$ for Sc^{3+}. Sharma[136] has incorporated

the effects of ligand distortions due to internal crystalline electric field in the overlap model and analysed the time-differential perturbed angular-correlation[137] (TDPAC) data on ^{117}In and ^{111}Cd $CdCl_2$. His analysis gives $Q(^{111}Cd) = 0.89 \pm 0.05$b which is very close to the value of 0.9 b obtained from the circular polarization measurements[138] of 247-keV γ-ray of ^{111}Cd.

In their interpretation of the e^2qQ data on metals obtained by TDPAC[137] and other methods Das and coworkers[139] have calculated the conduction electron and distant charges contribution to the field gradient in Be, Mg, Zn and Cd metals. The nuclear quadrupole moments obtained from their analysis are consistent with the nuclear structure systematics and the calculated field gradients are in quantitative agreement with the experimental values for Be and Mg.

Raghvan, Kaufmann and Raghvan[140] have shown that the major portion of extra-ionic field gradient in metals and dilute alloys is universally correlated to the antishielding-corrected ionic counterpart and is of the sign opposite to it. This correlation is the strongest evidence in favour of the existence of the term $(1 - \gamma_\infty)$.

A quantitative agreement between the estimates of $(1 - \gamma_\infty)$ obtained on the basis of a point-charge model in solids and the theoretical values cannot always be expected since several other important electronic effects might have been ignored. The best

way is to use the calculated lattice contribution to the field gradient corrected for the theoretical $(1 - \gamma_\infty)$ and interpret the discrepancy in terms of charge-transfer and overlap-covalency effects in the case of molecular solids or conduction electron contribution in the case of metals and alloys. If an agreement is obtained with the point charge model in the case of molecular solids, it is possible that the electronic effects are not important. However, this should be substantiated by independent experimental observations.

I.4.B Quadrupolar Interactions and (1-R)

The analysis[141] of hyperfine structure measurements on isolated atoms has produced striking evidences in favour of the Sternheimer shielding-antishielding factors. In order to evaluate Q from such data the field gradient, or equivalently the value of $\langle r^{-3} \rangle_q$, is calculated theoretically or deduced from other experimental quantities. The standard procedure has been to estimate a value of $\langle r^{-3} \rangle$ from the magnetic hyperfine structure or from fine structure. Using this $\langle r^{-3} \rangle$ value the uncorrected experimental quadrupole moment is obtained. In the case of np excited alkali atoms, for example,

$$Q_{\text{uncorrected}} = \frac{1.06395 \times 10^{-2}}{\langle r^{-3} \rangle_{np}} b_{3/2} \text{ (in barns)} \quad \text{(I.25)}$$

where the quadrupole interaction constant $b_{3/2}$ is given in MHz[141]

and $\langle r^{-3} \rangle_{np}$ in a.u. The Sternheimer correction is then applied to obtain the corrected spectroscopic Q as,

$$Q_{corrected} = Q_{uncorrected} / (1-R) \qquad (I.26)$$

Use of appropriate Sternheimer correction factors have been helpful in explaining several anomalous experimental results.

It has been observed[142] from hfs studies on ^{65}Cu in $3d^9 4s^2$ ($^2D_{3/2}$ or $^2D_{5/2}$) and $3d^{10}4p$ excited states that the estimated Q values differ by more than 40%. Sternheimer[74a] has shown that this difference can be quantitatively explained if the Sternheimer correction corresponding to 3d and 4p valence electrons are included in the interpretation. Murakawa[143] has studied 5d and/or 6p states of ^{139}La, ^{175}Lu and ^{201}Hg and estimated $R_Q(5d) = -0.4$ and $R_Q(6p) = -0.1$. Sternheimer[74a] has calculated $R_Q(5d) = -0.4$ for La which compares well with the experimental estimate. Childs[144] has measured the magnetic dipole and quadrupole coupling constants for 4f and 5d valence electrons from the hyperfine structure of ^{159}Tb in $4f^8 5d6s^2$ state. Similar to the case in ^{65}Cu, Sternheimer[74b] has shown that the experimental ratio of the coupling constants can be quantitatively attributed to the differential Sternheimer shielding for 5d and 4f electrons. The experimental studies on several np excited state alkali metal atoms have also shown[145] similar evidences. Belin and Svanberg[145j] have shown

that the quadrupole moments derived from the experimental quadrupole coupling factors for np $^2P_{3/2}$ (n = 5,6,7,8) sequence of ^{87}Rb shows a decreasing trend. The application of Sternheimer correction factor,[74b] R (np), in the sequence leads to a more consistent value of 0.13 b for all the cases studied.

Svanberg[145k] has similarly found that Q(^{39}K) corrected for Sternheimer shielding factor in np $^2P_{3/2}$ (n = 4,5,6) sequence leads to a more consistent value of 0.059 b as against the uncorrected values of 0.82, 0.85 and 0.86 respectively. From a comparison between Q values derived from hyperfine structure[146] of muonic $^{93}_{41}$Nb with the hfs measurements on $4d^4 5s$ and $4d^3 5s^2$ states, Buttgenbach and Dicke[147] have estimated $R_{4d} \sim -0.123$.

In the calculations of nuclear quadrupole moments from the atomic hfs data according to the semiempirical method, (e.g., in ^{65}Cu, ^{39}K, ^{87}Rb, and ^{93}Nb) no correction is applied to the magnetic dipole interaction (a/μ). Lindgren[71] has shown that such corrections are important for nd excited states of Rb. When $\langle r^{-3} \rangle$ is determined ab initio, the L=0 terms should be included in the calculations of R. In the semi-empirical procedure, however, these contributions are already contained in a/μ. Correlation effects should be also considered since they need not be the same for magnetic dipole

and electric quadrupole interactions. Thus, the apparent agreement between the quadrupole moments of $^{7}Li(2p)$ obtained from Sternheimer semi-empirical method and the calculation of Lindgren and coworkers[71] is due to the accidental cancellation of polarization effect on the magnetic interaction with the net correlation effect. In the case of $^{23}Na(^{3}P)$ these secondary effects are negligible and one expects the same to hold good for np states of heavier alkali metal atoms.

The Mössbauer experiments on the rare earth compounds[148] have predicted R = 0.1-0.3 for tripositive rare earth ions which compares well with the theoretical values of ∿0.15 obtained using Sternheimer method.

Dunlap, Kalvius and Shenoy[149] have presented a clear evidence of R for 5f electron from their Mössbauer quadrupole splitting studies on uranyl and neptunyl compounds. These authors have assumed that the difference in quadrupole splitting in the two cases should correspond to $(1 - R_{5f}) \langle r^{-3} \rangle_{5f}$ where $\langle r^{-3} \rangle_{5f}$ is derived from the relativistic HF wave functions for Np^{6+}. Their estimated R_{5f} value is +0.32. On the basis of the known values for R this value appears to be high.

I.4.C Hexadecapole Interactions

In a few recent experiments the electric hexadecapole interaction has been measured in solids[150a-c] and in the cases

of free atoms[150d,e] namely Ho and Es. Sternheimer[8] has calculated R_H and η_∞ and found that the hexadecapole polarization is more significant than the quadrupole case. The hexadecapole moment obtained for Ho has been corrected[8d] for the hexadecapole shielding effect $(1 - R_H)$. Theoretical calculations of η_∞ and R_H are however available in a very few cases.

I.4.D Shielding Factors $(1 - \sigma_2)$ and $(1 - \sigma_{nl})$ to the Crystalline Electric Field

The evidence for the shielding factor $(1 - \sigma_2)$ to the static crystalline electric field at the valence electron site has been obtained as a ratio of $\frac{1 - \gamma_\infty}{1 - \sigma_2}$ for several effect[148] nuclear alignment[151] and a combination[152] of electron paramagnetic resonance and optical spectroscopy experiments. These values are in reasonably good agreement with the theoretically calculated ratio. Pelzl[153] has analysed the available hyperfine interaction data on rare earth metals and concluded that $1 - \gamma_\infty$, and σ_2 increase with respect to the free ionic values.

Novakov and Hollander[154] have measured the splittings of $p_{3/2}$ atomic core levels caused by internal electric field gradients in the compounds of Th, U, Pu and Au by means of photoelectron-spectroscopy. Gupta and Sen[155] have shown that the measured splittings in $5p_{3/2}$ and $4p_{3/2}$ core levels can be qualitatively explained as due to the differential Sternheimer shielding $(1 - \sigma_{np})$ at 4p and 5p sites respectively. Their

estimate of the ratio of splitting is 1.7 for Au ($5d^{10}6s^{1}$) and 1.6 for Au ($5d^{10}6p^{1}$) which compares favourably with the measured value of ~ 2 in gold compounds.

I.4.E Shielding Factor $(1 - R_\theta)$ for Atomic Quadrupole Moments

Sternheimer[13] has shown that the significantly smaller values of atomic quadrupole moments measured on $np^5(n+1)s$ configuration of rare gases by atomic beams involving magnetic and electric field gradients can be quantitatively explained as arising due to the shielding effects (R_θ) of $(n+1)s \rightarrow d$ polarization caused by the hole in np shell.

I.5 Scope of the Present Work

In overall, it appears that there is overwhelming experimental evidence in favour of the Sternheimer polarization effects especially those corresponding to the quadrupole interaction. The experiments on hexadecapole interactions are presently being carried out in various laboratories and it is expected that similar polarization effects will be exhibited in these cases as well. An accurate knowledge of these shielding-antishielding factors is therefore extremely important in the interpretation of the experimental data. Accordingly, we have investigated in this thesis the Sternheimer shielding-antishielding factors of a variety of atoms and ions

using consistently one type of wave function, namely, the Hartree-Fock-Slater wave function.[41] The consistent use of this type of wave function enables us to compare all the results on various systems with some significance.

The present thesis is divided into seven chapters:

In Chapter II, we give the details of the method of calculations adopted by us. The procedure of generating Hartree-Fock-Slater (HFS) wave functions for free ions, and ions in crystal using Watson model are given. The Sternheimer perturbation-numerical approach is discussed and the expressions for various shielding-antishielding factors as given by Sternheimer presented.

In Chapter III we present the results of our calculation of α_q and γ_∞, for several free ions and ions in crystals. Estimates of relativistic and crystalline distortion effects on γ_∞ (and α_q) have been made. We have also studied the effect of crystalline distortion on σ_2 and R in the case of Ce^{3+}.

In Chapter IV we report our results of γ_∞ and R for several ions of interest in Mössbauer spectroscopy. The effect of crystal distortions on γ_∞ and R for $3d^6$ ions have been studied by correlating these values with the position of the outermost maximum in the total radial electron density distribution function and the experimental data on e^2qQ for several iron

compounds have been reanalysed using most reliable value of γ_∞ and R and a new range of values for Q (^{57m}Fe) has been derived.

In Chapter V we present our calculations on the hexadecapole antishielding factor η_∞ for several ions. Estimates of crystalline distortions on have been made in the cases of a few actinide ions. We also report our preliminary results on the second-order quadrupolar effect in the cases of a few actinide ions. A large value of $(1 - \eta_\infty)$ aided with the other favourable parameters such as nuclear quadrupole moment, natural abundance, and NMR sensitivity has been considered as a criterion to identify those nuclei which would be possible candidates for studying nuclear hexadecapole interaction.

In Chapter VI we present the results of our calculations on atomic shielding factor R_θ for np(n+1)s excited state atoms of C, Si, Ge, Sn, and Pb.

Chapter VII summarizes the various conclusions obtained in the present work. The scope of future work in this area is also outlined.

CHAPTER II

Sternheimer Perturbation-Numerical Method and the Calculation of Shielding-Antishielding Factors

CHAPTER II

Sternheimer Perturbation-Numerical Method and the Calculation of Shielding-Antishielding Factors

II.1 Introduction

The polarizabilities and shielding-antishielding factors calculated from Hartree wave functions have been found[5] to be significantly larger in magnitude than those calculated from Hartree-Fock (HF) wave functions. The marked sensitivity of these one-electron properties to the treatment of exchange potential in the zeroth-order wave functions attracted us to test the merits and demerits of Slater exchange approximation,[156] according to which the nonlocal HF exchange potential is replaced by

$$V_X = - 6\alpha \{ (3/8\pi)\ \rho^{1/3} \} \qquad \text{(II.1)}$$

One definite advantage in using Slater approximation[156] is that it reduces the computational time relative to the HF case by an order of magnitude without significantly affecting the accuracy in the wave functions. In passing we may mention that the Slater approximation provides the only feasible ab initio method for studying one-electron properties of large

molecules and metals.[157] Saxena and Narasimhan[158] have shown that the diamagnetic susceptibility and nuclear magnetic shielding factors for the closed-shell atoms and ions calculated from Hartree-Fock-Slater[159] (HFS) wave functions corresponding to $\alpha = 1$ in eq. (II.1) are in excellent agreement with HF calculations.[160] One might therefore expect that the HFS wave functions would be suitable for the study of polarizabilities.

As regards the choice of the method used for calculating the first-order perturbations, we have found from the survey of reported results that using the zeroth-order wave functions of similar accuracy, the UCHF method due to Sternheimer gives the values of the quadrupolar polarization effects which compare most favourably with the CHF methods. For example, Lahiri and Mukherji[24c,d] have noticed that the CHF results of α_q and γ_∞ do not differ as much as α_d and β_∞ when a comparison is made with the other uncoupled calculations. Sternheimer[161] has found that the CHF values of α_q for up to Argon isoelectronic sequence differ from the results obtained from the perturbation-numerical calculations by $\sim$ 5-15%. In recent LCMBPT and DE calculations[26,67] on γ_∞ it has been concluded that the coupling effects amount to $\sim$15% in most of the cases. The Sternheimer method therefore is an attractive substitute for the more difficult coupled calculations for heavier systems,

as far as quadrupolar polarization is concerned. Further, several reported calculations of α_q, γ_∞ , R and σ_2 have been generally based on UCHF methods using Hartree or Hartree-Fock wave functions. A comparison of HF and HFS wave functions corresponding to the zeroth-order is more justified, if a method of similar accuracy is used to obtain the first-order perturbed wave functions in both the cases. We have therefore chosen the HFS wave functions in our present study and have adopted the Sternheimer perturbation-numerical method to generate the appropriate quadrupolar and hexadecapolar polarizations in the case of a large number of free atoms and ions with the motivation of studying the Sternheimer shielding-antishielding factors in detail. We would like to make three comments which are related to the work embodied in this thesis.

(1) Since the HFS wave functions for all the neutral atoms are already available and since these can be generated with much less computational effort for most of the free ions of interest, it is worthwhile to compare the HFS polarizabilities and shielding results with the corresponding HF results and thus evaluate the merits of Slater exchange approximation in this context.

(2) The inter-shell and intra-shell consistency effects can be included by using the same moment, and external-charge perturbed wave functions, if desired.

(3) Due to a consistent choice of the zeroth-order wave functions, which are already known to be good approximations to the HF wave functions, coupled with the use of an accurate UCHF perturbation-numerical method, the general trends obtained from the study of a large number of atoms and ions are expected to be valid even in the case of more refined calculations.

In the previous chapters we have already referred to the pioneering work of Sternheimer who made calculations of α_q, γ_∞, η_∞, σ_2, R, R_H and R_θ for a variety of systems. Subsequently, calculations by others have also been reported. All these available values have been compared with the present calculations, in the following chapters. A fairly recent compilation of γ_∞ and R factors for the ground state atoms and ions has been given by Lucken.[162]

The experimental estimates of $(1 - \gamma_\infty)$ in highly ionic solids for the positive ions come out to be larger than the theoretical values whereas in the case of negative ions the estimated values are substantially lower than the theoretical counterparts. It is very likely that $(1 - \gamma_\infty)$ values themselves get substantially modified due to the changes in the outer orbitals of the ion in solids. To our knowledge, there have been only two calculations[29c,163] reported in the literature, both of which use the variation-perturbation method of Das and

Bersohn[27] and attempt to estimate the effects of crystalline potential on polarizabilities and shielding-antishielding factors. We therefore thought it worthwhile to calculate α_q, γ_∞, σ_2 and R for several ions using the Sternheimer perturbation-numerical method and HFS wave functions with Watson model[164] to simulate the ion within a crystal.

II.2 Calculation of Zeroth-order Wave-functions

II.2.A Free Ion

The Schrodinger equation for a one-electron orbital χ_i^o in an atom can be written as (energy in Rydbergs)

$$(-\nabla_i^2 + V_C + V_X) \quad \chi_i^o = E_i \chi_i^o \qquad \text{(II.2)}$$

where V_C is the Coulomb potential energy, i.e., the potential energy of an electron in the field of the nucleus and of all electrons, including itself. V_X is the exchange potential which can be thought of as a correction for the self-interaction energy of the electron. In the Hartree-Fock approximation,

$$V_{XHF} = E_i - V_C + (\nabla_i^2 \chi_i^o)/\chi_i^o \qquad \text{(II.3)}$$

In the theory of free-electron gas obeying Fermi statistics, Slater[156a] has shown that the exchange potential can be written as

$$V_{Xgas} = -8 F (n) \{(3/8\pi)\}^{1/3} \qquad \text{(II.4)}$$

where ρ is the total electron density, and $F(\eta)$ is given by

$$F(\eta) = \frac{1}{2} + \frac{1 - \eta^2}{4\eta} \ln \frac{1 + \eta}{1 - \eta}, \qquad \text{(II.5)}$$

where η is the ratio of the momentum of the electron to its momentum at the Fermi energy. In Slater's exchange approximation[156] to the atomic systems, $F(\eta)$ is taken as 3/4, which is the average value of $F(\eta)$ over all electrons in a Fermi gas at the absolute zero of temperature. The exchange potential then becomes,

$$V_{XS} = -6\{(3/8\pi)\rho\}^{1/3} \qquad \text{(II.6)}$$

The χ_i^o's obtained from eq. (II.2) using eq. (II.6) for V_X are called Hartree-Fock-Slater (HFS) wave functions.

We have used the computer program of Herman-Skillman (HS)[159] to generate the free-ion wave functions required in the present thesis over 441-point mesh.

II.2.B Crystal Ion

The crystal ion wave functions have been generated by including an extra stabilizing potential V shown in Fig. II.1 which is due to Watson.[164] In Watson model, the ion with an electric charge n_{ion}, is surrounded by a hollow sphere of radius r_{ion} and carries a uniformly distributed charge of $-n_{ion}$ units. The Coulomb potential V_C in eq. (II.2) then becomes;

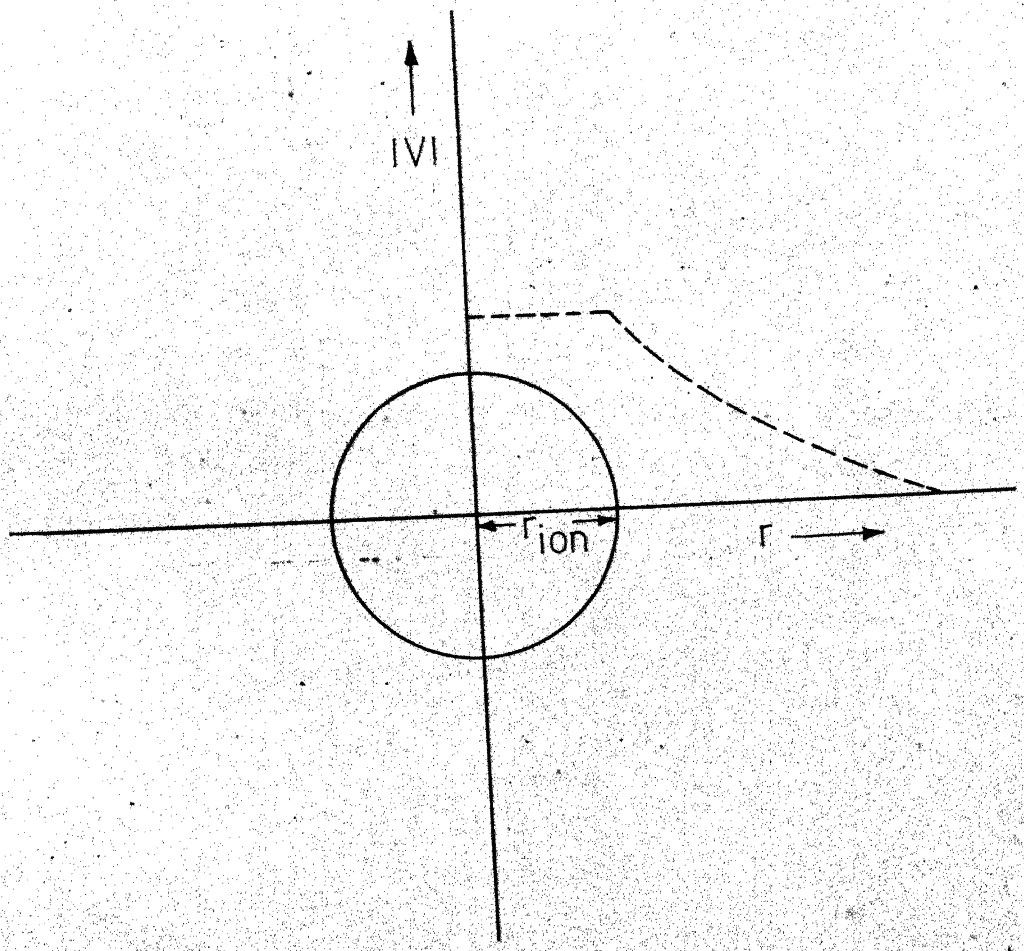

Fig.II.1 - The potential due to the superimposed charged hollow sphere with radius r_{ion} as a function of radial distance r.

$$V'_C = V_C + \frac{2n}{r_{ion}} \qquad \text{(II.7)}$$

for $r \leq r_{ion}$ and

$$V'_C = V_C + \frac{2n}{r} \qquad \text{(II.8)}$$

for $r \geq r_{ion}$, respectively.

Throughout this work, r_{ion} has been taken from Pauling's[165] table of ionic radii, except in the cases of Fr^+, Ra^{2+}, Ac^{3+}, At^- and rare earths and actinides where Zachariasens values[166] have been used.

II.3 External Charge-Perturbed Inhomogeneous Differential Equation: Quadrupolar Perturbation

In the following paragraphs we shall present the method of computation adopted by us which is essentially the same as that prescribed by Sternheimer[7b,11,74a] in his original papers.

The first-order perturbed Schrodinger equation can be written as

$$(H_o - E_o)\,\chi_i^1 = (E_1 - H_1)\,\chi_i^o \qquad \text{(II.9)}$$

where χ_i^o represents the first order perturbation of the unperturbed wave function χ_i^o; H_o and E_o correspond to the unperturbed Hamiltonian and eigenfunction for the unperturbed state n . The unperturbed wave function can be written as

$$\chi_i^o = \frac{u_o(nl)}{r} Y_l^m \qquad \text{(II.10)}$$

where $u_o(nl)$ is r times the radial part of the unperturbed wave function. $u_o(nl)$ is normalized according to

$$\int_o^\infty u_o^2(nl)\, dr = 1 \qquad \text{(II.11)}$$

The crystal potential at the ionic site can be written[11c]

$$V_{crystal} = \sum_{n,m} A_n^m r^n Y_n^m \qquad \text{(II.12a)}$$

where A_n^m are the constants characteristic of the ionic distribution in the lattice and Y_n^m is the normalized spherical harmonic. The term corresponding to n=2, and m=0, is the quadrupolar potential given by

$$H_1 = -A_2^o r^2 Y_2^o \qquad \text{(II.12b)}$$

Under the influence of this perturbing field the spherical shells get polarized according to,

$$\chi_i^o(l=0) \rightarrow N_o\{ \chi_i^o(l=0) + \chi_i^1 (l' = 2)\}$$

$$\chi_i^o(l=1) \rightarrow N_1 \{\chi_i^o(l=1) + \chi_i^1 (l' = 1) + \chi_i^1 (l' = 3)\}$$

$$\chi_i^o(l'=l) \rightarrow N_1 \{\chi_i^o(l) + \chi_i^1 (l' = l) + \chi_i^1 (l' = l + 2) + \chi_i^1 (l' = l - 2)\} \qquad \text{(II.13)}$$

The part of the polarization characterized by the same l value as the unperturbed wave function is called the radial perturbation and those with $\Delta l = \pm 2$ are called angular perturbations.

The perturbed wave function can be separated into radial angular variable as

$$\chi_i^l \ (l = l') = \frac{u_l' \ (nl \to l')}{r} \ Y_{l'}^m \qquad \text{(II.14)}$$

Substituting eq. (II.10) and (II.14) in eq. (II.9) and separating the variables, u_l' can be obtained from the following inhomogeneous radial Schrodinger equation

$$\{ - \frac{d^2}{dr^2} + \frac{l'(l'+1)}{r^2} + V_o - E_o \} \ u_l' \ (nl \to l')$$

$$= u_o(nl) \{ r^2 - \langle r^2 \rangle_{nl} \ \delta_{ll'} \} \qquad \text{(II.15)}$$

where $V_o = V_{XS} + V_C$ and $u_l'(nl \to l')$ represents r times the perturbed radial wave function corresponding to the polarization $(nl \to l')$. According to Sternheimer local approximation,

$$(V_C + V_{XS} - E_o) - \frac{1}{u_o} \frac{d^2 u_o}{dr^2} - \frac{l(l+1)}{r^2} \qquad \text{(II.16)}$$

We have solved the finite difference equivalent of eq. (II.15) by writing eq. (II.16) as

$$V_o(r) - E_o = \frac{u_o'(r+\delta) - 2.u_o'(r) + u_o'(r-\delta)}{\delta^2 \ u_o'(r)} - \frac{l(l+1)}{r^2} \qquad \text{(II.17)}$$

and substituting in eq. (II.15),

$$u_l'(r+\delta) = u_l'(r) \{ 2. + \delta^2 \ \frac{l'(l'+1) - l(l+1)}{r^2}$$

$$+ \frac{u_o'(r+\delta) - 2u_o'(r) + u_o'(r-\delta)}{u_o'(r)} \}$$

$$- u_l'(r-\delta) - u_o'(r) \ \delta^2 \{ r^2 - \langle r^2 \rangle_{nl} \delta_{ll'} \} \qquad \text{(II.18)}$$

We have used this form for the outward integration which requires the knowledge of the unperturbed wave functions and the perturbed wave functions at two initial points to start the direct solution. The two boundary conditions $u_1'(0)$ and $u_1'(\infty) = 0$ define the solution uniquely. The starting slope of the solution is changed in an iterative way till the solution at large r decays exponentially. The behaviour of the solution for the first few points on the r mesh when fed in the computer results in a faster convergence. Three to four iterations are generally required to achieve convergence. For $\Delta l = +2$ the behaviour of $u_1'(r \to 0)$ has been taken as r^{l+3} whereas for $\Delta l = -2$ and 0, it is taken as r^{l-1}.

For large r the inward integration has been started with a multiplicative constant in $u_1'(r)$ according to the relation

$$u_1'(r+\delta) = u_1'(r) \exp[-\{N(r)\}^{1/2} \delta] \qquad \text{(II.19)}$$

where

$$N(r) = \frac{u_o'(r+\delta) - 2u_o'(r) + u_o'(r-\delta)}{2\, u_o'(r)} + \frac{l'(l'+1) - l(l+1)}{r^2} - \frac{r u_o'(r)}{u_1'(r)} \qquad \text{(II.20)}$$

In eq. (II.19) to start with we have taken $N = -E_o$. The multiplicative constant is varied till the boundary condition at r=0 is bracketed within a desired limit.

We have employed both the inward and outward integrations and matched them iteratively near the outer peak of the unperturbed wave functions for all the excitations.

II.4 Moment-Perturbed Inhomogeneous Differential Equation: Quadrupolar Perturbation

In an alternative approach the source of perturbation is the nuclear moment itself.

$$H_1 = -Q \frac{(3\cos^2\theta - 1)}{2r^3} \qquad \text{(II.21)}$$

The first-order perturbed differential equation takes the form,

$$\left\{ \frac{-d^2}{dr^2} + \frac{l'(l'+1)}{r^2} + V_o - E_o \right\} u_1 = u_o \left\{ \frac{1}{r^3} - \left\langle \frac{1}{r^3} \right\rangle_{nl} \delta_{ll'} \right\} \qquad \text{(II.22)}$$

which has the equivalent difference equation as

$$u_1(r+\delta) = u_1(r) \left\{ 2. + \delta^2 \frac{l'(l'+1) - l(l+1)}{r^2} + \frac{u_o(r+\delta) - 2u_o(r) + u_o(r-\delta)}{u_o(r)} \right\}$$

$$- u_1(r-\delta) - u_o(r) (\delta)^2 \left\{ \frac{1}{r} - \left\langle \frac{1}{r^3} \right\rangle_{nl} \delta_{ll'} \right\} \qquad \text{(II.23)}$$

The method of solving the moment-perturbed equation is exactly the same as the external charge-perturbed case, except that the boundary condition near the nucleus is different. Thus, in the case of $s \rightarrow d$ type excitation

$$u_1(0) = \frac{a_o}{6} \qquad \text{(II.24)}$$

where

$$a_o = \left\{ \frac{u_o(ns)}{r} \right\}_{r \to 0} \qquad \text{(II.25)}$$

In the case of np→f, $u_1(0)$ is zero and near the origin it behaves as

$$u_1 \text{ (r small)} = \left\{ \frac{b_o r}{12} \right\} \qquad \text{(II.26)}$$

where

$$b_o = \left\{ \frac{u_o(np)}{r^2} \right\}_{r \to 0} \qquad \text{(II.27)}$$

For other excitations $u_1(0) = 0$ and its behaviour near the nucleus has been similarly obtained from the appropriate logarithmic series. It should be noted that the constants a_o, b_o, are calculated in the Herman-Skillman routine and then recalculated in the independent perturbation program to check that the wave functions have been correctly transferred.

The inward integration in the case of $u_1(nd \to s)$ perturbation was very unstable and this is one of the reasons why we have chosen to match inward and outward integrations for the angular cases as well.

II.5 Moment-Perturbed Inhomogeneous Differential Equation: Hexadecapolar Perturbation

In the case of hexadecapole moment-perturbed wave function $u_{1,H}$ the inhomogeneous equation can be written as,

$$\{-\frac{d^2}{dr^2} + \frac{l'(l'+1)}{r^2} + V_o - E_o\} u_{l,H} = u_o\{\frac{1}{r^5} - \langle \frac{1}{r^5} \rangle_{nl}\} \delta_{ll'} \quad \text{(II.28)}$$

and only nd d and nf f perturbations have been considered. For nd d excitation, the boundary condition at r=0 is given by c/6, where c is the coefficient of r^3 in the power series expansion of nd wave function near the nucleus.

II.6 Method for Integral Evaluation

The 'presentation mesh' of HS has been used as the 'integration mesh' to perform the block-wise integration through adjacent intervals[167] according to

$$\int_{x=a}^{x=b} F(X)\, dx = \frac{1}{2}\,\delta\Big[\sum_{j=1}^{J}\{F(X_{j+1}) + F(X_j)\} - \frac{1}{12}\sum_{j=1}^{J}\{\Delta^2 F(X_{j+1}) + \Delta^2 F(X_j)\} + \frac{11}{720}\sum_{j=1}^{J}\{\Delta^4 F(X_{j+1}) + \Delta^4(X_j)\}\Big] \quad \text{(II.29)}$$

In order to calculate the differences up to fourth it is necessary, that the two extra entries at both the ends of each block are included. This sequence of entries gives J=41 points in the first block and J=44 in the rest. This is achieved before the integration is started and the final result is of course the sum over all the blocks.

Table II.1: The various coefficients pertaining to the quadrupolar polarization, obtained as a result of integration over angular variables and summation over magnetic substates

$C(nl \to l;\ l_e)$	$c(nl \to l')$	$C(L_1)$	$C(L_2)$	$C(L_3)$
(ns→d; p)	8/5	4/3(1)		
(np→p; p)	48/25	4(0)	4/25(2)	
(np→f; p)	72/25	36/25(2)		
(nd→d; p)	16/7	4/3(1)	12/49(3)	
(nd→g; p)	144/35	72/49(3)		
(nf→h; p)	16/3	40/27(4)		
(nf→f; p)	224/75	24/25(2)	8/27(4)	
(ns→d; d)		4/5(2)		
(np→p; d)		28/25(1)	36(175(3)	
(np→f; d)		12/25(1)	144/175(3)	
(nd→d; d)		4(0)	-12/49(2)	16/49(4)
(nd→g; d)		144/245(2)	40/49(4)	
(nf→h; d)		40/63(3)	80/99(5)	
(nf→f; d)		48/25(1)	-88/225(3)	40/99(5)
(ns→d; f)		4/7(3)		
(np→p; f)		108/175(2)	4/21(4)	
(np→f; f)		72/175(2)	4/7(4)	
(nd→g; f)		12/49(1)	24/49(3)	300/539(5)
(nd→d; f)		72/49(1)	-44/147(3)	500/1617(5)
(nf→f; f)		4(0)	76/225(2)	-4/11(4), 500/1287(6)
(nf→h; f)		20/63(2)	40/77(4)	700/1287(6)

electric field at the valence electron site will be referred to as σ_2^D and is given by,

$$\sigma_2^D(nl\to l') = c(nl\to l') \frac{\int_0^\infty w^2(n_e l_e)\, f(r)\, dr}{\langle r^2\rangle_{n_e l_e}} \qquad \text{(II.34)}$$

where $f(r) = \frac{1}{r^3}\int_0^r u_o\, u_1'\, r'^2 dr' + r^2 \int_r^\infty u_o u_1' r'^{-3} dr'$ (II.35)

and $w(n_e l_e)$ denotes the unperturbed valence electron wave function. The corresponding exchange contribution will be referred to as σ_2^E and is given by

$$\sigma_2^E(nl\to l'; n_e l_e; L) = -C(nl\to l'; L) \frac{K(nl\ l'; L)}{\langle r^2\rangle_{n_e l_e}} \qquad \text{(II.36)}$$

where $K = \int_0^\infty u_o(nl)\, w(n_e l_e)\, G(r)\, dr$

with $G = \frac{1}{r^{L+1}} \int_0^\infty u_1'(nl\to l')\, w(n_e l_e)\, r'^{L}\, dr'$

$$+ r^L \int_r^\infty u_1'(nl\to l')\, w(n_e l_e)\, r'^{-L-1}\, dr' \qquad \text{(II.37)}$$

The coefficients $C(nl\ l'; n_e l_e; L)$ are given by,

$$C(nl\to l'; n_e l_e; L) = \frac{4 \sum_{m=-l}^{l} C^{(2)}(lm, l'm)\, C^{(L)}(lm, l_e m_e)\, C^{(L)}(l'm; l_e m_e)}{C^{(2)}(l_e m_e; l_e m_e)} \qquad \text{(II.38)}$$

The integers L correspond to the expression in spherical harmonics of r_{12}^{-1} in the exchange interaction. The coefficients

$C(nl \to l'; n_e l_e; L)$ have been compiled in Table II.1.

The total σ_2 is given by

$$\sigma_2 = \sum_{nl} \{ \sigma_2^D(nl \to l') + \sum_L \sigma_2^E (nl \to l'; n_e l_e, L)\} \qquad (II.39)$$

II.7.B Calculation of γ_∞ and R from the Moment-Perturbed Equation

From the quadrupole moment perturbed wave function $u_1(nl \to l)$ the γ_∞ can be expressed as,

$$\gamma_\infty = \sum_{nl} c(nl \to l') \int_0^\infty u_1(nl \to l')\, u_o(nl)\, r^2 dr \qquad (II.40)$$

Denoting the valence electron wave functions by $w(n_e l_e)$, the direct contribution to R, by $(nl \to l')$ excitation of the core orbital is given by

$$R_D(nl \to l';\ n_e l_e) = \frac{\int_0^\infty \gamma(nl \to l'; r)\{ w(n_e l_e)\}^2 r^{-3} dr}{\langle r^{-3} \rangle_{n_e l_e}} \qquad (II.41)$$

where

$$\gamma(nl \to l'; r) = \frac{1}{Q} \{ \int_0^r Q_i(nl \to l')\, dr' + r^5 \int_r^\infty Q_i(nl \to l') r'^{-5} dr' \} \qquad (II.42)$$

with $Q_i(nl \to l') = c(nl \to l')\, Q\, u(nl)\, u_1(nl \to l') r^2 \qquad (II.43)$

which gives the direct contribution to the density of the induced moment corresponding to $(nl \to l')$ excitation. The contribution to R, by the exchange term arising from $(nl \to l')$ is given by

$$R_E(nl\to l';n_e l_e;L) = -\frac{C(nl\to l';n_e l_e;L)}{\langle r^{-3}\rangle_{n_e l_e}} \int_0^\infty u_1(nl)w(n_e l_e)g\,dr \qquad (II.44)$$

where $g_L(nl\to l';n_e l_e) = \frac{1}{r^{L+1}} \int_0^r u_1(nl\to l')w(n_e l_e)\, r'^L\, dr'$

$$+ r^2 \int_r^\infty u_1(nl\to l')w(n_e l_e)\, r^{L-1}\, dr' \qquad (II.45)$$

the net R is given by

$$R = \sum_{nl} \{ R_D(nl\to l';\ n_e l_e) + \sum_L R_E(nl\to l';\ n_e l_e, L) \} \qquad (II.46)$$

The constants $C(nl\to l';n_e l_e;L)$ are given in Table II.1.

II.7.C Calculation of η_∞ from the Moment-Perturbed Equation

The hexadecapole antishielding factor η_∞ has been calculated as,

$$= \sum_{nd} \eta_\infty(nd\to d) + \sum_{nf} \eta_\infty(nf\to f) \qquad (II.47)$$

where, $$(nd\to d) = \frac{80}{63} \int_0^\infty u'_o(nd)\, u'_{1,H}(nd\to d)\, r^4\, dr$$

and $$(nf\to f) = \frac{112}{99} \int_0^\infty u'_o(nf)\, u'_{1,H}(nf\to f)\, r^4 dr \qquad (II.48)$$

The net angular contribution to η_∞ has been estimated by using the approximation

$$\frac{\gamma_{\infty,ang}}{\eta_{\infty,ang}} = \frac{9}{5} \qquad (II.49)$$

where γ_{∞} , ang are calculated from moment-perturbed equation (II.22).

II.8 Typical Results of Calculations

For illustration purposes we present here a few typical numerical and graphical results. Thus, our numerical values of $u_1(5p \to p)$ for Tm^{3+} have been given in Table II.2. This function has been represented graphically along with $4 \times u_o(5p)$ in Fig. II.2. The free ion HFS wave functions for Tm^{3+} were generated in $\sim 1\frac{1}{2}$ min and single iteration in the case of $u_1(5p \to p)$ took $\sim$2 sec in our IBM 7044/1401 computer system at the Indian Institute of Technology, Kanpur. We have given in Fig. II.3 the plots of $u_{1,H}(5d \to d)$ along with $2500 \times u_o(5d)$ in the case of Au^+.

II.9 Computer Programs

The computer listings of the following three main programs used in the present work have been given in Appendix I: (a) the free and crystal ion HFS wave function program, (b) γ_{∞} and R routine, and (c) polynomial fitting program.

The quantitative estimates of the effects due to crystal distortions on shielding-antishielding factors have been obtained by expressing these in terms of suitable polynomial series in r_{ion}, $\langle r^{-3} \rangle$ and ρ_m, the position of the outermost peak

Table II.2: The moment perturbed radial wave functions $u_1(5p \rightarrow p)$ as a function of r (in a.u.) for Tm^{3+} ion.

r (a.u.)	$u_1(5p \rightarrow p)$	r (a.u.)	$u_1(5p \rightarrow p)$
0.0000	0.0000	1.2563	11.1452
0.0048	1.5539	1.5671	20.4203
0.0097	2.6399	1.8779	21.7037
0.0016	3.1168	2.1887	18.9976
0.0019	3.0298	2.4996	15.0938
0.0183	3.0932	2.5341	14.6514
0.0280	1.7986	3.1558	7.7172
0.0378	-0.5717	3.7774	3.5415
0.0475	-3.2644	4.3991	1.4893
0.0572	-5.7451	5.0208	0.5955
0.0583	-5.9917	5.0898	0.5375
0.0777	-9.0211	6.3331	0.0724
0.0971	-9.1619	7.5765	0.0087
0.1166	-6.8807	8.8198	0.0009
0.1360	-3.1008	10.0631	0.0001
0.1381	-2.6295		
0.1770	5.8894		
0.2158	11.9292		
0.2547	13.9431		
0.2936	12.2773		
0.2979	11.9121		
0.3756	2.1018		
0.4533	-9.0335		
0.5310	-17.0507		
0.6087	-20.8103		
0.6173	-20.9793		
0.7727	-18.1110		
0.9282	-8.6681		
1.0836	1.7156		
1.2390	10.3431		

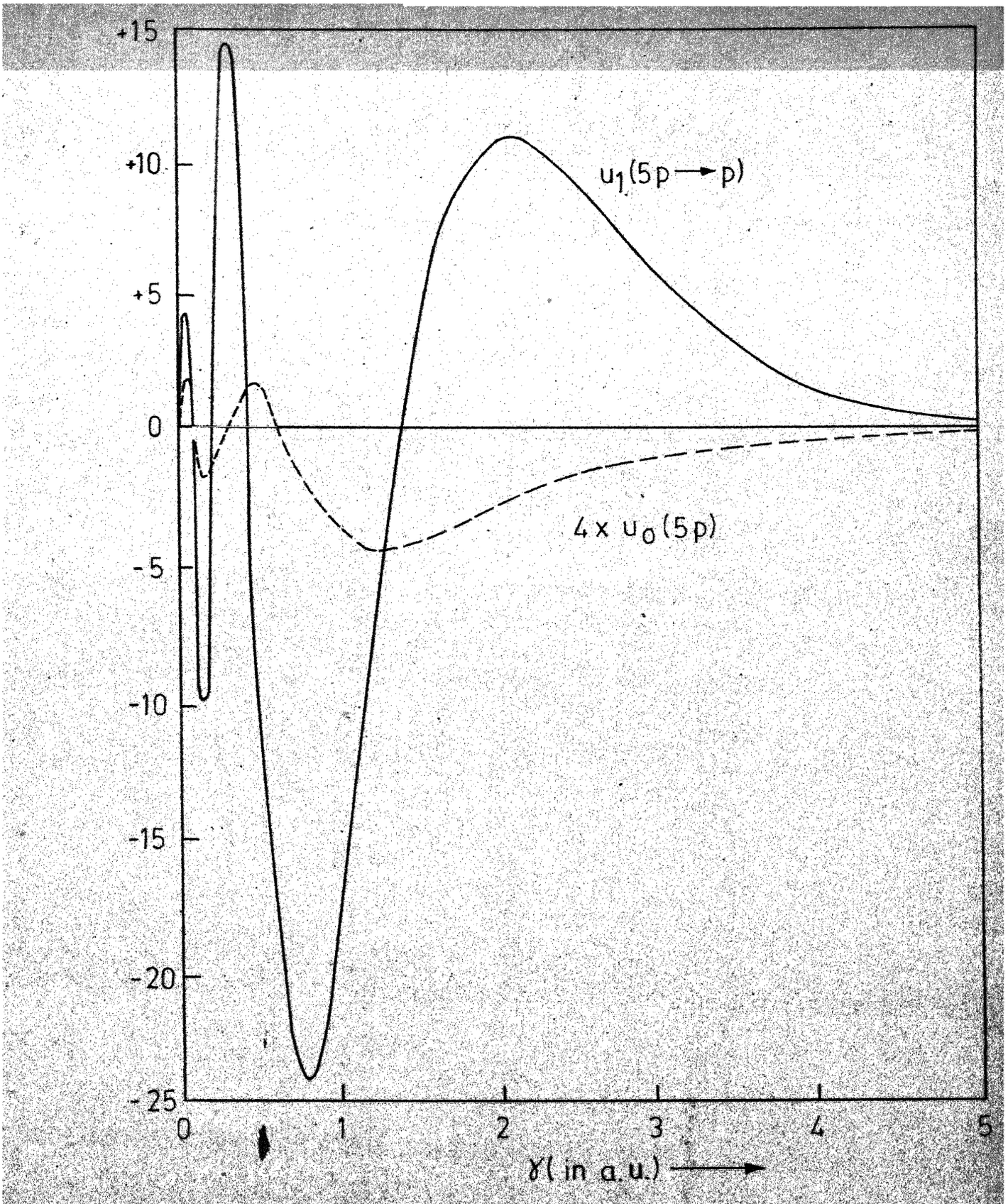

Fig. II. 2 - The plot of Quadrupole moment - perturbed radial wav function $u_1(5p \longrightarrow p)$ along with the $4 \times u_0(5p)$ wave function for Tm^{3+} ion.

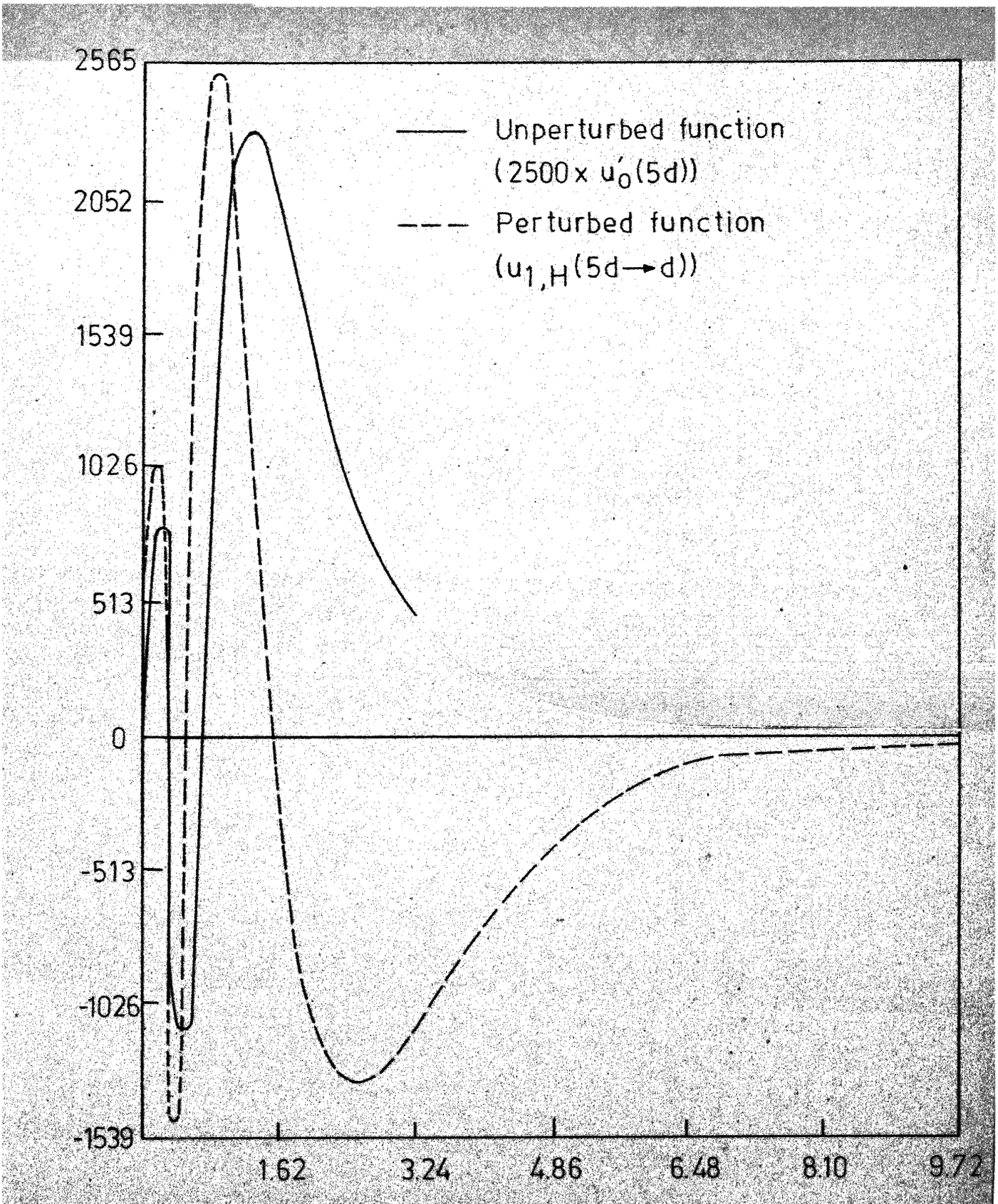

Fig. II.3 - Perturbed wave function $u_{1,H}(5d \rightarrow d)$ and 2500 time unperturbed 5d function $u_0(5d)$ for Au^+ ion.

in the total radial charge density distribution of the atom or ion. The various polynomial fittings have been carried out by using standard method of minimizing the average percentage error via normal equations.[168] The listing of the computer program for this purpose is given in Appendix I under polynomial fitting program. The routines corresponding to (i) the inward and outward integration, (ii) the integrals, and (iii) the polynomial fitting have been developed by the author.

CHAPTER III

Sternheimer Quadrupole Shielding-Antishielding Factors for Several Closed Shell Ions, A Rare Earth Ion and Ions in Actinide Series: Estimates of Relativistic Effects and Crystalline Distortions

CHAPTER III

Sternheimer Quadrupole Shielding-Antishielding Factors for Several Closed Shell Ions, A Rare Earth Ion and Ions in Actinide Series: Estimates of Relativistic Effects and Crystalline Distortions*

III.1 Introduction

From a survey of the reported theoretical calculations till 1971, it became clear to us that extensive calculations of α_q and γ_∞ utilizing nonrelativistic HFS wave functions for free ions and ions in crystals represented by the Watson model,[164] adopting the Sternheimer perturbation-numerical method will serve the following two purposes:

(1) a comparison of our γ_∞ and α_q values with those of Feiock and Johnson[169] (FJ), who have used relativistic HFS wave functions and the uncoupled method similar to Sternheimer, would give an estimate of net relativistic-effects on and α_q, and γ_∞

---

* The work presented in this chapter has been published in the following papers:
(1) K. D. Sen and P. T. Narasimhan, Adv. Nucl. Quadrupole Res., 1, 277 (1974); (2) Phys. Rev. B (in press) (1976); (3) Phys. Rev. A (in press) (1976).

(2) a comparison of our free ion and ion in crystal values would give an approximate estimate of the changes brought about in γ_∞ and α_q due to the lattice potential.

The interpretation of nuclear quadrupole coupling data is generally based on eq. (I.5). It is therefore necessary to make estimates of the net relativistic and lattice potential effects on the shielding-antishielding parameters.

III.2 Results and Discussion

III.2.A γ_∞ and α_q for Closed-Shell Free Ions and Ions in Crystals

We have considered the following six sequences of closed-shell free ions isoelectronic with He, Ne, A, Kr, Xe, and Rn respectively,

(i) Li^+, Be^{2+}, B^{3+}, C^{4+}, N^{5+}, O^{6+};

(ii) F^-, Na^+, Mg^{2+}, Al^{3+}, Si^{4+}, P^{5+}, S^{6+};

(iii) Cl^-, K^+, Ca^{2+}, Sc^{3+}, Ti^{4+}, V^{5+}, Cr^{6+};

(iv) Br^-, Rb^+, Sr^{2+}, Yt^{3+}, Zr^{4+}, Nb^{5+}, Mo^{6+};

(v) I^-, Cs^+, Ba^{2+}, La^{3+}; and

(vi) At^-, Fr^+, Ra^{2+}, Ac^{3+}.

With the use of nonrelativistic HFS wave functions for these ions we have generated the external charge-perturbed wave functions and calculated γ_∞ and α_q according to the

method described in Chapter II. The calculated values of γ_∞ and α_q have been presented in Table III.1 and Table III.2 respectively. For purposes of comparison, the values calculated by FJ have been given in column 3 of these tables. As expected, our γ_∞ (or α_q) values in the case of lighter ions ($Z \leq 18$) are in excellent agreement with FJ calculations. For the heavier ions FJ values are consistently larger than the presently calculated values. Comparing the negative halogen ions in the two cases we have obtained the upper limit of the net relativistic effect on γ_∞ in each series. It has been found that the relativistic effects increase the nonrelativistic γ_∞ value by 7% for the ions up to Kr isoelectronic series. For Xe series this effect becomes as high as $\sim$19%.

The results of other available calculations of γ_∞ and α_q have been compiled in column 4 of Tables III.1 and III.2, respectively. Our values for the positive ions are in good agreement with those of Sternheimer and Lahiri and Mukherji (see the references appearing at the end of Table III.2), which are based on HF wave functions. For F^-, Cl^- and Br^- the present γ_∞ values are -41, -82 and -195 respectively which are significantly larger than the antishielding effect obtained from HF wave functions. It would be useful to modify the Slater exchange potential in the outer regions to make the wave functions more internal.

Table III.1*: Total γ_∞ values for the free ions and ions in crystals. The crystal ion values correspond to Pauling ionic radius.

	Free ion			Crystal Ion		
Ion	Present	Feiock and Johnson	Others	Present	Others	Experimental**
Li^+	0.261	0.257	0.256[a]; 0.248[c]; 0.247[d]; 0.248[e]; 0.257[i]	0.282	0.271[x]	+4.4, +0.5
Be^{2+}	0.187	0.185	0.185[a]; 0.189[b]; 0.181[c]; 0.180[d]; 0.186[i]	0.208	0.190[x]	
B^{3+}	0.146	0.145	0.145[a]; 0.142[c]; 0.142[d]; 0.147[f]; 0.145[i]	0.162		
C^{4+}	0.119	0.119	0.117[d]	0.131		
N^{5+}	0.101		0.099[d]	0.110		
O^{6+}	0.088			0.094		
O^{2-}			-429.4; -950.5[i]	-24.19	-28.22, -25.30 -33.90[g]; -9.056[x]	
F^-	-41.109	-42.190	-66.86, -23.22, -25.71, -21.11[g]; -22.53[h]; -23.03, -22.15; -22.12, -22.0[i]; -29.88[j]; -37.61[l]	-14.583	-10.62[x]	

Table III.1 (...Contd.)

Ion	Free ion			Crystal Ion		
	Present	Feiock and Johnson	Others	Present	Others	Experimental**
Na^{+}	-5.029	-5.072	-4.514[a]; -4.514, -4.505, -4.497[i]; -5.178[j]; -4.56[b,k]; -5.961[l]	-7.686	-4.747[x]	
Mg^{2+}	-3.320	-3.350	-3.038[i]; -3.485[j]; -3.898[l]			
Al^{3+}	-2.434	-2.462	-2.59[a]; -2.4[f]; -2.236[i]; -2.57[j]; -2.749[l]	-5.715	-3.217[x]	-4.9
Si^{4+}	-1.902	-1.927	-1.32[l]	-4.508		
P^{5+}	-1.550			-3.449		
S^{6+}	-1.302	-1.323		-2.594		
Si^{4-}				-131.99		
P^{3-}				-80.15		
S^{2-}			-197.1[x]	-54.99	-37.64[x]	
Cl^{-}	-82.047	-83.50	-53.91[i]; -101.116[l]; -56.6[m]; -49.28[n]; -78.3[o]; -63.21[p]	-38.915	-27.04[g]; -37.90[x]	-10
K^{+}	-18.768	-19.16	-12.17[i]; -17.32[b,k]; -27.21[l]; -12.84[n]; -18.27[p]	-28.701	-22.83[x]	

Table III.1 (...Contd.)

Ion	Free ion			Crystal ion		
	Present	Feiock and Johnson	Others	Present	Others	Experimental**
Ca^{2+}	-13.625	-13.95	-12.12[i]; -19.66[l]; -13.32[p]	-25.71	-20.58[x]	
Sc^{3+}	-10.677		-9.461[g]	-20.04	-20.34[x]	-19
Ti^{4+}	-8.761	-9.006	-7.721[i]; -12.50[x]	-14.616	-25.51[x]	
V^{5+}	-7.417			-10.744		
Cr^{6+}	-6.423	-6.636		-8.368		
Ge^{4-}				-323.47		
As^{3-}				-201.53		
Se^{2-}				-137.36		
Br^{-}	-195.014	-210.0	123.0[h]; -244.3[l]; -99.0[n]; -100[q]	-97.424		-35
Rb^{+}	-51.196	-54.97	-47.9[e]; -113.776[b]; -49.29[n], -50[q]	-77.063		
Sr^{2+}	-38.423	-41.35		-70.063		
Yt^{3+}	-30.889		-33.6[s]	-53.326		
Zr^{4+}	-25.867	-28.09		-38.398		

Table III.1 (..Contd.)

	Free ion			Crystal ion		
Ion	Present	Feiock and Johnson	Others	Present	Others	Experimental**
Nb^{5+}	-22.204			-28.991		
Mo^{6+}	-19.215	-21.43		-23.861		
Sn^{4-}				-546.85		
Sb^{3-}				-344.18		
Te^{2-}				-241.33		
I^{-}	-331.633	-396.10	-173.75^{n}; -175^{q}; -138.4^{r}	-177.732		-45
Cs^{+}	-102.755		-103.05^{e}; -110.44^{n}; -110^{q}	-156.896		
Ba^{2+}	-79.397			-141.187		
La^{3+}	-65.278		-65.82^{y}			
Fr^{+}	-192.035		-193.01^{y}	-295.958		
Ra^{2+}	-150.746		-151.60^{y}	-261.234		
Ac^{3+}	-125.049		-126.06^{y}	-196.517		

Table III.2*: The free and crystal ion total quadrupole polarizability values, α_q, in a_0^5 units.

	Free Ion			Crystal Ion
Ion	Present	Feiock and Johnson	Others	Present
Li^+	0.005214	0.004712	0.00471[a]; 0.004648[c]; 0.00466[d]; 0.004699[i]; 0.00473[t]	0.007992
Be^{2+}	0.000683	0.000637	0.000633[a]; 0.000630[c]; 0.000638[d]; 0.000642[i]	0.001217
B^{3+}	0.000150	0.000143	0.000142[a]; 0.000141[c]; 0.000143[d]; 0.000144[i]	0.000262
C^{4+}	0.000045	0.000043	0.000043[d]	0.000074
N^{5+}	0.000016		0.000016[d]	0.000026
O^{6+}	0.000007			0.000010
O^{2-}				4.391510 (6.238, 7.738, 3.227[g])
F^-	6.89807	7.843	3.457[i]; 2.937[j]; 4.409[l]; 21.76, 2.877, 2.332[g]	1.028660 (1.802[g])
Na^+	0.063013	0.063250	0.067[a]; 0.06417, 0.0641, 0.06387[i]; 0.0632[j]; 0.08848[l]; 0.0634; 0.0649[v]	0.115088

Table III.2 (...Contd.)

	Free Ion			Crystal Ion
Ion	Present	Feiock and Johnson	Others	Present
Mg^{2+}	0.020956	0.021000	0.02188[i]; 0.0215[j]; 0.030[l]	0.059505
Al^{3+}	0.008668	0.008671	0.00101[a]; 0.009104[i]; 0.00895[j]; 0.01185[l]	0.032727
Si^{4+}	0.004158		0.00597[l]	0.018167
P^{5+}	0.002139			0.014177
S^{6+}	0.001197	0.001192		0.005960
Si^{4-}				276.15878
P^{3-}				50.88831
S^{2-}				14.16375
Cl^{-}	19.17835	19.46	13.1[g]; 11.79, 19.44[i]; 19.759[l], 11.92[p]; 13.77[t]; 13.05[u]	4.770722
K^{+}	0.638469	0.637500	0.7194[i]; 1.047[l]; 0.674[p]; 0.735[t]; 0.717[u]; 0.721[v]	1.199525
Ca^{2+}	0.273318	0.27200	0.3008[i]; 0.4381[l]; 0.290[p]	0.778462

Table III.2 (...Contd.)

	Free Ion			Crystal Ion
Ion	Present	Feiock and Johnson	Others	Present
Sc^{3+}	0.137123		0.1524[i]	0.479939
Ti^{4+}	0.076042	0.07532		0.289070
V^{5+}	0.045287			0.169139
Cr^{6+}	0.028438	0.02799		0.099532
Ge^{4-}				280.10462
As^{3-}				62.26001
Se^{2-}				19.80673
Br^{-}	27.86503	28.99	31.442[l]	7.541961
Rb^{+}	1.407357	1.376	3.117[l]; 1.592[W]	2.705311
Sr^{2+}	0.691121	0.6692		2.029917
Y^{3+}	0.391197			1.406932
Zr^{4+}	0.241542	0.2310		0.909730
Nb^{5+}	0.158216			0.573686
Mo^{6+}	0.108594	0.1027		0.367894

Table III.2 (...Contd.)

	Free Ion			Crystal Ion
Ion	Present	Feiock and Johnson	Others	Present
Sn^{4-}				377.02949
Sb^{3-}				93.98383
Te^{2-}				33.72970
I^{-}	44.87240	49.84		14.55947
Cs^{+}	3.660668	3.443	4.907[w]	6.89371
Ba^{2+}	2.052602	1.892		5.603819
La^{3+}	1.383249	1.214	1.390[y]	4.112645
Fr^{+}	5.759481			10.973830
Ra^{2+}	3.438726			8.892337
Ac^{3+}	2.36332			7.665737
At^{-}	57.03699			19.78638

References to the Tables III.1 and III.2

* A preliminary account of this work has been published in 'Advances in Nuclear Quadrupole Resonance' (Ed. by J. A. S. Smith, Hyden, London, 1974), p. 277. Due to errors in transcription a few values in this paper are misleading. The Tables I and II given here contain the correct values.

**Experimental values have been discussed in section III of the text.

a See reference 27 of text.

b R. M. Sternheimer, Phys. Rev. 115, 1198 (1959).

c J. Lahiri and A. Mukherji, Phys. Rev. 141, 428 (1966).

d P. W. Langhoff, M. Karplus and R. P. Hurst, J. Chem. Phys. 44, 565 (1966).

e R. M. Sternheimer and R. F. Peierls, Phys. Rev. A3, 837 (1971).

f R. M. Sternheimer, Phys. Rev. A 4, 1723 (1971).

g See reference 29c of text.

h R. M. Sternheimer, Phys. Rev. 132, 1638 (1963).

i P. W. Langhoff and R. P. Hurst, Phys. Rev. 139, 1415 A (1965).

j J. Lahiri and A. Mukherji, Phys. Rev. 153, 386 (1967).

k See reference 175.

l C. Litt, Phys. Rev. A 7, 911 (1973).

m R. M. Sternheimer and H. M. Foley, Phys. Rev. 102, 731 (1956).

n E. G. Wikner and T. P. Das, Phys. Rev. 109, 360 (1958).

[o] R. E. Watson and A. J. Freeman, Phys. Rev. 123, 521 (1961).

[p] J. Lahiri and A. Mukherji, Phys. Rev. 155, 24 (1967).

[q] R. E. Watson and A. J. Freeman, Phys. Rev. 135, 1209 A (1964).

[r] R. M. Sternheimer, Phys. Rev. 146, 140 (1966).

[s] R. M. Sternheimer, Phys. Rev. 159, 266 (1967).

[t] R. M. Sternheimer, Phys. Rev. 107, 1565 (1957).

[u] P. G. Khubchandani, R.R. Sharma and T. P. Das, Phys. Rev. 126, 594 (1962).

[v] G. Burns, Phys. Rev. 115, 357 (1959).

[w] R. M. Sternheimer, Phys. Rev. A 1, 321 (1970).

[x] See reference 163 of text.

[y] R. P. Gupta and S. K. Sen, Phys. Rev. A 7, 850 (1973); ibid, 1169 (1973).

In the case of multinegative ions corresponding to Ne, A, Kr, Xe, and Rn series it has not been possible for us to generate the self-consistent wave functions. Such a situation is well known[170] in the case of O^{2-} where the stable free ion does not exist and it is doubtful that a HF solution would converge to a state with all the 10 electrons bound to it. On the other hand oxides, sulphides etc. exist as stable ionic solids and the approximation of ions with a certain radius is a useful physical concept which explains many properties of ionic solids. In order to obtain the wave functions for ions in crystals it is necessary to include the stabilizing potential due to the lattice. Yamashita and coworkers[171] have obtained the wave functions of O^{2-} in MgO crystal by a variational method. Watson has proposed a spherical potential surrounding O^{2-} ion according to the method described in Chapter II. As compared to the free atomic or ionic cases these wave functions give better agreement with the experimental properties such as dipole polarizabilities, diamagnetic susceptibilities,[162] atomic scattering factors, and Compton profiles.[171] Fukamachi and coworkers[172a] have shown that the contracted wave functions of Yamashita and coworkers and Watson for O^{2-} give more or less similar results for atomic scattering factors and Compton profiles in MgO. Burns and Wikner[29c] and Paschalis and Weiss[163] have earlier calculated γ_∞ values in a few cases using the

Watson model[164] and the variational method of Das and Bersohn.[27] We thought it worthwhile to study these ions as well as other ions of interest to the experimentalist by means of a more accurate perturbation-numerical procedure and using HFS wave functions.

With the use of the Watson model[164] to describe the lattice potential, we generated the SCF wave functions for all the ions considered above and additional 10 negative ions given by O^{2-}, S^{2-}, P^{3-}, Si^{4-}; Se^{2-}, As^{3-}, Ge^{4-}; Te^{2-}, Sb^{3-}, Sn^{4-}. To our knowledge, the self-consistent numerical HFS wave functions for these ten ions have been generated for the first time. We have used these wave functions to calculate γ_∞ and α_q values by means of external charge-perturbed procedure and the results obtained have been given in column 5 of Table III.1 and Table III.2 respectively. For the purpose of comparison we have also included the γ_∞ results obtained with the Watson model by Burns and Wikner[29c] (BW) and Paschalis and Weiss[163] (PW) in column 6 of Table III.1.

For heavier positive ions the results based on the variation-perturbation method of Das and Bersohn[27] underestimates the antishielding effect. This has also been observed in the case of free ion calculations. In the cases of K^+, Ca^{2+}, Sc^{3+}, and Ti^{4+}, Paschalis and Weiss[163] have quoted γ_∞ as respectively -22.83, -20.58, -20.34 and -25.51. This trend seems to be

erroneous since one expects the 3p wave function in Ti^{4+} to be more internal than that in Sc^{3+}. As compared to our free ion values the γ_∞ in crystal is $\sim$ 50% smaller for the negative ions. For the positive ions also a similar increase is obtained in a large number of cases. Thus the effect due to crystalline distortion is estimated to be $\sim$3 times larger than the relativistic or coupling effects discussed earlier.

Experimental estimates of γ_∞ are available for a large number of ions in ionic solids (vide Chap. I, Sec. 4.A). The effective γ_∞ for Na^+ has been estimated to be $\sim$-9. The present value of -7.7 compares favourably with this value. Raymond[92] has estimated the best fit value of γ_∞ for Al^{3+} in Al_2SiO_5 polymorphs as -4.9 which is in satisfactory agreement with our crystal ion value of -5.7. Bhide and Hegde[135] have combined the electric field gradient data on ^{44}Sc and ^{57}Fe to estimate γ_∞ =-19 for Sc^{3+} which is to be compared with the present value of -20. Recently Anderson and Karra[125] have estimated γ_∞ = +4.4 for Li^+ in LiF single crystal via acoustic-saturation studies. The interpolated result of 0.34 due to Lahiri and Mukherji[24] and the present value of 0.28 are significantly lower than the above experimental estimate. Gupta and Sen[155] have calculated γ_∞ for Li in $1s^2 2p^1$ configuration and noticed that the theoretical value of -4.4 so obtained is in reasonably good agreement with Anderson and Karra's[125] estimate in LiF crystals.

However, such an electronic configuration for the lithium ion is highly improbable in solid LiF and the two values cannot be meaningfully compared. We have found that in an analogous experiment on LiF single crystal, Shutilov and coworkers[124] have estimated γ_∞ to be 0.5 ± 0.3 which is very close to the crystal ion value predicted by Lahiri and Mukherji,[24] Paschalis and Weiss[163] and by us. It therefore appears that overall agreement between theoretical and experimental estimates in the cases of positive ions in ionic solids is quite satisfactory.

Burns and Wikner[29c] have estimated the values of γ_∞ for Cl^-, Br^- and I^- to be centred around -10, -35 and -45 respectively. As mentioned in Chapter I, this choice has been criticized by Das and Dick[90] on the grounds that the models used to interpret the experimental results in these cases are rather crude. However, Ikenbery and Das[121] have subsequently found that a fairly contracted γ_∞ in the cases of halogen negative ions would be required to interpret the quadrupole coupling data in alkali halide solid-solutions. Since our free ion γ_∞ values for halogen negative ions significantly overemphasize the antishielding effect as compared to HF results we cannot directly compare our results with the experimental estimates. Beri et al.[26b] have recently included the consistency corrections to γ_∞ values based on HF wave functions for F^-, Cl^- and Br^- ions. Assuming the net contraction effect to be similar in the cases of HF and HFS approximations, we have

estimated the contracted HF value of γ_∞ for F^-, Cl^- and Br^- to be -5, -28 and -74, respectively. In view of the recent estimates of $\gamma_\infty \sim -30$ for Cl^- in $CoCl_2.2H_2O$[100] and alkali metal hexachlorostanates, $GdCl_3$,[101] the agreement can be considered as satisfactory. We think that Burns and Wikner's estimate of contraction of γ_∞ for halogen negative ions needs a careful rechecking.

Our nonrelativistic α_q values are in excellent agreement with the FJ values for the lighter ions. In the cases of heavy positive ions the present nonrelativistic values are consistently larger than the corresponding relativistic values. This can be qualitatively explained as arising due to the relativistic contraction of the outer loops of the external p orbitals which leads to decrease in relativistic α_q values. For the mono-negative ions however, our values are slightly lower than the relativistic values of FJ. We do not have a satisfactory explanation for such a trend observed in the cases of negative ions.

Due to the easy deformability of the negative ions, it is natural to expect a range of ionic radii for them. We have studied γ_∞ and α_q values as a function of the radius of the Watson sphere for F^-, Cl^-, Br^-, I^-, O^{2-}, S^{2-}, Se^{2-}, and Te^{2-}. These results have been shown in Table III.3. It is evident from these results that γ_∞ and α_q values critically depend upon

Table III.3: The variation of γ_∞ and α_q as a function of radius of the charged sphere around the mono and dinegative ions. Pauling ionic radii r_{ion} and α_q are given respectively in $\mathring{A}$ and $\mathring{A}^5$ units.

Ion (r_{ion})		r_{ion}-0.3	r_{ion}-0.2	r_{ion}-0.1	r_{ion}	r_{ion}+0.1	r_{ion}+0.2	r_{ion}+0.3
F^-	$-\gamma_\infty$	11.76	12.73	13.65	14.583	15.35	16.12	16.81
(1.36)	α_q	0.73112	0.82500	0.92186	1.02866	1.11937	1.21753	1.31372
Cl^-	$-\gamma_\infty$	34.27	35.852	37.367	38.91	40.12	41.31	42.40
(1.81)	α_q	3.91686	4.201256	4.476530	4.77072	4.99956	5.24830	5.48522
Br^-	$-\gamma_\infty$	87.12	90.62	93.98	97.42	100.06	102.75	105.20
(1.95)	α_q	6.32263	6.72065	7.11244	7.541961	7.86092	8.21185	8.54506
I^-	$-\gamma_\infty$	161.83	167.19	172.34	177.73	181.71	185.88	189.70
(2.16)	α_q	12.63354	13.26593	13.88220	14.55947	15.04711	15.58797	16.09956
O^{2-}	$-\gamma_\infty$		17.61	20.69	24.19	28.13		
(1.40)	α_q		2.73887	3.47623	4.39151	5.52979		
S^{2-}	$-\gamma_\infty$	41.19	45.43	50.03	54.99	60.28	65.98	72.06
(1.84)	α_q	9.15833	10.61811	12.27850	14.16375	16.28388	18.70592	21.44842

Table III.3 (...Contd.)

Ion (r_{ion})		r_{ion}-0.3	r_{ion}-0.2	r_{ion}-0.1	r_{ion}	r_{ion}+0.1	r_{ion}+0.2	r_{ion}+0.3
Se^{2-}	$-\gamma_\infty$	106.38	115.93	126.26	137.36	149.15	161.64	174.78
(1.98)	α_q	13.31641	15.23805	17.39608	19.80673	22.50776	25.51939	28.84786
Te^{2-}	$-\gamma_\infty$	195.73	210.02	225.23	241.33	258.27	276.01	294.54
(2.21)	α_q	24.45348	27.27590	30.36075	33.72970	37.40221	41.40090	45.75437

the choice of the ionic radius. With increase in this radius, as expected, the γ_∞ and α_q values approach the free ionic result. We have obtained polynomial-fittings in each case for γ_∞ and α_q, as a function of the ionic radius r_{ion}. The polynomial

$$\gamma_\infty (\text{or } \alpha_q) = \sum_{i=0}^{2 \text{ or } 3} a_i \, (r_{ion})^{-1} \qquad \text{(III.1)}$$

has been used and the various coefficients have been listed in Table III.4. From such a correlation it is found that a typical reduction by $\sim$ 20% in the Pauling ionic radius results in 15-20% and 25-30% decrease respectively in values of γ_∞ for mono-negative and di-negative ions considered here. In the cases of negative ions due to their easy deformability, it is very likely that the size of the ion is different in different ionic solids. As estimated above, the γ_∞ values undergo significant changes as a result of the variation in r_{ion}. It would be highly desirable to have estimates of r_{ion} in a given system by semi-empirical means so that more appropriate values of γ_∞ can be used in interpreting the experimental e^2qQ data in solids.

III.2.B γ_∞, α_q, σ_2 and R for Ce^{3+} in Crystal

The experimental estimates[151-153] of the Sternheimer shielding-antishielding factors for rare earth ions in solids are generally higher than the corresponding free ion values.[12b]

Table III.4: The parameters a_i in the equation $|\gamma_\infty|$ (or α_q) = $\sum_{i=0}^{2 \text{ or } 3} a_i (r_{ion})^{-i}$. The average percentage error, APE, in each fit has been given in the last column.

Ion	a_i	a_0	a_1	a_2	a_3	APE
F^-	$\|\gamma_\infty\|$	41.109	-70.142	63.751	-23.777	0.2
	α	6.898	-18.631	20.344	-7.984	0.7
Cl^-	$\|\gamma_\infty\|$	82.047	-138.379	154.426	-82.365	0.1
	α	19.178	-56.394	77.357	-40.820	0.2
Br^-	$\|\gamma_\infty\|$	195.014	-311.460	315.728	-156.969	0.1
	α	27.865	-81.764	113.142	-60.741	0.3
I^-	$\|\gamma_\infty\|$	331.633	-545.901	658.673	-430.379	0.05
	α	44.872	-130.374	195.036	-119.285	0.1
O^{2-}	$\|\gamma_\infty\|$	158.062	-300.195	158.005		0.2
	α	46.932	-93.498	54.567		0.4
S^{2-}	$\|\gamma_\infty\|$	319.261	-787.365	553.842		0.5
	α	142.118	-395.202	293.815		1.5
Se^{2-}	$\|\gamma_\infty\|$	755.323	-1976.609	1490.665		0.3
	α	189.063	-561.066	447.203		1.0

Table III.4 (...Contd.)

Ion	a_i	a_0	a_1	a_2	a_3	APE
Te^{2-}	$\lvert\gamma_\infty\rvert$	1208.988	-3441.039	2878.0738		0.2
	α_q	278.854	- 900.622	792.930		0.6

We therefore thought it worthwhile to estimate the effects of crystalline potential on γ_∞, α_q, σ_2 and R for the rare earth ion of Ce^{3+}.

We have used the Watson model to calculate γ_∞, α_q, σ_2 and R for Ce^{3+} to estimate the effects due to the lattice potential. The calculations of γ_∞, α_q, and σ_2 were carried out using external charge-perturbed wave functions. In the calculation of R we have used the moment-perturbed procedure. All the direct and exchange terms have been included in the calculation of σ_2 and R. These results have been given in Table III.5. Our free ion values of α_q, γ_∞, σ_2 and R for Ce^{3+} are 1.26, -65, 0.71 and 0.11 respectively. These are in quantitative agreement with the results of Gupta and Sen[12b] who have used the HFS wave functions and Sternheimer perturbation-numerical method to calculate σ_2, γ_∞ and R_D for the free tripositive rare-earth ions. Our crystal ion values of α_q, γ_∞, σ_2 and R for Ce^{3+} are 3.52, -107, 0.53 and 0.2 respectively. In the cases of α_q, γ_∞, and R values we observe a significant increase over the free ion values. The decrease of σ_2 in the crystal ion case is not clear to us. We note here that the experimental estimates[151-153] of σ_2 are consistently $\sim$40-50% higher than the free ion values. We are studying in greater detail, the effects of lattice potential on σ_2.

Table III.5: The individual contributions to α_q, γ_∞, σ_2 and R in the case of Ce^{3+} in crystal. Pauling ionic radius has been taken as 1.12 Å.

Exct.	α_q	γ_∞	σ_2	R
1s→d	0.0000	0.0116	0.0000	0.0116
2s→d	0.0000	0.0269	0.0000	0.0248
3s→d	0.0000	0.0487	0.0008	0.0286
4s→d	0.0018	0.0845	0.0178	0.0150
5s→d	0.5592	0.2768	0.2114	0.0039
2p→f	0.0000	0.0339	0.0000	0.0350
3p→f	0.0000	0.0808	0.0006	0.0472
4p→f	0.0029	0.1710	0.0226	0.0265
5p→f	2.7577	0.6608	0.4197	0.0050
3d→s	0.0000	-0.0279	-0.0007	-0.0159
4d→s	0.0011	-0.0891	-0.0199	-0.0089
3d→g	0.0000	0.0915	0.0005	0.0606
4d→g	0.0058	0.2301	0.0270	0.0391
Total (Ang.)	2.8317	1.534	0.3529	0.2720
2p→p	0.0000	-0.2462	0.0000	-0.2084
3p→p	0.0000	-1.4521	0.0000	-0.3646
4p→p	0.0006	-8.0337	-0.0013	0.1011
5p→p	0.6384	-95.805	-0.1710	0.4275
3d→d	0.0000	-0.3244	0.0000	-0.0332
4d→d	0.0019	-2.5267	-0.0046	0.0016
Total (Rad.)	0.6409	-108.388	0.1769	-0.0760
Grand Total	3.5226	-106.854	0.5298	0.1960

III.2.C γ_∞ for Actinide Free Ions and Ions in Crystals

The quadrupole coupling measurements on actinides have recently become available mainly through Mössbauer effect[149] and atomic beam magnetic resonance[150e] methods. In this region the first calculation of γ_∞ was carried out by Sternheimer[173] on Am^{2+}. He used the HFS wave functions corresponding to the neutral atom and predicted that these functions overestimate the antishielding effect by ~5%. Feiock and Johnson[169] (FJ) have calculated γ_∞ for Th^{4+} and U^{6+} using relativistic HFS wave functions.

With the aim to estimate relativistic and lattice potential effects we have calculated free ion values of γ_∞ for all tetrapositive actinide ions and crystal ion γ_∞ for Pa^{4+}, Bk^{4+} and Lw^{4+}. We have used the moment-perturbed wave functions in both cases and the results so obtained have been presented along with the other available results in Table III.6. In view of the fact that the actinide elements show variable valency we have also calculated γ_∞ for U^{3+}, U^{5+}, U^{6+} and Am^{2+}.

The 5f contribution has been included by considering the occupancy of 5f shell. After the completion of our work, we came across the paper by Gupta and Sen[155] where these authors have calculated γ_∞ for Th^{4+}, Pa^{4+}, U^{3+}, U^{4+}, U^{6+}, Np^{4+} and Pu^{4+} using external charge-perturbed wave functions but without the inclusion of 5f contributions. Although we used the moment-

Table III.6. The non-relativistic total γ_∞ values to zeroth order for the ions in actinide series ($90 \leq Z \leq 103$). The electronic configuration considered in each case has been shown in column 3.

Ion	Z	Configuration	Free Ion (Present)	Free Ion (Others)	Crystal Ion
Th^{4+}	90	$(Rn)5f^0$	-107.170	-177.5[a] -108.46[c]	
Pa^{4+}	91	$(Rn)5f^1$	-105.325	-104.9[c]	-145.23
U^{3+}	92	$(Rn)5f^3$	-117.987		
U^{4+}	92	$(Rn)5f^2$	-103.805	-103.0[c]	
U^{5+}	92	$(Rn)5f^1$	- 95.530		
U^{6+}	92	$(Rn)5f^0$	- 85.155	-143.9[a] - 88.3[c]	
Np^{4+}	93	$(Rn)5f^3$	-102.170		
Pu^{4+}	94	$(Rn)5f^4$	-100.970	-100.4[c]	
Am^{2+}	95	$(Rn)5f^7$	-132.867	-137.3[b]	
Am^{4+}	95	$(Rn)5f^5$	- 99.786		
Cm^{4+}	96	$(Rn)5f^6$	- 98.842		
Bk^{4+}	97	$(Rn)5f^7$	- 97.985		-141.7
Cf^{4+}	98	$(Rn)5f^8$	- 98.890		
E^{4+}	99	$(Rn)5f^9$	- 96.47		
Fm^{4+}	100	$(Rn)5f^{10}$	- 96.40		
Md^{4+}	101	$(Rn)5f^{11}$	- 95.417		
No^{4+}	102	$(Rn)5f^{12}$	- 95.210		
Lw^{4+}	103	$(Rn)5f^{13}$	- 94.211		-139.7

[a] See reference 168; [b] See reference 173; [c] See reference 146.

perturbed wave functions, the agreement in the case of Th^{4+} is to within ~ 3% and this provides a good check on the accuracy of both these calculations. It is gratifying to note that the use of ionic wave functions actually reduces γ_∞ of Am^{2+} by ~5% as has been earlier predicted by Sternheimer.[173] The for heavier tetrapositive actinide ions in free state seem to be constant at -95 and γ_∞ for actinide series of ions can be taken as $-100(\pm 5)$. This is not unexpected since like the tripositive rare earth ions, the tetrapositive actinide ions are characterized by an ionic radii of ~ 0.9 Å.

A comparison with FJ[169] values for Th^{4+} and U^{6+} shows that in this region of the periodic table relativistic effects would increase γ_∞ by ~65%. Freeman and Watson[21a] have indicated that such an increase might result because of a severe relativistic contraction of the inner loops of p shells. However, one expects the contraction in outer loops of p shells due to relativistic effects and a detailed analysis of the relativistic two-component unperturbed and perturbed functions is necessary before arriving at any physical reasoning for such an effect.

In the cases of Pa^{4+}, Bk^{4+} and Lw^{4+}, it is found that the lattice effects would increase the free ion γ_∞ value by ~45% which is comparable to the relativistic effect in this region, as mentioned earlier.

III.2.D Some Comments on the Watson Model for Ions in Solids

The Watson model provides a means to generate the zeroth order crystalline wave functions and makes it possible to estimate the effect of the lattice potential on Sternheimer shielding-antishielding factors. It preserves the electron-eutrality of the crystal and can be further extended to incorporate the proper symmetry of the ion within crystalline lattice. Such a model can also be used to estimate the changes in shielding-antishielding factors due to partial compensation of charges in ionic solids.

The choice of the radius of Watson sphere is arbitrary and it would be more appropriate to choose r_{ion} in some semi-empirical manner. The complete neglect of overlap, the point charge like potential outside the sphere and the use of similar potentials for both positive and negative ions, however, remain the main drawbacks of the model. But keeping in mind the fact that the simple Watson model qualitatively reproduces the experimental trends in γ_∞ values it would be highly desirable to improve upon this model in order to obtain more accurate values of shielding-antishielding factors for ions in solids.

CHAPTER IV

Sternheimer Shielding-Antishielding Factors for Some Ions and Metals of Interest in Mössbauer and TDPAC Studies

CHAPTER IV

Sternheimer Shielding-Antishielding Factors for Some Ions and Metals of Interest in Mössbauer and TDPAC Studies*

IV.1 Introduction

The experimental studies on the nuclear quadrupole coupling in solids via Mössbauer effect and TDPAC studies have been largely concerned with the transition metal elements. In Mössbauer effect studies the nuclei of ^{57m}Fe, ^{99}Ru and ^{189}Os occupy a central role and in order to interpret the experimental data according to eq. (I.17) it is necessary to have reliable estimates of γ_∞ and R. The calculations of γ_∞ and R for Fe^{3+} and Fe^{2+} have been carried out by several workers using methods of varying accuracy. Burns and Wikner[29c] have reported γ_∞ as -6.81 and -9.47 for Mn^{2+} and Fe^{3+} respectively using the variational method of Das and Bersohn.[27] Gupta and Sen[155] have calculated γ_∞ for most of the transition metal ions but their calculations do not include the important contribution from the outermost d shell. Ray et al.[174] have compared the

* The work presented in this chapter has been published in the following papers:
(1) K. D. Sen and P. T. Narasimhan, Phys. Rev. A (in press) (1976); (2) Phys. Rev. B (in press) (1976); (3) Phys. Rev. A, (in press) (1976).

LCMBPT and DE calculations of γ_∞ for Fe^{3+} and found that the two results including consistency terms agree within 12%. The net effect of intra-shell and inter-shell consistency terms on γ_∞ is only 8% of the first-order result due to Sternheimer.[175] Ingalls[30] has calculated γ_∞ and R for Fe^{2+} using the variational method of Das and Bersohn.[27] Freeman and Watson[21b](FW) have calculated the radial contribution to R using the orbital-polarized unrestricted HF method. The generally employed less-accurate estimate of R = +0.32 for Fe^{2+} is based on the addition of FW estimate of radial terms to Ingalls'[30] calculation of the angular terms. A more reliable value of +0.12 has been given by Sternheimer.[74d] In the overlap model of Sharma[128c] a major source of inaccuracy arises from the uncertainty in the shielding-antishielding parameters $(1-\gamma_\infty)$ and (1-R) respectively. In the analysis of quadrupole splitting obtained from Mossbauer effect studies on $FeSiF_6.6H_2O$ Ingalls[132] has used a 10% covalency reduction in $\langle r^{-3}\rangle_{3d}$. Such changes in the electron density distribution of ions in solids are expected to alter the values of $(1-\gamma_\infty)$ and (1-R) and it is of interest to make an estimate of these using some simple assumptions.

IV.2 Results and Discussion

IV.2.A Calculation of γ_∞ for nd^5 Sequences

Lahiri and Mukherji[24] have suggested that within a given

isoelectronic series the correlation of γ_∞ (or α_q) values to the position of the outermost peak in the total radial electronic charge density distribution, ρ_m, can be used to estimate the effect of distortion of the ion in going from the free state to within a crystal. A similar treatment of γ_∞ and R in the cases of nd^5 (n = 3,4,5) and $3d^6$ isoelectronic sequences has been carried out by us. Thus, in our γ_∞ calculations the following ions have been considered,

n=3 : Cr^+, Mn^{2+}, Fe^{3+}, Co^{4+}, Ni^{5+}, Cu^{6+};
n=4 : Mo^+, Tc^{2+}, Ru^{3+}, Rh^{4+}, Pd^{5+}, Ag^{6+}, and
n=5 : W^+, Re^{2+}, Os^{3+}, Ir^{4+}, Pt^{5+}, Au^{6+}.

The radius of maximum charge density has been calculated according to,

$$\rho_m = \int \sum_i \chi_i^{o*}(j)\chi_i^o(j)\, r_i^2\, d\,\Omega_i \qquad \text{(IV.1)}$$

where i varies over all occupied core orbitals, including the outermost d orbitals, and χ_i^o gives the wave function of the j-th electron in the i-th orbital.

In the case of the $5d^5$ series we have not attempted such a correlation owing to a rather flat density distribution obtained in the outer region. Our results of γ_∞ and ρ_m (in a.u.) for these ions are given in Table IV.1. For comparison purposes we have also included the earlier available calculations. Here

Table IV.1: Zeroth order ionic antishielding factor (γ_∞) for various ions. ρ_m gives the distance of the farthest peak in the total electron density distribution (Eq. VI.1)

Ion	$-(\gamma_\infty)$	ρ_m (a.u.)
Cr^{+}	16.67 (10.57)[a]	0.767
Mn^{2+}	11.96 (6.81[b], 11.37[c], 9.19[a])	0.721
Fe^{3+}	9.64 (6.17[b], 9.47[d], 7.97[a])	0.675
Co^{4+}	8.13 (6.97)[a]	0.643
Ni^{5+}	7.04	0.600
Cu^{6+}	6.21	0.571
Mo^{+}	39.36 (27.53)[a]	1.014
Tc^{2+}	30.62 (24.21)[a]	0.986
Ru^{3+}	25.71 (21.40)[a]	0.938
Rh^{4+}	22.27 (19.08)[a]	0.891
Pd^{5+}	19.70	0.865
Ag^{6+}	17.68	0.819

Table IV.1 (...Contd.)

Ion	$-(\gamma_\infty)$	ρ_m (a.u.)
W^{+}	77.31 (56.85)[a]	
Re^{2+}	61.67	(e)
Os^{3+}	52.66	(e)
Ir^{4+}	46.10 (39.78)[a]	(e)
Pt^{5+}	41.35	(e)
Au^{6+}	37.49	(e)

[a] See ref. 155; [b] See ref. 29c; [c] See ref. 175;

[d] See ref. 174; [e] Precise ρ_m values in the $5d^5$ sequence could not be obtained with HFS wave functions on account of their rather flat behaviour at larger r values.

again, the variational calculations[32c] on Mn^{2+} and Fe^{3+} seem to underestimate the antishielding effect. In these two cases our values are in excellent agreement with Sternheimer's calculations[175] based on HF wave functions.[176] Due to the increased binding effect as Z increases γ_∞ values decrease. The difference between the presently calculated values and those of Gupta and Sen[155] is due to the contribution from the d^5 shell which has not been included in the latter calculations. As is evident, this contribution can by no means be neglected.

In Table IV.2 we have presented the results of the polynomial fitting according to

$$|\gamma_\infty| = \sum_{i=0}^{3} a_i \rho_m^i \qquad \text{(IV.2)}$$

for $3d^5$ and $4d^5$ series. The average percentage error in the fitting is $\sim$4%. From this correlation we have concluded that for a typical increase in ρ_m value by 10% the antishielding factor is expected to increase by $\sim$ 40% for Fe^{3+} and 60% for Ru^{3+} respectively.

IV.2.B Calculation of R for $3d^6$ Sequence

The calculations of R including all the direct and exchange terms[74a] have been carried out for the following $3d^6$ series of ions: Cr, Mn^+, Fe^{2+}, Co^{3+}, Ni^{4+}. The results of individual contributions along with ρ_m, $\langle r^{-3} \rangle_{3d}$ and 3d eigenvalue $-\varepsilon_{3d}$ have been given in Table IV.3.

Table IV.2: Values of coefficients a_i in $|\gamma_\infty| = \sum_{i=0}^{3} a_i \rho_m^i$ for $3d^5$ and $4d^5$ isoelectronic series.

Series	i	a_i
$3d^5$	0	+ 9.94331934
	1	+ 56.51866168
	2	-247.48745045
	3	+241.13786680
$4d^5$	0	+ 25.88997667
	1	+254.74583419
	2	-671.61179214
	3	+426.21804032

Table IV.3: The individual direct and exchange contributions R_D and R_E to the Sternheimer valence shielding factor R for Cr, Mn^+, Fe^{2+}, Co^{3+} and Ni^{4+} in $3d^6$ configuration. R_E values have been given in parentheses in each case below R_D values. ρ_m and $\langle r^{-3} \rangle_{3d}$ values are in Bohr units and the 3d orbital eigenvalues are given in Rydberg units.

Perturbation	Cr	Mn^+	Fe^{2+}	Co^{3+}	Ni^{4+}
1s→d	0.0279	0.0268	0.0257	0.0247	0.0237
	(-0.0008)	(-0.0008)	(-0.0008)	(-0.0008)	(-0.0008)
2s→d	0.0476	0.0444	0.0416	0.0389	0.0367
	(-0.0127)	(-0.0122)	(-0.0118)	(-0.0113)	(-0.0109)
3s→d	0.0236	0.0207	0.0184	0.0161	0.0145
	(-0.0091)	(-0.0079)	(-0.0070)	(-0.0060)	(-0.0053)
2p→f	0.0703	0.0661	0.0624	0.0590	0.0560
	(-0.0146)	(-0.0141)	(-0.0137)	(-0.0132)	(-0.0128)
3p→f	0.0376	0.0335	0.0300	0.0271	0.0248
	(-0.0137)	(-0.0122)	(-0.0108)	(-0.0097)	(-0.0087)
3d→s	-0.0090	-0.0085	-0.0084	-0.0081	-0.0078
3d→g	0.0167	0.0171	0.0169	0.0164	0.0158
R_D(Ang):	0.2147	0.2001	0.1866	0.1741	0.1637
R_E(Ang):	(-0.0509)	(-0.0472)	(-0.0441)	(-0.0410)	(-0.0385)
Tot.(Ang)	0.1638	0.1529	0.1425	0.1331	0.1252
2p→p	-0.3626	-0.3308	-0.3027	-0.2782	-0.2569
	(0.2698)	(0.2535)	(0.2387)	(0.2251)	(0.2127)

Table IV.3 (...Contd.)

Perturbation	Cr	Mn^{+}	Fe^{2+}	Co^{3+}	Ni^{4+}
$3p \rightarrow p$	0.1587	0.1750	0.1790	0.1748	0.1667
	(-0.1275)	(-0.1581)	(-0.1773)	(-0.1848)	(-0.1848)
$3d \rightarrow d$	0.1558	0.0625	0.0389	0.0283	0.0223
R_D(Rad):	-0.0481	-0.0933	-0.0848	-0.0751	-0.0679
R_E(Rad):	(0.1423)	(0.0954)	(0.0614)	(0.0403)	(0.0279)
Tot.(Rad)	0.0942	-0.0021	-0.0234	-0.0348	-0.0400
Net R	0.2580	0.1550	0.1191	0.0983	0.0852
ρ_m	0.76733	0.73273	0.68735	0.64335	0.61227
$\langle r^{-3} \rangle_{3d}$	2.967471	4.264828	5.773645	7.49987	9.458906
$-\epsilon_{3d}$	0.292534	1.161839	2.418018	3.984175	5.82547

The most significant contributions to R come from the radial excitation of np→p type. The exchange contribution R_E corresponding to these excitations is always ~70% of the direct R_D and is opposite in sign. In the case of 2p→p excitations the direct contribution predominates over the exchange term and the net effect is antishielding. As Z increases within the isoelectronic series the valence electrons experience greater binding and a stronger overlap effect is obtained between 3d and p orbitals in the core. This is reflected in the increasing percentage of the exchange term with respect to the direct term corresponding to 2p→p contributions to R presented in Table IV.3. Thus, R_E (2p→p, 3d) is respectively 74.4%, 76.6%, 78.8%, 80.9%, and 82.8% of R_D (2p→p, 3d) for Cr, Mn^+, Fe^{2+}, Co^{3+} and Ni^{4+}. Interestingly, an even larger effect corresponding to 3p→p excitations can be noticed in Table IV.3. For Cr, R_E (3p→p, 3d) is 80% of the direct term and the net effect is shielding. Beyond the case of Fe^{2+} ion in the series where the two contributions almost cancel each other, the exchange term corresponding to 3d→d excitation is zero and the direct term gives rise to shielding which decreases with increasing Z in the series. As a result, except in the case of Cr atom, where due to a large 3d→d direct contribution to R one obtains a net shielding effect, the total radial contribution to R is antishielding and increases in magnitude

with increase in Z. The total angular contribution to R is always shielding, and predominates over the total radial contribution to R. With increasing Z the total angular contribution decreases and the net R is shielding and decreases with increasing Z.

After the completion of this work on $3d^6$ isoelectronic series a paper by Gupta and Sen[155] came to our notice. These authors have calculated R for Mn^{+}, Fe^{2+}, Co^{3+}, and Ni^{4+} as 0.034, 0.053, 0.062 and 0.065 respectively. We note here that these authors have not considered the contributions due to the 3d orbital and exchange terms. Our calculations in Table IV.3 show that the sum of these contributions amount to 0.121, 0.065, 0.035, and 0.020 for Mn^{+}, Fe^{2+}, Co^{3+}, and Ni^{4+}, respectively. On subtracting these contributions from our total R given in Table IV.2 we obtain the values 0.034, 0.054, 0.063, and 0.066 which are in excellent agreement with the results of Gupta and Sen.[155] We conclude from such a comparison that the exchange and 3d orbital contributions should be included in order to obtain reliable values of R.

Our calculated value of +0.12 for Fe^{2+} based on HFS wave functions is in excellent agreement with Sternheimer's[74d] value of +0.12 obtained using analytic HF wave functions of Clementi.[177] In order to estimate the effect of solid-state distortions of the ion on the field gradient due to valence

electrons we have expressed $(1-R)\langle r^{-3}\rangle_{3d}$ as a polynomial in ρ_m according to

$$q_{val} = \sum_{i=1}^{4 \text{ or } 5} a_i \rho_m^{-i} \qquad \text{(IV.3)}$$

The values of a_i are presented in Table IV.4. From this correlation we have concluded that an increase in ρ_m by 10% brings down the valence contribution to the field gradient by ~47%. We note here that the experimental estimates of ρ_m can be obtained from single-crystal X-ray data and this can be used in correlations based on eqs. (IV.2) and (IV.3)

IV.2.C Reanalysis of Mössbauer Quadrupole Splitting Data on Ferric and Ferrous Compounds

We have used the best value[67a,72,174] of $1-\gamma_\infty = 10.47$ and $1-R = 0.88$ for Fe^{3+} and Fe^{2+} respectively to recalculate $Q(^{57m}Fe)$ following Sharma's analysis[134] of quadrupole coupling data on Fe_2O_3, $Al_2O_3:Fe^{3+}$ and the T_d and O_h Fe^{3+} sites in yttrium iron garnet. These values come out to be 0.154 b, 0.179 b, 0.146 b and 0.139 b, respectively, which are to be compared with the original values of 0.18 b for Fe_2O_3 and 0.204 b for $Al_2O_3:Fe^{3+}$. We have also recalculated $Q(Fe^{57m})$ from the $FeSiF_6.6H_2O$ quadrupole splitting data by using $1-R = 0.855$ and $\gamma_\infty = 12.07$ corresponding to Ingalls'[132] $\langle r^{-3}\rangle_{3d}$ value of 4.622 a.u. In order to evaluate the appropriate values

of γ_∞ and R we have expressed these in terms of the following polynomials:

$$R \text{ (or } \gamma_\infty) = \sum_{N=1}^{3,4 \text{ or } 5} a_N \langle r^{-3} \rangle_{3d}^{-N} \qquad \text{(IV.4)}$$

The values of various coefficients along with the respective average percentage error in the various fittings have been given in Table IV.4. In both the cases (R and γ_∞), we have utilized the exact polynomial to evaluate the values of R and γ_∞ at $\langle r^{-3} \rangle$ = 4.622 a.u.

The new value comes out to be 0.156 b which is in closer agreement with $Q(Fe^{57m})$ obtained from ferric compound data. We note here that in the interpretation[134] of the latter no account has been taken of the covalency effect although there is a good deal of evidence for such effects in the ferric systems. The present estimates of $Q(^{57m}Fe)$ may be compared with the theoretical estimate[177] of 0.16±0.02 b based on nuclear-model calculations.

IV.2.D The Results of R Factor Calculations for A Few Other Ions of Interest in Mössbauer Spectroscopy

In Table IV.5 we have presented the results of our calculations of R factors including the exchange contributions for $Ru^{2+}(4d^6)$, $Os^{2+}(5d^6)$, $Pr^{3+}(4f^2)$, $Tm^{3+}(4f^{12})$ and $Np^{6+}(5f^1)$ ions, which are of interest in Mössbauer studies. The small

Table IV.4: The values of various coefficients, a_N, defining R, γ_∞ and $(1-R)\langle r^{-3}\rangle_{3d}$ in terms of polynomials* in $\langle r^{-3}\rangle_{3d}$, $\langle r^{-3}\rangle_{3d}$ and ρ_m respectively. APE denotes the average percentage error in each fit.

Coefficients	R			γ_∞			$(1-R)\langle r^{-3}\rangle_{3d}$	
	N = 3	N = 4	N = 5	N = 3	N = 4	N = 5	N = 4	N = 5
a_1	1.14968	1.24624	1.73606	90.95005	102.79519	113.32834	-365.05260	-1027.30895
a_2	-4.28426	-5.86794	-17.05343	-285.63862	-479.90153	-834.61981	730.95160	2548.88001
a_3	9.33127	17.22054	107.63916	483.22657	1450.96739	4313.35606	-488.03859	-2354.99749
a_4		-12.01283	-318.37110		-1473.55779	-11188.90540	109.80178	959.93666
a_5			367.20465			11644.93049		-144.82862
APE	0.4	0.3	Exact	0.6	0.1	Exact	0.3	Exact

* See equations (IV.2) and (IV.3) of text.

Table IV.5: The separate direct and exchange contributions R_D and R_E to R for $Ru^{2+}(4d^6)$, $Os^{2+}(5d^6)$, $Pr^{3+}(4f^2)$, $Tm^{3+}(4f^{12})$ and $Np^{6+}(5f^1)$ ions. R_E values appear in the parentheses below the R_D values

Perturbation	Ru^{2+}	Os^{2+}	Pr^{3+}	Tm^{3+}	Np^{6+}
1s→d	0.0148	0.0083	0.0114	0.0097	0.0072
	(-0.0008)	(-0.0005)	(0.0000)	(0.0000)	(-0.0000)
2s→d	0.0180	0.0082	0.0252	0.0208	0.0145
	(-0.0059)	(-0.0027)	(-0.0008)	(-0.0008)	(-0.0009)
3s→d	0.0096	0.0044	0.0328	0.0249	0.0139
	(-0.0005)	(-0.0005)	(-0.0054)	(-0.0044)	(-0.0026)
4s→d	0.0082	0.0038	0.0177	0.0117	0.0091
	(-0.0037)	(-0.0002)	(-0.0038)	(-0.0023)	(-0.0003)
5s→d		0.0042	0.0036	0.0028	0.0187
		(-0.0019)	(-0.0004)	(-0.0003)	(-0.0046)
6s→d					0.0037
					(-0.0006)
2p→f	0.0299	0.0149	0.0351	0.0294	0.0209
	(-0.0077)	(-0.0041)	(-0.0008)	(-0.0008)	(-0.0009)
3p→f	0.0164	0.0077	0.0537	0.0411	0.0235
	(-0.0011)	(-0.0006)	(-0.0078)	(-0.0065)	(-0.0041)
4p→f	0.0123	0.0065	0.0323	0.0224	0.0151
	(-0.0051)	(-0.0005)	(-0.0068)	(-0.0046)	(-0.0006)
5p→f		0.0055	0.0072	0.0043	0.0171
		(-0.0023)	(-0.0009)	(-0.0005)	(-0.0041)

Table IV.5 (...Contd.)

Perturbation	Ru^{2+}	Os^{2+}	Pr^{3+}	Tm^{3+}	Np^{6+}
6p→f					0.1202
					(-0.0315)
3d→s	-0.0034	-0.0037	-0.0165	-0.0124	-0.0073
	(0.0026)	(0.0012)	(0.0011)	(0.0008)	(0.0007)
4d→s	0.0021	-0.0014	-0.0116	-0.0087	-0.0024
		(0.0006)	(0.0029)	(0.0022)	(0.0004)
5d→s		-0.0001			0.0005
					(-0.0004)
3d→g	0.0225	0.0110	0.0667	0.0526	0.0324
	(-0.0028)	(-0.0012)	(-0.0077)	(-0.0065)	(-0.0046)
4d→g	(0.0059)	0.0085	0.0401	0.0287	0.0203
		(-0.0007)	(-0.0081)	(-0.0056)	(-0.0005)
5d→g		0.0028			0.0160
		-			(-0.0036)
4f→p		-0.0045			-0.0146
		(0.0003)			(0.0021)
4f→h		0.0096			0.0256
		(-0.0006)			(-0.0020)
R_D(Ang):	0.1233	0.0857	0.2977	0.2273	0.3344
R_E(Ang):	(-0.0222)	(-0.0137)	(-0.0385)	(-0.0293)	(-0.0581)
Tot (Ang)	0.1011	0.0720	0.2592	0.1980	0.2763

Table IV.5 (...Contd.)

Perturbation	Ru^{2+}	Os^{2+}	Pr^{3+}	Tm^{3+}	Np^{6+}
2p→p	-0.1076	-0.0430	-0.2222	-0.1795	-0.1183
	(0.0847)	(0.0299)	(0.0190)	(0.0188)	(0.0175)
3p→p	-0.1386	-0.0579	-0.5876	-0.3961	-0.1576
	(-0.0161)	(+0.0221)	(0.2399)	(0.1741)	(0.0524)
4p→p	0.0183	-0.1299	0.1903	0.1974	-0.2367
	(0.0613)	(-0.0482)	(-0.0769)	(-0.0930)	(0.0028)
5p→p		-0.0275	0.5130	0.3279	-0.1093
		(+0.1618)	(-0.1684)	(-0.0941)	(0.1432)
6p→p					0.4390
					(-0.1943)
3d→d	-0.0336	-0.0110	-0.1462	-0.1015	-0.0470
	(-0.0598)	(-0.0189)	(0.0736)	(0.0542)	(0.0348)
4d→d	0.0291	-0.0374	0.0648	0.0573	-0.0580
		(-0.0438)	(-0.0402)	(-0.0372)	(-0.0036)
5d→d		0.0281			-0.0010
					(+0.0330)
4f→f		-0.0283			-0.0278
		(0.0146)			(-0.0392)
R_D(Rad)	-0.2324	-0.3069	-0.1879	-0.0945	-0.3167
R_E(Rad)	(0.0701)	(0.1175)	(0.0470)	(0.0228)	(0.0466)
Tot (Rad)	-0.1623	-0.1894	-0.1409	-0.0717	-0.2697
Net R	-0.0612	-0.1174	+0.1183	+0.1264	+0.0066

net antishielding effect of -0.0612 and -0.1174 is obtained in the cases of $Ru^{2+}(4d^6)$ and $Os^{2+}(5d^6)$, respectively and these results are believed to be accurate to within 20%.

The earlier calculations on rare earth ions have not included the exchange terms. It is clear from Table IV.5 that although the individual exchange contributions are important the net effect adds up to a small fraction of the total direct contribution. Thus, in the cases of Pr^{3+} and Tm^{3+} the R values become +0.1183 and +0.1264 respectively, while without exchange the corresponding values are +0.1098 and 0.1328 respectively. These R values are in reasonably good agreement with the experimental estimate[152,153] of R $\sim$0.2-0.4.

In the case of $Np^{6+}(5f^1)$, the present calculations using nonrelativistic HFS wave functions give a net shielding of R = +0.0066. The only literature value available in this case is the estimate of +0.32 obtained by Dunlap et al.[149] from Mössbauer studies on $(UO_2)^{2+}$ and $(NpO_2)^{2+}$ coordination compounds. These authors, however, assumed that the difference in the principal component of the field gradient tensor in the two cases is directly related to the valence electron contribution due to 5f shell in Np^{6+}. The relativistic effects for the actinides have been shown to be quite significant ($\sim$60%) in γ_∞ calculations and we expect an effect of similar magnitude for R as well.

IV.2.E Ionic Antishielding Factors in Metals and Their Relevance to Mössbauer and TDPAC Studies

In recent years a number of experimental studies on nuclear quadrupolar interactions in metals have been made using especially the Mössbauer and TDPAC methods. In the interpretation of quadrupole coupling data on metals and dilute alloys it is more appropriate to include the screening effects of the conduction electrons in calculating γ_∞ values. Most of the calculations reported so far in the literature correspond to free ion cases, whereas, it is well known that in metals the core electrons are more similar to those in the neutral atoms with appropriate electronic configurations given by $3d^n4s^1$, $4d^n5s^1$ and $5d^n6s^2$ for the three transition metal series.

We have calculated γ_∞ using moment-perturbed wave functions for the neutral atom cores in third-, fourth-, and fifth row elements in the periodic table. The transition metal elements have been assumed to be in $3d^n4s^1$, $4d^n5s^1$ and $5d^n6s^2$ configurations in these three rows, respectively. We have also calculated γ_∞ contribution due to single electron (in the cases where d shell is occupied) by using the c coefficients (vide eqn. II.32) as $\frac{1}{10}$ c(nl→l). These results have been given in Table IV.6.

Das and coworkers[139] have found that the use of appropriate neutral atom wave functions for Zn and Cd increases γ_∞ by 10% over the values based on Zn^{2+} and Cd^{2+} wave functions. In the

Table IV.6: Sternheimer antishielding factor γ_∞ corresponding to the closed shells and per d electron in the elements of third, fourth and fifth row of the periodic table. The transition metal elements have been assumed in $3d^n4s^1$, $4d^n5s^1$ and $5d^n6s^2$ electron configuration respectively.

Ion	Core (A)	Contribution per 3d electron	Ion	Core (Kr)	Contribution per 4d electron	Ion	Core (Xe)	Contribution per 5d electron
K	-17.86	-	Rb	-49.34	-	Cs	-99.65	-
Ca	-13.67	-	Sr	-38.93	-	Ba	-81.07	-
Sc	-13.37	-4.57	Y	-36.00	-9.12	La	-72.66	-5.42
Ti	-12.21	-2.93	Zr	-32.51	-5.54	Hf	-61.50	-5.11
V	-11.29	-2.21	Nb	-29.75	-3.97	Ta	-56.9	-4.92
Cr	-10.53	-1.80	Mo	-27.57	-3.09	W	-52.83	-4.15
Mn	-9.90	-1.53	Tc	-25.65	-2.56	Re	-49.60	-3.52
Fe	-9.34	-1.38	Ru	-24.10	-2.20	Os	-46.83	-3.09
Co	-8.85	-1.27	Rh	-22.59	-1.93	Ir	-44.29	-2.77
Ni	-8.43	-1.17	Pd	-21.55	-1.73	Pt	-42.23	-2.51
Cu	-8.04	-1.10	Ag	-20.52	-1.57	Au	-40.28	-2.30
Zn	-7.33	-0.58	Cd	-18.98	-1.07	Hg	-38.52	-2.13

Table IV.6 (...Contd.)

Ion	Core (A)	Contribution per 3d electron	Ion	Core (Kr)	Contribution per 4d electron	Ion	Core (Xe)	Contribution per 5d electron
Ga	-6.64	-0.31	In	-17.28	-0.79	Tl	-35.22	-1.66
Ge	-6.03	-0.27	Sn	-16.18	-0.63	Pb	-33.27	-1.32
As	-5.51	-0.21	Sb	-14.76	-0.52	Bi	-31.03	-1.12
Se	-5.06	-0.17	Te	-13.70	-0.45	Po	-29.14	-0.96

case of highly positive ions such as those in the intermediate regions in the three rows considered here, one expects a more significant difference. Indeed, the neutral atom values for Ti, V and Cr are -13.4, -12.2 and -11.3 which are to be compared with -8.8, -7.4 and -6.4 for Ti^{4+}, V^{5+} and Cr^{6+} as obtained in Table III.1. Similarly, in the cases of Zr, Nb, and Mo, the γ_∞ values of -32.5, -29.7 and -27.6 are significantly larger in magnitude than the corresponding ionic values of -26, -22 and -19.

The universal correlation obtained by Raghavan, Kaufmann and Raghavan[140] emphasizes the role of $(1 - \gamma_\infty)$ in determining the extra-ionic field gradient contribution in metals and alloys. From the available experimental data on e^2qQ on metals and dilute alloys obtained mainly from Mössbauer and TDPAC studies, Raghvan et al.[140] have extracted the extra-ionic field gradient, eq', by subtracting the antishielding corrected lattice field gradient from the total field gradient according to

$$eq' = eq - (1 - \gamma_\infty)\, eq_{lat} \qquad \text{(IV.5)}$$

where q_{lat}'s were calculated using the point charge model. These authors have found that eq' is universally proportional to the ionic counterpart $(1 - \gamma_\infty)\, eq_{lat}$ and is opposite in sign. Such a proportionality indicates that the conduction electron

contribution to the field gradient in metals and dilute alloys cannot be adequately represented by $(1-R)\ q_{cond}$. Das and coworkers[139] have noted that the calculation of the field gradient for Cd metal based on the usual expression,

$$q = (1 - \gamma_\infty)\ q_{lat} + (1-R)\ q_{cond} \qquad \text{(IV.6)}$$

leads to a value of the nuclear quadrupole moment for ^{111}Cd which is three times larger than that derived from ionic data. Patnaik, Thompson and Das[178] have found in a detailed analysis of the field gradient contribution from the conduction electrons in Zn and Cd metals that the plane wave component is antishielded by $\frac{1}{2}(1 - \gamma_\infty)$ instead of the usual factor of $(1-R)$. Now, such a prescription emphasizes all the more strongly the need of using more appropriate values of γ_∞ in the cases where the antishielding effect is sizeable. We, therefore, strongly feel that the presently calculated γ_∞ values are more appropriate to the cases of metals and alloys, and should be used to interpret the quadrupole coupling data in these systems.

CHAPTER V

Sternheimer Hexadecapole Antishielding Factors: nd-(n=3,4,5) Shell Ions, 4f-, and 5f-Shell Ions

CHAPTER V

Sternheimer Hexadecapole Antishielding Factors: nd-(n=3,4,5) Shell Ions, 4f-, and 5f-Shell Ions*

V.1 Introduction

Nuclei with spin $I \geq 2$ can possess a nonvanishing electric hexadecapole moment, H. The nuclear calculations[179,180] using Nilsson model give H values of the order of 0.5-5b^2 for the nuclei in rare earth (lanthanide) and transuranium (actinide) regions. Nuclear hexadecapole deformations have been studied by Coulomb excitation methods[181] for several Wolfram, lanthanide and actinide nuclei. However, the values of H cannot be always derived from such measurements. Dankwort, Ferch and Gebauer[150d] have measured H in the ground state of holmium atom using atomic beam magnetic resonance technique. In solid state the interaction of H with the fourth derivative of electrostatic potential at the nucleus, i.e. the nuclear hexadecapole coupling $e^4m_{16}H$ has been first measured by Wang[150a] for ^{123}Sb ($I = \frac{7}{2}$) in $SbBr_3$ via NQR. Mahler and

---

* The work presented in this chapter has been/is to be published in the following papers:
(1) K. D. Sen and P. T. Narasimhan, Phys. Rev. A 11, 1162 (1975); (2) Phys. Rev. A (to be communicated); (3) Pramāṇa (to be communicated).

coworkers[150b] have detected ultrasonically-induced hexadecapole transition of ^{115}In in InAs. More recently, Dinesh and Smith[150c] have estimated the $e^4m_{16}H$ for ^{93}Nb in $NbCl_5$ via pulsed NQR studies.

The effects of nuclear electric hexadecapole moments are generally masked by the more dominant effects due to the nuclear quadrupole moment ($e^2qQ/e^4m_{16}H \sim 10^5$ for ^{121}Sb and ^{123}Sb in $SbBr_3$). Sternheimer[8a,b] has shown for the first time that the hexadecapole moment induced in the closed d and f shells can be represented, analogous to the quadrupolar case, as

$$H_{ind} = -\eta_\infty H \qquad (V.1)$$

where η_∞ can be as large as 10^3-10^4 for medium and heavy atoms with closed d shells. For example, η_∞ for Cu^+, Ag^+, Cs^+, In^{3+}, Ho^{2+} and Hg^{2+} has been calculated to be -1200, -8050, -670, -3791, -660, and -63000 respectively. A few values[150a,c] of $e^4m_{16}H$ in solids are available and it is of interest to calculate η_∞ in the cases of several other experimentally important ions.

In addition to the direct hexadecapolar perturbation due to the nuclear hexadecapole moment (cf eq. V.1), the quadrupolar perturbation taken to second-order[8c] also has the transformation properties resembling the hexadecapole moment. In the complete interpretation of hexadecapole interaction therefore

it is essential to include the second-order quadrupolar effects. The induced hexadecapole moment due to the second order quadrupolar effects can be written[3c] as

$$H^{Q}_{ind} = H_{11} + H_{02} \qquad (V.2)$$

H_{11} arises from the electron density u_1^2, where u_1 is the first-order quadrupolar perturbation of u_o and is given by

$$H_{11} = 16\, C^{H}(nl \rightarrow l)\, Q^2\, K_{11} \qquad (V.3)$$

with $$K_{11} = \int_o^\infty u_1^{\,2}\, r^4\, dr \qquad (V.4)$$

$C^{H}(nl \rightarrow l)$ is the result of integration over the angular variables and the summation over magnetic substates. For $(nd \rightarrow d)^2$ and $(nf \rightarrow f)^2$, C^{H} values are 0.373 and 0.749 respectively.

H_{02} arises from the second-order perturbation u_2 of the u_o which is determined from the equation,

$$(H_o - E_o)\, u_2 = -(H_1 - E_1)\, u_1 + E_2 u_o \qquad (V.5)$$

and is given by

$$H_{02} = 32\, C^{H}(nl \rightarrow l_1 \rightarrow l_2)\, Q^2\, K_{02} \qquad (V.6)$$

where

$$K_{02} = \int_o^\infty u'_o\, u'_2\, r^4\, dr \qquad (V.7)$$

$$l_2 = l_1 \quad \text{or} \quad l_2 = l_1 \pm 2.$$

Sternheimer[8c,d] has shown that for Ho, the ratio $H^{Q}_{ind}/-\eta_{\infty}H \sim 0.34$, which shows that the second-order quadrupolar effects are quite significant as compared to the direct hexadecapolar effects due to H and therefore H^{2}_{ind} should be considered in interpreting the data on hexadecapole interaction.

Sternheimer[8d] has recently calculated the valence shielding factor (R_H) corresponding to the hexadecapolar polarization in the case of holmium atom as +0.24. The shielding-corrected value of H for holmium atom as obtained from the atomic beam experiments of Dankwort et al.[150d] then becomes 1.06 b^2. We note here that η_{∞} and R_H values are significantly larger than the corresponding values of γ_{∞} and R in the quadrupolar case. The hexadecapole interaction data on free atoms are now becoming available from atomic beam magnetic resonance experiment and in order to derive the nuclear hexadecapolar moment from such data it is essential to have the knowledge of reliable values of R_H.

V.2 Results and Discussion

V.2.A Sternheimer Hexadecapole Antishielding Factors for nd^1, nd^5 and nd^{10} Ions

It appeared to us that nuclei with large η_{∞} and favourable natural abundance, quadrupole moment, magnetic resonance sensitivity should be more likely candidates for studying nuclear

Sternheimer[8c,d] has shown that for Ho, the ratio $H^{Q}_{ind}/-\eta_{\infty}H \sim 0.34$, which shows that the second-order quadrupolar effects are quite significant as compared to the direct hexadecapolar effects due to H and therefore H^{2}_{ind} should be considered in interpreting the data on hexadecapole interaction.

Sternheimer[8d] has recently calculated the valence shielding factor (R_H) corresponding to the hexadecapolar polarization in the case of holmium atom as +0.24. The shielding-corrected value of H for holmium atom as obtained from the atomic beam experiments of Dankwort et al.[150d] then becomes 1.06 b^2. We note here that η_{∞} and R_H values are significantly larger than the corresponding values of γ_{∞} and R in the quadrupolar case. The hexadecapole interaction data on free atoms are now becoming available from atomic beam magnetic resonance experiment and in order to derive the nuclear hexadecapolar moment from such data it is essential to have the knowledge of reliable values of R_H.

V.2 Results and Discussion

V.2.A Sternheimer Hexadecapole Antishielding Factors for nd^{1}, nd^{5} and nd^{10} Ions

It appeared to us that nuclei with large η_{∞} and favourable natural abundance, quadrupole moment, magnetic resonance sensitivity should be more likely candidates for studying nuclear

hexadecapole interaction in ionic solids via NQR. For this purpose we have calculated η_∞ values for a number of positive ions using the moment-perturbed method of Sternheimer described in Chapter II. In Table V.1, we have presented our values of individual radial contribution to η_∞, $\langle r^{-5} \rangle_{nd}$, and total for all the ions considered by us.

In all these cases we have found that the nd→d perturbations contribute most significantly and nf→f perturbations produce a much weaker effect. In Fig. V.1 we have plotted η_∞ vs Z for 3d, 4d, and 5d ions. It is found that in these three cases the η_∞ value attains a maximum at Cu^+, Ag^+, Au^+, respectively, where the nd shell is complete and most external. With further increase in Z, η_∞ again decreases. Sternheimer[8b] has earlier observed a similar trend in the case of 4d ions. With increase in ionic charge within an isoelectronic series it is found that η_∞ values get drastically reduced.

The angular contributions to η_∞ in the case of Cu^+, Ag^+, and Au^+ have been estimated[8] from

$$(\gamma_{\infty \text{ang}} / \eta_{\infty, \text{ang}})_{HFS} = \frac{9}{5}$$

The values of $\gamma_{\infty, \text{ang}}$ are obtained as 0.58, 0.79 and 1.15 for Cu^+, Ag^+ and Au^+ respectively. The neglect of angular contribution therefore does not cause significant inaccuracy in η_∞ values reported in Table V.1. In the following discussion we shall assume $\eta_\infty = \eta_{\infty, \text{radial}}$.

Table V.1: Individual radial contributions to the total nuclear hexadecapole anti-shielding factor $\eta_\infty . \langle \frac{1}{r^5} \rangle_{nd}$ gives the expectation value of $\frac{1}{r^5}$ over the outermost nd orbital.

Ion	Perturbation 3d→d	4d→d	4f→f	5d→d	5f→f	6d→d	$\langle \frac{1}{r^5} \rangle_{nd}$	η_∞, radial
Ti^{3+}	-26.234						44.458	-26.234
Mn^{2+}	-274.63						101.13	-274.63
Cu^{+}	-1471.7						262.76	-1471.74
Zn^{2+}	-352.51						361.38	-352.51
Ge^{4+}	-161.58						637.85	-161.58
Rb^{+}	-57.688						1943.1	-57.688
Zr^{3+}	-35.668	-711.85					308.36	-747.53
Nb^{5+}	-30.865						4085.20	-30.865
Tc^{2+}	-25.560	-3947.5					563.04	-3973.1
Ag^{+}	-18.194	-9562.3					1138.2	-9580.4
In^{3+}	-15.757	-2859.1					1841.3	-2875.0
Sb^{3+}	-13.835	-1686.1					2724.2	-1699.9
Cs^{+}	-11.018	-866.58					5319.1	-877.60
Hf^{3+}	-5.833	-376.69	-70.031	-6794.8			2504.2	-7247.4

Table V.1 (...Contd.)

Ion	Perturbation	3d→d	4d→d	4f→f	5d→d	5f→f	6d→d	$\langle \frac{1}{r^5} \rangle_{nd}$	η_∞, radial
Re^{2+}		-5.376	-309.13	-33.262	-34841.0			3766.7	-35189.0
Au^{+}		-4.859	-242.77	-17.010	-71279.0			6208.1	-71544.0
Hg^{2+}		-4.743	-229.37	-14.762	-37141.0			7606.8	-37390.0
Bi^{3+}		-4.423	-194.90	-10.297	-14506.0			12372.0	-14716.0
Fr^{+}		-4.052	-160.165	- 7.116	-7818.1			20687.0	-7989.4
Th^{3+}		-3.808	-139.98	-5.674	-4956.0		-28452.0	3860.0	-33557.0
Am^{2+}		-3.458	-115.49	-4.270	-4067.2	-303.674		44280.0	-4994.1

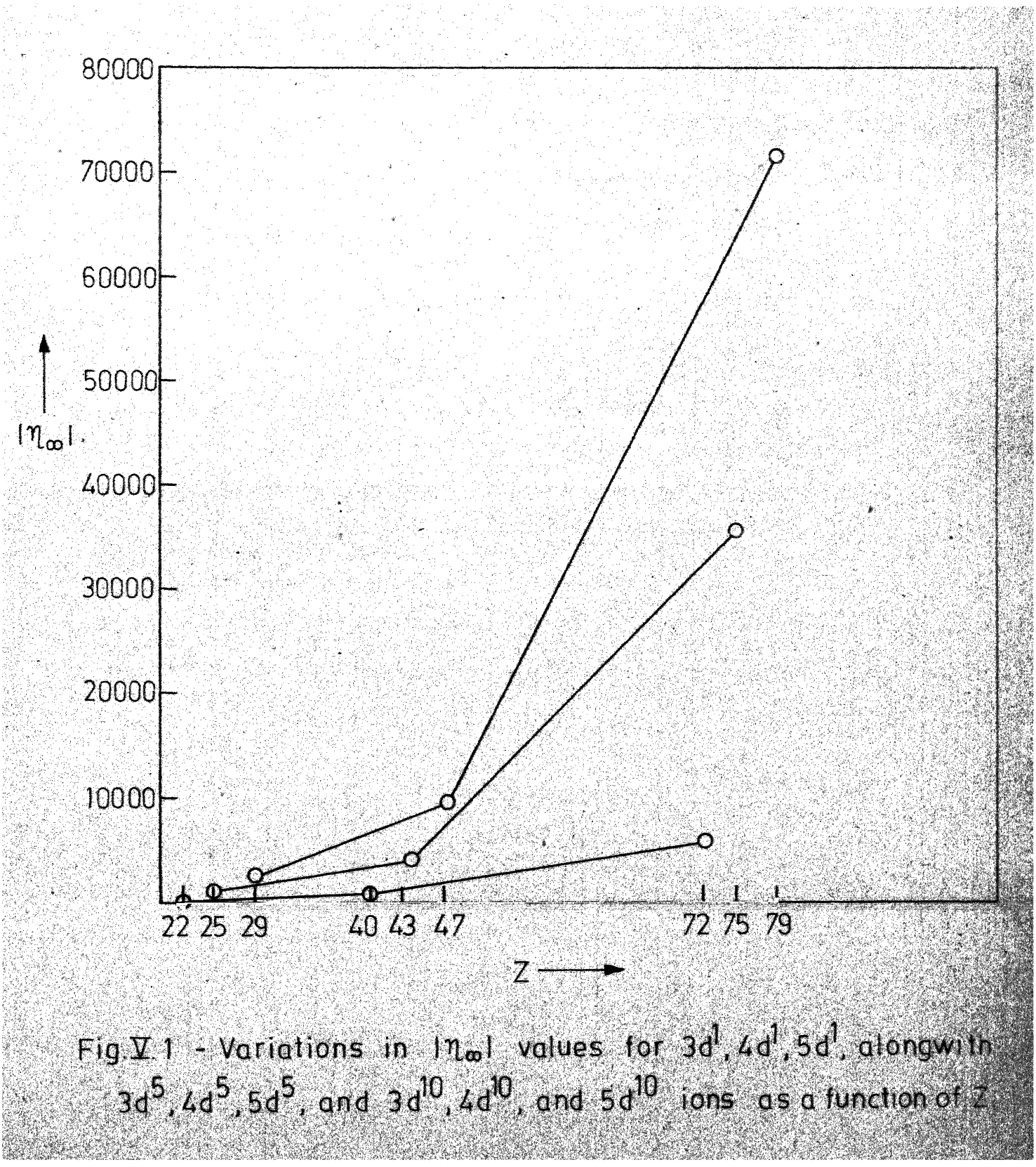

Fig V.1 - Variations in $|\eta_\infty|$ values for $3d^1, 4d^1, 5d^1$, alongwith $3d^5, 4d^5, 5d^5$, and $3d^{10}, 4d^{10}$, and $5d^{10}$ ions as a function of Z

In Table V.2 we have compiled the values of mass number, nuclear spin, natural isotopic abundance, nuclear moment, nuclear magnetic sensitivity, nuclear quadrupole moments, and the presently calculated η_∞ values for some favourable cases up to the rare earth ions. It appears from Table V.2 that Bi^{3+} and Re^{2+} are the most suitable candidates for studying hexadecapole interaction. The ions Sb^{3+}, In^{3+}, and Mn^{2+} also appear to be prominent in this regard.

In the recent NQR studies on ^{93}Nb in $NbCl_5$, Dinesh and Smith[150c] have estimated the hexadecapole coupling constant as 372 kHz and 396 kHz at 2/m and m Nb sites, respectively. In the case of a perfectly ionic compound, niobium in $NbCl_5$ would exist as a closed shell ion of Nb^{5+} ($3d^{10}4s^24p^6$) and only 3d→d perturbation would contribute to the η_∞ value. From Table V.1 we obtain $\eta_\infty = -30.86$ for Nb^{5+} which is a small value. In Table V.3 we have presented the η_∞ values corresponding to Nb^+, Nb^{2+}, Nb^{3+}, Nb^{4+} and Nb^{5+} ions, respectively. In actual case, however, one expects significant covalency effects in $NbCl_5$ and it is therefore natural to anticipate contribution to η_∞ due to the low-lying 4d orbitals in niobium. The contribution to η_∞ due to the single 4d electron in the case of Nb^{4+} ($3d^{10}4s^24p^64d^1$) is calculated to be -390.52 and this makes the total η_∞ value as -421.77 which is an order of magnitude larger than η_∞ for Nb^{5+} case. Due to the significant increase in value as a result of charge transfer covalency it is not surprising that the hexadecapole interaction in $NbCl_5$ has been

Table V.2: Relevant data on some systems containing nuclei with hexadecapole moments

Ion	A	I	α%	μ_{BM}	S	Ω	$-\eta_\infty$
$Ti^{3+}(3d^1)$	47	5/2	7.75		2.09×10^{-3}		26.2
	49	7/2	5.57		3.76×10^{-3}		26.2
$Mn^{2+}(3d^5)$	55	5/2	100.0	3.46	0.178	0.4 - 0.6	274.6
$Ge^{4+}(3d^{10})$	73	9/2	7.61		1.4×10^{-3}	-0.22	161.6
$Rb^{+}(3d^{10})$	85	5/2	72.8		1.05×10^{-2}	0.24 -0.31	57.7
$Zr^{3+}(4d^1)$	91	5/2	11.23		9.4×10^{-3}		747.5
$Nb^{5+}(3d^{10})$	93	9/2	100.0	6.147	0.432	-(0.16- 4)	26.0

Table V.2 (...Contd.)

Ion	A	I	α%	μ_{BM}	S	Q	$-\eta_\infty$
$In^{3+}(4d^{10})$	113	9/2	4.2	5.507	0.345	0.75-1.18	2875.0
	115	9/2	95.8		0.347	0.76-1.2	
$Sb^{3+}(4d^{10})$	121	5/2	57.2	3.341	0.16	-(0.5-1.2)	1700.0
	123	7/2	42.8	2.533	4.57×10^{-2}	-(0.68-1.5)	
Cs^{+} $(4d^{10})$	133	7/2	100.0		4.74×10^{-2}	-0.3×10^{-2}	877.0
$Hf^{3+}(5d^{1})$	177	7/2	18.4		6.38×10^{-4}	3.0	7247.4
	179	9/2	13.8		2.16×10^{-4}	3.0	
$Re^{2+}(5d^{5})$	185	5/2	37.0	3.143	0.133	2.9	35189.0
	187	5/2	63.0	3.147	0.137	2.7	
$Bi^{3+}(5d^{10})$	209	9/2	100.0	4.037	0.137	-0.4	14716.0

A : Mass Number, I : Nuclear spin, α % : Natural Isotopic Abundance, μ_{BM} : Nuclear Moment (in B.M.), S: Sensitivity at constant field relative to an equal number of protons, Q : Nuclear Quadrupole Moment (10^{-24} cm^2).

Table V.3: Individual radial contributions to the total nuclear hexadecapole antishielding factor η_∞ for Nb^+, Nb^{2+}, Nb^{3+}, Nb^{4+}, and Nb^{5+} ions. $\langle \frac{1}{r^5} \rangle_{nd}$ gives the expectation value of $\frac{1}{r^5}$ over the outermost nd orbital.

Ion Perturbation	3d→d	4d→d	$\langle \frac{1}{r^5} \rangle_{nd}$	η_∞, radial
$Nb^+(4d^4)$	-31.813	-11039.1	299.05	-11071.0
$Nb^{2+}(4d^3)$	-31.716	-3300.8	340.29	-3332.5
$Nb^{3+}(4d^2)$	-31.531	-1209.8	399.07	-1241.3
$Nb^{4+}(4d^1)$	-31.249	-390.52	451.11	-421.77
$Nb^{5+}(3d^{10})$	-30.865		4085.2	-30.865

detected[150c] since the values of the other parameters in Table V.2 are quite favourable in this case.

V.2.B Sternheimer Hexadecapole Antishielding Factors for Rare Earths and Actinides

Extensive evidence has been obtained[182] for the existence of hexadecapole deformation in the nuclei of rare earth and actinide region. We have therefore calculated η_∞ values for all the tripositive rare earth (excepting Nd^{3+}) and tetrapositive actinide ions using nonrelativistic HFS wave functions. We note here that the relativistic effects will be extremely important in this region as has been already seen in the case of γ_∞. In any case, the presently calculated values should prove to be useful in making quantitative estimates of relativistic effects when the relativistic calculations become available. Our results of η_∞ for rare earth and actinide series are presented in Table V.4. As is evident from these values, η_∞ for tripositive lanthanides and tetrapositive actinides can be taken as approximately constant at -550 ($\pm$50) and -4500 ($\pm$500) respectively. Such a trend has already been observed in the case of γ_∞ for these ions where a value of -80 and -100 has been arrived at by similar calculations. The approximate constancy of γ_∞ and η_∞ in these regions can be qualitatively explained on the basis of almost similar sizes of the ions within each series.

Table V.4: Hexadecapole antishielding factors for the lanthanide and actinide ions

Ion	Configuration	$-\eta_\infty$
Ce^{3+}	$4f^1$	616.61
Pr^{3+}	$4f^2$	597.54
Nd^{3+}	$4f^3$	- SCF Program does not converge
Pm^{3+}	$4f^4$	567.54
Sm^{3+}	$4f^5$	554.72
Eu^{3+}	$4f^6$	545.31
Gd^{3+}	$4f^7$	536.37
Tb^{3+}	$4f^8$	530.21
Dy^{3+}	$4f^9$	524.28
Ho^{3+}	$4f^{10}$	519.59
Er^{3+}	$4f^{11}$	516.01
Tm^{3+}	$4f^{12}$	513.51
Yb^{3+}	$4f^{13}$	511.86
Lu^{3+}	$4f^{14}$	511.35

Table V.4 (...Contd.)

Ion	Configuration	$-\eta_\infty$(Free)	$-\eta_\infty$(crystal Ion)
Th^{4+}	$5f^0$	5002.27	
Pa^{4+}	$5f^1$	4753.18	7550.9
U^{4+}	$5f^2$	4534.68	
Np^{4+}	$5f^3$	4347.64	
Pu^{4+}	$5f^4$	4176.17	
Am^{4+}	$5f^5$	4024.16	
Cm^{4+}	$5f^6$	3892.54	
Bk^{4+}	$5f^7$	3765.39	6904.94
Cf^{4+}	$5f^8$	3659.01	
Es^{4+}	$5f^9$	3553.23	
Fm^{4+}	$5f^{10}$	3459.47	
Md^{4+}	$5f^{11}$	3377.36	
No^{4+}	$5f^{12}$	3296.44	
Lw^{4+}	$5f^{13}$	3194.12	5250.99
Hypothetical	$5f^{14}$	3155.77	

V.2.C Effect of Crystalline Potential on Hexadecapole Antishielding Factors

We have estimated the effect of lattice potential on using the Watson model (see Chapt. II.2.B) for Pa^{4+}, Bk^{4+} and Lw^{4+}. These η_∞ values corresponding to the core electrons have been given in Table V.4. Similar to the case in calculations we have found that in the cases of positive ions in crystals as a result of expansion of electron density, values get enhanced with respect to the free ion values. The enhancement in η_∞ values due to crystal potential is found to be ~150%. Such a dramatic enhancement obtained in η_∞ values for actinide ions in solids calls for a need to investigate the hexadecapole interaction in the cases of actinide nuclei in solids.

V.2.D Second Order Quadrupolar Effects, H_{11}: Free Ions and Ions in Crystal

The additional induced hexadecapole moment H_{11} (eq. V.3) has been calculated for Pa^{4+}, Bk^{4+} and Lw^{4+} using free and crystalline wave functions. These values have been presented in Table V.5. It is evident from these values that the $(5f \rightarrow f)^2$ contribution to H_{11} gets significantly enhanced by an order of magnitude as a result of the crystalline potential. We have not calculated the second-order contributions corresponding to H_{02} (eq. V.5) and it is difficult to comment about the

Table V.5: The second order quadrupolar effect H_{11} (eq. VI.2) for Pa^{4+}, Bk^{4+} and Lw^{4+} in free and crystalline states

Perturbation	$Pa^{4+}(5f^1)$		$Bk^{4+}(5f^7)$		$Lw^{4+}(5f^{13})$	
	Free ion	Crystal	Free ion	Crystal	Free ion	Crystal
3d→d	0.03	0.03	0.02	0.02	0.02	0.02
4d→d	1.08	1.06	0.77	0.76	0.58	0.57
5d→d	40.99	58.20	28.01	31.93	21.00	22.92
4f→f	0.18	0.17	0.11	0.10	0.07	0.07
5f→f	3.29	221.99	14.19	455.92	19.36	285.09
H_{11} (Total)	45.57	281.45	43.10	488.73	41.03	308.67

total H^{Q}_{ind}. We have tested our program for the calculation of H_{O2} corresponding to (4d→d→d) polarization in Ag^{+}. Complete calculations of H^{Q}_{ind} for rare earth ions are currently under progress. Our preliminary results, however, indicate that it is necessary to consider the second order quadrupolar effects in analysing the experimentally measured hexadecapole interaction.

CHAPTER VI

Sternheimer Shielding Factors for Atomic Quadrupole Moments: np(n+1)s Configuration of C, Si, Ge, Sn and Pb

CHAPTER VI

Sternheimer Shielding Factors for Atomic Quadrupole Moments: np(n+1)s Configuration of C, Si, Ge, Sn and Pb

VI.1 Introduction

The atomic quadrupole moment θ is the first non-vanishing multipole moment for an atom. The initial measurements of the atomic quadrupole moments of the $^2P_{3/2}$ ground states of Al and In have shown that the experimental values are slightly lower than the theoretical result of $\frac{1}{5}\langle r^2\rangle_{np}$ based on the central field theory due to Buckingham.[184] Sandars and Stewart[185] have measured the atomic quadrupole moments of Ne, Ar, Kr and Xe in $^3P_2$ states with configuration $np^5n's$, where n is the principal quantum number of the outermost p shell and n'=n+1. These authors have found that not only the experimental values are smaller in magnitude than the theoretical result of $\frac{1}{5}\langle r^2\rangle_{np}$ but there is a change in sign of the values for Kr and Xe. Sandars[186] has suggested that the significant shielding effect is probably due to the n's→d type polarization of the n's shell by the quadrupole moment of the np^5 vacancy.

* The work presented in this chapter has been published in the following paper:
K.D. Sen and P. T. Narasimhan, Phys. Rev. A (in press).

Denoting the quadrupole moment associated with the np^5 vacancy and the n's→d perturbation as θ (np) and θ(n's→d) respectively, one can define a shielding factor R_θ by,

$$R_\theta = - \frac{\theta(n's \rightarrow d)}{\theta(np)} \qquad \text{(VI.1)}$$

The total quadrupole moment, θ , of the atom is now given by,

$$\theta_{atom} = \theta(np) + \theta(n's \rightarrow d) = \theta(np)(1 - R_\theta). \quad \text{(VI.2)}$$

Sternheimer[13] has formulated the perturbation theory for such a shielding effect and calculated R_θ values up to second order for Ne, A, Kr, and Xe in the np^5n's configuration. These theoretical values of R_θ are in excellent agreement with the experimental results of Sandars and Stewart[185] which afford an important direct evidence on the existence and magnitude of Sternheimer shielding effects.

Theoretically, it is interesting to calculate R_θ values for the excited state atoms with a single electron each in np and n's shells. In this chapter we present the R_θ values for C, Si, Ge, Sn and Pb in the npn's excited state configuration with n=2 for C, n=3 for Si, n=4 for Ge, n=5 for Sn and n=6 for Pb.

VI.2 Method of Calculation

The following derivation is identical with the equations derived by Sternheimer in Ref. 13.

In Buckingham's[184] theory of quadrupole moments, the quadrupole moment, $\theta(np)$, associated with the np electron with magnetic quantum number m=+1 is given by the expectation value of $P_2 r^2$ over the np wave function. On integration over the angular variables, it can be shown that

$$\theta(np) = + \frac{1}{5} e \int_o^\infty u_{np}^2 \, r^2 \, dr \qquad \text{(VI.3)}$$

where e is the magnitude of the electron charge and u_{np} gives r times the radial wave function of the np electron with the normalization condition,

$$\int_o^\infty u_{np}^2 \, dr = 1 \qquad \text{(VI.4)}$$

The repulsive electrostatic quadrupolar interaction between the np electron and the n's electron in Rydberg units is given by

$$V(r_2, \theta_2) = +2 \{ \left(\frac{1}{r_2^3}\right) \int_o u_{np}^2 \, r_1^2 dr_1 + r_2^2 \int_{r_2}^\infty u_{np}^2 r_1^{-3} dr_1 \} P_2(\theta_2) \times \int (\theta_1^1)^2 \, P_2(\theta_1) \sin\theta_1 d\theta_1 \qquad \text{(VI.5)}$$

where (r_1, θ_1) and (r_2, θ_2) are the coordinates of np and n's electrons respectively, P_2 is the Legendre polynomial for l=2, and θ_1^1 is the spherical harmonic θ_1^m with l=1, m=1 obeying the normalization condition

$$\int_o^\pi (\theta_1^1)^2 \sin\theta \, d\theta = 1 \qquad \text{(VI.6)}$$

Integrating over θ_1 we get,

$$V(r_2, \theta_2) = \frac{2}{5} V_{np}(r_2) P_2(\theta_2) = H_1, \qquad \text{(VI.7)}$$

where $V_{np}(r_2)$ is minus the function in the square bracket of equation (VI.5). H_1 gives the perturbation due to the quadrupole potential of the np electron which polarizes the n's orbital to d states. The first order polarization (n's→d) is given by:

$$\{ -\frac{d^2}{dr^2} + \frac{6}{r^2} + V_o - E_o \} v_1' (n's \to d) = V_{np}(r)\, v_o'(r) \qquad \text{(VI.8)}$$

where $v_1'(n's \to d)$ and $v_o'(r)$ represent r times the radial part of the perturbed and the unperturbed wave functions respectively, V_o is the effective potential and E_o is the energy eigenvalue corresponding to the unperturbed n's shell. In eq. (VI.8) r_2 has been replaced by r for convenience. The term $V_o - E_o$ is replaced by the Sternheimer[6,7c] local approximation,

$$V_o - E_o = \frac{1}{v_o'} \frac{d^2 v_o'}{dr^2} \qquad \text{(VI.9)}$$

The quadrupole moment induced due to first order overlap density is given by,

$$\theta(n's \to d) = \frac{4}{25}(e) \{ \int_o^\infty v_o' (n's)\, v_1' (n's \to d)\, r^2 dr \} \qquad \text{(VI.10)}$$

From eq. (VI.1), the first-order shielding factor $R_{\theta,1}$ is given by,

$$R_{\theta,1} = \frac{-4}{5} \{ \int_o^\infty v_o'(n's)\, v_1' (n's \to d)\, r^2 dr \} / \langle r^2 \rangle_{np} \qquad \text{(VI.11)}$$

We note that eq. (VI.11) is effectively the same as the first-order contribution corresponding to the $np^5n's$ configuration, where $v_1'(n's\rightarrow d)$ are obtained by replacing V_{np} by $-V_{np}$ due to attraction between the np^5 vacancy and the n's electron.

There are two types of second-order contribution to R_θ. The first arises from the square of the first order perturbed density and is given by

$$R_{\theta,2a} = +\frac{8}{175}\,\frac{\int_o^\infty v_1'^2 r^2 dr}{\langle r^2\rangle_{np}} \qquad \text{(VI.12)}$$

The other arises from the second-order overlap density and is given by

$$R_{\theta,2b} = +\frac{16}{175}\,\frac{\int_o^\infty v_o' v_2'\, r^2 dr}{\langle r^2\rangle_{np}} \qquad \text{(VI.13)}$$

where v_2' is r times the radial part of the second-order perturbation which satisfies the following inhomogeneous equation,

$$\left\{ \frac{-d^2}{dr^2} + \frac{6}{r^2} + V_o - E_o \right\} v_2'(n's\rightarrow d) = V_{np} v_1'(n's\rightarrow d) \qquad \text{(VI.14)}$$

The total second-order contribution to R_θ is given by,

$$R_{\theta,2} = R_{\theta,2a} + R_{\theta,2b} \qquad \text{(VI.15)}$$

Finally, the total R_θ is given by,

$$R_\theta = R_{\theta,1} + R_{\theta,2} \qquad \text{(VI.16)}$$

The perturbed Hartree-Fock-Slater (HFS) wave functions corresponding to the excited state configuration were generated

over the 521 point mesh using a modified Herman-Skillman program.[159] It may be pointed out here that we have used an extended mesh of 521 points as compared to the usual 441 point mesh to satisfactorily describe the external radial wave functions for the excited states considered in this chapter. The integration of the difference equation corresponding to the inhomogeneous eq. (VI.8) was started at the last mesh point r_1 of the unperturbed function and $v_1'(r_1)$ was gradually varied in an iterative way till the solution became well-behaved near r=0. The appropriate boundary condition near r=0 is given by $v_1'(r) \propto r^3$ as $r \to 0$ and $v_1'(0)=0$. In a similar manner, using $v_1'(n's \to d)$ and V_{np} obtained previously, the second-order perturbed wave function $v_2'(n's \to d)$ is obtained by solving eq. (VI.14). Three to four iterations were sufficient to achieve the required boundary condition.

VI.3 Results and Discussion

In Table VI.1 we have listed the energy eigenvalue corresponding to n's orbital in Rydberg units, the expectation value r^2 over the np electron wave function, the first-order shielding factor $R_{\theta,1}$, the total second-order contribution $R_{\theta,2}$, and the total atomic quadrupole shielding factor R_θ for all the cases considered by us. The total R_θ value is calculated as 1.041 for C, 1.390 for Si, 1.371 for Ge, 1.616 for Sn and 1.703 for Pb.

Table VI.1: Values of the atomic quadrupole shielding factor R_θ and other relevant quantities

Atom	State	$-E_{n's}$(Ry)	$\langle r^2 \rangle_{np}$	$R_{\theta,1}$	$R_{\theta,2}$	R_θ
C	2p3s	0.2686	2.560	1.025	0.016	1.041
Si	3p4s	0.2268	6.545	1.345	0.045	1.390
Ge	4p5s	0.2277	7.067	1.324	0.047	1.371
Sn	5p6s	0.2095	9.049	1.548	0.068	1.616
Pb	6p7s	0.2035	10.004	1.627	0.076	1.703

In all the cases, the first-order perturbation v_1' is found to have a sign opposite to that of v_o' in the external region of r. The integral in the numerator of eq. (VI.11) therefore becomes negative and the first-order shielding factor assumes a positive value. $R_{\theta,2a}$ is always positive due to the v_1^2 term in the numerator of eq. (VI.12). The second-order perturbed wave function v_2' has the same sign as v_o' in the region of large r values. This makes the numerator of eq. (VI.13) positive and therefore $R_{\theta,2b}$ is also positive. Thus, in contrast to the case of the vacancy-induced shielding effect, both the second-order terms make a positive contribution to the total R_θ. However, the total $R_{\theta,2}$ values are much smaller than the first-order term $R_{\theta,1}$.

Except in the case of Ge, $R_{\theta,1}$ increases with increase in Z. The rather anomalous behaviour obtained as we go from Si(3p4s) to Ge(4p5s) is probably due to the fact that the binding energy of n's electron in both the cases is almost similar whereas the values of $\langle r^2 \rangle_{np}$ maintain the increasing order of magnitude. The values of R_θ reported here are somewhat larger than those obtained earlier by Sternheimer[13] with HFS wave functions on the $np^5(n+1)s$ states of rare gases and this may be due to the somewhat tighter binding of the np and (n+1)s electrons in the present case.

It has been indicated[13] that the use of HFS wave functions to describe the unperturbed state leads to a slight overestimate in the calculated values of R_θ. However, except for C(2p3s) where R_θ is very close to unity, the present calculations predict that the total atomic quadrupole moment θ_{atom} of the atoms considered here should be smaller in magnitude and opposite in sign to that calculated from the central field theory due to Buckingham.[184]

CHAPTER VII

Summary and Future Work

CHAPTER VII

Summary and Future Work

VII.A Summary

The interpretation of experimental data on the nuclear quadrupole and hexadecapole interactions, and atomic quadrupole moments obtained from NMR, NQR, Mössbauer, TDPAC, and atomic beam experiments requires the knowledge of appropriate values of γ_∞, R, σ_2, η_∞, and R, which are more commonly known as Sternheimer shielding-antishielding factors. A survey of the experimental evidence in favour of Sternheimer factors in this respect has been given in Chapter I.

Most of the available theoretical values of Sternheimer factors pertain to the free ions and it is important to estimate the changes in the free ionic Sternheimer factors due to the crystal potential, charge-transfer, covalency, and relativistic effects. Further, a literature survey of the various theoretical calculations on Sternheimer factors revealed that for some ions of interest to the experimentalists even free ionic values of reasonable accuracy are not available.

In this thesis we have made an attempt to bridge the gaps mentioned above by adopting the reasonably accurate Sternheimer perturbation-numerical method and HFS wave functions.

and calculated Sternheimer factors for a variety of free atoms and ions, and ions in solids. We have used the Watson model to simulate the lattice potential around positive and negative ions in solids.

In Chapter III we have presented the results of our calculations on

(a) γ_∞ and α_q values for the following free ions:

Li^+, Be^{2+}, B^{3+}, C^{4+}, N^{5+}, O^{6+};
F^-, Na^+, Mg^{2+}, Al^{3+}, Si^{4+}, P^{5+}, S^{6+};
Cl^-, K^+, Ca^{2+}, Sc^{3+}, Ti^{4+}, V^{5+}, Cr^{6+};
Br^-, Rb^+, Sr^{2+}, Yt^{3+}, Zr^{4+}, Nb^{5+}, Mo^{6+};
I^-, Cs^+, Ba^{2+}, La^{3+}; and
At^-, Fr^+, Ra^{2+}, Ac^{3+}.

(b) γ_∞ and α_q values for the following crystal ions:

Li^+, Be^{2+}, B^{3+}, C^{4+}, N^{5+}, O^{6+};
O^{2-}, F^-, Na^+, Mg^{2+}, Al^{3+}, Si^{4+}, P^{5+}, S^{6+};
Si^{4-}, P^{3-}, S^{2-}, Cl^-, K^+, Ca^{2+}, Sc^{3+}, Ti^{4+}, V^{5+}, Cr^{6+};
Ge^{4-}, As^{3-}, Se^{2-}, Br^-, Rb^+, Sr^{2+}, Yt^{3+}, Zr^{4+}, Nb^{5+}, Mo^{6+};
Sn^{4-}, Sb^{3-}, Te^{2-}, I^-, Cs^+, Ba^{2+}, La^{3+};
At^-, Fr^+, Ra^{2+}, Ac^{3+}.

(c) mono and dinegative ions γ_∞ and α_q as a function of the radius of the Watson sphere, r_{ion}, and expressed γ_∞ and α_q in terms of polynomials in r_{ion}^{-1}.

(d) γ_∞, α_q, R and σ_2 values for the crystal ion of Ce^{3+}. For R and σ_2 we have calculated all the direct and exchange contributions.

(e) γ_∞ values for the free ions in the actinide series given by,
Th^{4+}, Pa^{4+}, U^{4+}, Np^{4+}, Pu^{4+}, Am^{4+}, Cm^{4+}, Bk^{4+}, Cf^{4+},
E^{4+}, Fm^{4+}, Md^{4+}, No^{4+}, Lw^{4+}, U^{3+}, U^{5+}, U^{6+}, and Np^{6+}.

(f) γ_∞ values for the crystal ions of Pa^{4+}, Bk^{4+}, and Lw^{4+}.

In Chapter IV we have presented,

(a) γ_∞ values for $3d^5$, $4d^5$ and $5d^5$ isoelectronic sequences of:
Cr^+, Mn^{2+}, Fe^{3+}, Co^{4+}, Ni^{5+}, Cu^{6+};
Mo^+, Tc^{2+}, Ru^{3+}, Rh^{4+}, Pd^{5+}, Ag^{6+};
W^+, Re^{2+}, Os^{3+}, Ir^{4+}, Pt^{5+}, Au^{6+}.

(b) Polynomial fitting of the γ_∞ values for $3d^5$ and $4d^5$ sequences in terms of ρ_m, where ρ_m is the distance of the outermost maximum in the total radial electron density distribution of the ion.

(c) R factors for the following free ions,
Cr, Mn^+, Fe^{2+}, Co^{3+}, Ni^{4+} (all in $3d^6$ configuration);
Ru^{2+}, Os^{2+}, Pr^{3+}, Tm^{3+}, Np^{6+}.
All the direct and exchange terms in R have been computed. The field gradient due to valence electrons has been correlated to ρ_m values in $3d^6$ series.

(d) γ_∞ values for the following atoms in their appropriate electronic configurations in metals.

K, Ca, Sc, Ti, V, Cr, Mn, Fe, Co, Ni, Cu, Zn, Ga, Ge, As; Rb, Sr, Y, Zr, Nb, Mo, Tc, Ru, Rh, Pd, Ag, Cd, In, Sn, Sb; Cs, Ba, La, Hf, Ta, W, Re, Os, Ir, Pt, Au, Hg, Tl, Pb, Bi.

In Chapter V we have presented

(a) η_∞ values for the free ions of Ti^{3+}, Mn^{2+}, Cu^{+}, Zn^{2+}, Ge^{4+}, Rb^{+}, Zn^{3+}, Nb^{5+}, Tc^{2+}, Ag^{+}, In^{3+}, Sb^{3+}, Cs^{+}, Hf^{3+}, Re^{2+}, Au^{+}, Hg^{2+}, Bi^{3+}, Fr^{+}, Th^{3+}, Am^{2+}, Ce^{3+}, Pr^{3+}, Pm^{3+}, Sm^{3+}, Eu^{3+}, Gd^{3+}, Tb^{3+}, Dy^{3+}, Ho^{3+}, Er^{3+}, Tm^{3+}, Yb^{3+}, Lu^{3+}, Th^{4+}, Pa^{4+}, U^{4+}, Np^{4+}, Pu^{4+}, Am^{4+}, Cm^{4+}, Bk^{4+}, Cf^{4+}, E^{4+}, Md^{4+}, No^{4+}, and Lw^{4+}.

(b) η_∞ values for the crystal ions of Pa^{4+}, Bk^{4+}, and Lw^{4+}.

(c) The second order quadrupolar contribution, H_{11} to the total induced hexadecapole moment for the free ions and crystal ions of Pa^{4+}, Bk^{4+}, and Lw^{4+},

In Chapter VI we have presented our results of the shielding factor R_θ to the atomic quadrupole moment for the np(n+1)s excited states of C(n=2), Si(n=3), Ge(n=4) and Sn(n=5).

For the positive ions our results of Sternheimer factors are in excellent agreement with those based on HF wave functions.

For the negative ions HFS wave functions are significantly more external.

The free ion γ_∞ values for tetra-positive actinide ions appear to be constant at $-100(\pm 5)$. A comparison with Feiock and Johnson's[169] values based on relativistic HFS wave functions suggests that the relativistic effects would increase the magnitude of quadrupolar antishielding factors by $\sim$ 65%.

The superimposed potential due to the Watson sphere reproduces the empirical trend that the Sternheimer factors in the case of positive ions in solids are larger than the free ionic values, while for the negative ions there is a significant contraction. In the case of σ_2 in the crystal ion of Ce^{3+}, however, the free ion values are larger in magnitude. The γ_∞ values using the Watson model for positive ions are in excellent agreement with the experimental estimates for Li^+, Na^+, Al^{3+}, Sc^{3+}. For the Cl^- case also the crystal ion calculation of γ_∞ is in excellent agreement with the experimental estimates. For Br^-, and I^- a careful rechecking of the experimental estimates is required.

The problem of estimating crystalline potential effects has been attempted in two different ways. Firstly, for the mono and dinegative ions, γ_∞ and α_q values have been expressed as a function of the Watson sphere radius, r_{ion}. The calculated values of γ_∞ and α_q get significantly affected due to changes

in r_{ion}. If the values of r_{ion} can be estimated within a particular solid in some semiempirical manner, the correlations of γ_∞ and α_q obtained in this thesis would be helpful in estimating γ_∞ and α_q values for ions in ionic solids in situ.

Secondly, the crystalline potential effects have been estimated for positive ions by correlating γ_∞ and σ_{val} in the case of experimentally important nd^5 (n=3,4,5) and $3d^6$ configurations respectively to the position of the outermost peak in the total radial electron density distribution of the ions within a given isoelectronic series. When the experimental estimates of ρ_m by means of single crystal X-ray studies become available these correlations would give the estimates of γ_∞ and (1-R) for ions in solids.

A large value of η_∞ coupled with the favourable values of the parameters such as nuclear spin, nuclear quadrupole moment, NMR sensitivity, and natural abundance has been chosen as a criterion to predict the systems with detectable hexadecapolar interactions in solids. In this respect the ions of Bi^{3+}, Re^{2+}, Sb^{3+}, In^{3+}, Mn^{2+}, tripositive rare earths and tetrapositive actinides seem to be high in the priority list. The covalency effects due to 4d participation in Nb-Cl bonding for $NbCl_5$ have been shown to significantly enhance the η_∞ value for niobium. A dramatic enhancement in η_∞ values of ~150% for tetrapositive ions in solids suggests the need of examining these ions for hexadecapolar interactions in solids.

The calculation of the atomic quadrupole shielding factor R_θ for np(n+1)s excited states predicts that the measured quadrupole moment in such excited states of C, Si, Ge, Sn and Pb would be smaller in magnitude and opposite in sign to the theoretical estimate based on the central field theory.

VII.B Future Work

The future activity in the theoretical calculations of Sternheimer factors for atoms and ions is going to involve the use of better starting wave functions and a more complete perturbation procedure. The relativistic many-body perturbation theory (MBPT) calculations, though expensive, have to be carried out at least in the cases of a few representative systems in alkali metals, VIII group elements, and rare earths and actinides. This would ascertain the relativistic, consistency, and correlation effects on Sternheimer factors and help in evaluating the accuracy of various other coupled and uncoupled calculations.

The recently developed 'effective-operator' form of MBPT by Lindgren and coworkers[71] seems to be extremely promising in carrying out ab initio calculations of hyperfine interactions. Owing to its local character, the HFS potential with the appropriate 'potential-corrections' can be used in this method

to reproduce the results based on HF potential as the starting point. A relativistic formulation of the effective-operator form of MBPT is highly desirable since this would enable the evaluation of relativistic, consistency and correlation effects on Sternheimer factors to be done simultaneously.

In the regions where the two-electron effects on Sternheimer factors are shown to be small by MBPT calculations,[67] it would be interesting to estimate the relativistic and crystal potential effects on shielding-antishielding factors by using HF wave functions. In the case of positive ions, however, we have shown that the HFS results of shielding-antishielding factors are in excellent agreement with the corresponding HF calculations. It would be therefore more economical to perform relativistic HFS calculations of R and γ_∞ and compare the results with the presently calculated nonrelativistic HFS results and thus estimate the relativistic effects on these Sternheimer factors. Such a comparison has already been carried out for γ_∞ in Chapter III.

Very little is known about R_H and H^{Ω}_{ind} even at the nonrelativistic level of approximation. We are currently engaged in the calculations of H^{Ω}_{ind} and R_H for the rare earth free and crystal ions.

With the first-order wave functions generated in the present thesis one can improve upon the values of Sternheimer

factors in an approximate manner via the geometric-approximation[46], or more completely using the differential equation procedure of Ray et al.[26] Such improvements in the cases of more polarizable C^{2-} and S^{2-} ions would be welcome. Alternatively, one can use the presently calculated uncoupled perturbed wave functions as input to the more complete coupled calculations such as those of Kaneko[19b,20] and obtain the fully coupled results of Sternheimer shielding-antishielding factors.

In the semiempirical procedure adopted by Sternheimer to calculate R factors for high angular momentum states of alkalis some correlation effects are included indirectly into the potential. It would be interesting to see if the improvements can be achieved by using a similar method to calculate other Sternheimer factors. However, as pointed out by Lindgren[73g] one has to be extremely careful in such calculations since two local potentials without 'potential-corrections', though fitted to the same experimental parameter, yield significantly different results of R for nd excited states of alkali metal atoms.

For several metals, the band structure calculations have recently[187] become available using the renormalized atom approach. It is hoped that these results would be utilized in the calculation of the conduction electron contribution to the field gradient. In such a case it would be more appropriate to use Sternheimer factors pertaining to the renormalized atoms. The calculations of γ_∞ for several renormalized atoms are currently being carried out by us.

REFERENCES

1. (a) A. Hochheim, Verh. Deutsch Phys. Ges. 40, 446 (1908); (b) K. Fajans and G. Joos, Z. Physik 23, 1 (1928); (c) M. Born and W. Heisenberg, ibid. 23, 388 (1924).

2. (a) E. Bederson and E. J. Robinson in 'Advances in Chemical Physics' (Edited by J. Ross, Academic, New York, 1966), Vol. 10, p 1; (b) R. R. Teachout and R. T. Pack, Atomic Data 3, 195 (1971). For an exhaustive compilation of theoretical and experimental results on atomic dipole polarizabilities of neutral atoms till 1970.

3. A. D. Buckingham and D. A. Dunmur, Trans. Faraday Soc. 64, 1776 (1968).

4. (a) P. S. Epstein, Phys. Rev. 28, 695 (1926); (b) E. Schrodinger, Ann. Physik 80, 437 (1926); (c) G. Wentzel, Z. Physik 38, 518 (1926); (d) I. Waller, ibid., 28, 635 (1926); (e) S. Doi, Proc. Phys.-Meth. Soc. (Japan) 10, 223 (1928).

5. A. Dalgarno, Advances in Physics 11, 281 (1962). For an excellent review of theoretical methods for multipole polarizabilities and shielding-antishielding factors.

6. R. M. Sternheimer, Phys. Rev. 86, 316 (1952).

7. (a) R. M. Sternheimer, Phys. Rev. 80, 102 (1950); (b) ibid. 84, 244 (1951); (c) ibid. 95, 736 (1954); (d) ibid. 105, 158 (1957); (e) R. M. Sternheimer and H. M. Foley, ibid. 92, 1460 (1953); (f) ibid 102, 731 (1956); (g) H. Foley, R. M. Sternheimer and D. Tycko, ibid. 93, 734 (1954).

8. (a) R. M. Sternheimer, Phys. Rev.Lett. 6, 190 (1967); (b) Phys. Rev. 123, 870 (1961); (c) ibid. 127, 812 (1962); (d) ibid. A10, 1964 (1974).

9. R. M. Sternheimer, Phys. Rev. 96, 951 (1954).

10. (a) G. Burns, Phys. Rev. 128, 2121 (1962); (b) J. Chem. Phys. 42, 377 (1965); (c) M. T. Hutchings and D. K. Ray, Proc.Phys. Soc. (London) 81, 663 (1963);

(d) D. K. Ray, ibid. 82, 47 (1963); (e) C. J. Lenander and E. Y. Wong, J. Chem. Phys. 38, 2750 (1963); (f) R.E. Watson and A. J. Freeman, Phys. Rev. 139, A1606 (1965); (g) M. N. Ghatikar, A. K. Raychaudhuri and D. K. Ray, Proc. Phys. Soc. (London) 86, 1235 (1965).

11. (a) R. M. Sternheimer, Bull. Am. Phys. Soc. 10, 597 (1965); (b) Phys. Rev. 146, 140 (1966); (c) ibid. 173, 376 (1968).

12. (a) R. P. Gupta, B. K. Rao and S. K. Sen, Phys. Rev. A3, 545 (1971); (b) R. P. Gupta and S. K. Sen, ibid. A7, 850 (1973).

13. (a) R. M. Sternheimer, Phys. Rev. A 7, 887 (1973); (b) ibid. 8, 685 (1974).

14. (a) P. Gombas, Z. Physik 122, 497 (1944); (b) Hand. Phys. (Springer, Berlin, 1956) pp 36.

15. (a) R. M. Sternheimer, Phys. Rev. 107, 1565 (1957); (b) ibid. 115, 1198 (1959).

16. (a) H. Peng, Proc. Roy. Soc. (London) A178, 499 (1941); (b) P. Vinti, Phys. Rev. 41, 813 (1932).

17. L. C. Allen, Phys. Rev. 118, 167 (1960).

18. P. W. Langhoff, M. Karplus and R. P. Hurst, J. Chem. Phys. 44, 505 (1966).

19. (a) A. Dalgarno, Proc. Roy. Soc. (London) A251, 282 (1959); (b) S. Kaneko, J. Phys. Soc. Japan 11, 1600 (1959); (c) A. Dalgarno and J. M. McNamee, Proc. Phys. Soc. 77, 673 (1961); (d) A. Dalgarno and H. A. J. McIntyre, ibid. 85, 47 (1965).

20. S. Kaneko and S. Arai, J. Phys. Soc. Japan 26, 170 (1969).

21. (a) R. E. Watson and A. J. Freeman, Phys. Rev. 131, 252 (1963); (b) ibid. 131, 2566 (1963); (c) ibid. 131, 2573 (1963); (d) ibid. 132, 706 (1963); (e) ibid. 133, A1571 (1964); (f) ibid. 135, A1209 (1964).

22. R. K. Nesbet, Proc. Roy. Soc. (London) A230, 312 (1955).

23. (a) H. D. Cohen, Bull. Am. Phys. Soc. 9, 624 (1964); (b) H. D. Cohen and C. C. J. Roothaan, J. Chem. Phys. 43, S34 (1965); (c) ibid. 43, 3558 (1965); (d) ibid. 45, 10 (1966).

24. (a) J.Lahiri and A. Mukherji, J. Phys. Soc. Japan 21, 1178 (1966); (b) Phys. Rev. 141, 428 (1966); (c) ibid. 153, 386 (1967); (d) ibid. 155, 24 (1967).

25. P. G. Khubchandani, R. R. Sharma and T. P. Das, Phys. Rev. 126, 594 (1962).

26. (a) S. N. Ray, T. Lee, T. P. Das and R. M. Sternheimer, Phys. Rev. A 9, 1108 (1974); (b) A. C. Beri, S. N. Ray, T. P. Das and R. M. Sternheimer, ibid. A 12, 1168 (1975).

27. T. P. Das and R. Bersohn, Phys. Rev. 102, 733 (1956).

28. E. G. Wikner and T. P. Das, Phys. Rev. 109, 360 (1958).

29. (a) G. Burns, Phys. Rev. 115, 357 (1959); (b) J. Chem. Phys. 31, 1253 (1959); (c) G. Burns and E. G. Wikner, Phys. Rev. 121, 155 (1961).

30. R. Ingalls, Phys. Rev. 128, 1155 (1962).

31. (a) A. Dalgarno and D. Parkinson, Proc. Roy. Soc. (London) A 250, 422 (1959); (b) A. Dalgarno and J. M. McNamee, J. Chem. Phys. 35, 1517 (1961).

32. M. Yoshimine and R. P. Hurst, Phys. Rev. 135, A 612 (1964).

33. P. W. Langhoff and R. P. Hurst, Phys. Rev. 139, A 1415 (1965).

34. (a) M. Karplus and H. J. Kolker, J. Chem. Phys. 38, 1263 (1963); (b) H. J. Kolker and M. Karplus, ibid. 39, 2011 (1963).

35. A. Temkin, Phys. Rev. 107, 1004 (1957).

36. K. J. Duff and T. P. Das, Phys. Rev. 168, 43 (1968).

37. (a) A. J. Sadlej, Mol. Phys. 21, 145 (1971); (b) ibid. 22, 705 (1971).

38. (a) J. A. Pople and P. Schofield, Phil. Mag. 2, 591 (1957); (b) J. Thorhallsson, C. Frisk and S. Fraga, Theoret. Chim. Acta 10, 388 (1968); (c) J. Chem. Phys. 49, 1987 (1968); (d) K. M. S. Saxena and S. Fraga, ibid. 57, 1800 (1972).

39. S. A. Adelman and A. Szabo, J. Chem. Phys. 58, 687 (1963).

40. R. Ahlberg and O. Goscinski, J. Phys. B 6, 2254 (1973).

41. J. C. Slater, "Quantum Theory of Atomic Structure", (McGraw Hill, New York, 1960), Vol. II.

42. (a) D.F.-T. Tuan, S. T. Epstein, and J. O. Hirschfelder, J. Chem. Phys. 44, 431 (1966); (b) S. T. Epstein, "The Variation Method in Quantum Chemistry" (Academic, New York, 1974), Chap. IX.

43. J. Musher, J. Chem. Phys. 46, 369 (1967).

44. S. T. Epstein and R. E. Johnson, J. Chem. Phys. 47, 2275 (1967).

45. T. C. Caves and M. Karplus, J. Chem. Phys. 50, 3649 (1969).

46. J. M. Shulman and J. I. Musher, J. Chem. Phys. 49, 4845 (1968).

47. A. T. Amos, J. Chem. Phys. 52, 603 (1970).

48. D.F.-T. Tuan, Chem. Phys. Lett. 7, 115 (1970).

49. A. J. Sadlej and M. Jaszunski, Mol. Phys. 22, 761 (1971).

50. M. J. Jamieson and A. Gafarian, Mol. Phys. 30, 1611 (1975).

51. D.F.-T. Tuan and A. Davidz, J. Chem. Phys. 55, 1286 (1971).

52. A. J. Sadlej, Mol. Phys. 26, 1444 (1973).

53. R. F. Stewart, Mol. Phys. 29, 787 (1975).

54. (a) C. Litt, Phys. Rev. A 1, 258 (1970); (b) C. Litt, Phys. Rev. A 7, 911 (1973).

55. (a) A. K. Bhattacharya, R. K. Moitra and A. Mukherji, Int. J. Quantum Chem. IX, 385 (1975); (b) H. P. Roy and A. K. Bhattacharya, IX, 495 (1975).

56. R. F. Stewart, Mol. Phys. 30, 1283 (1975).

57. (a) W. E. Donath, J. Chem. Phys. 39, 2685 (1963); (b) C. Schwartz, Phys. Rev. 123, 1700 (1961).

58. (a) H. J. Volker and H. H. Michels, J. Chem. Phys. 43, 1027 (1965); (b) G. M. Stacey, Proc. Phys. Soc. (London), 88, 897 (1966); (c) W. D. Robb, J. Phys. B 6, 945 (1973); (d) ibid. B 7, L369 (1974).

59. R. E. Sitter and R. P. Hurst, Phys. Rev. A 5, 5 (1972).

60. (a) F. P. Billingsley, II and M. Krauss, Phys. Rev. A 6, 855 (1972); (b) W. J. Stevens and F. P. Billingsley, II, ibid. A 8, 2236 (1973).

61. (a) H.-J. Werner and W. Meyer, Mol. Phys. 31, 855 (1976); (b) Phys. Rev. A 13, 13 (1976).

62. (a) R. Ahlrichs, H. Lischka, V. Staemmler and W. Kutzelnigg, J. Chem. Phys. 62, 1225 (1975); (b) R. Ahlrichs, F. Driessler, H. Lischka, V. Staemmler and W. Kutzelnigg, ibid. 62, 1235 (1975).

63. (a) H. P. Kelly, Phys. Rev. 136, B897(1964); (b) H. P. Kelly, Atomic Physics 2, 227 (1972).

64. (a) K. A. Brueckner, Phys. Rev. 97, 1357 (1955); (b) ibid. 100, 36 (1955); (c) J. Goldstone, Proc. Roy. Soc. (London) A239, 267 (1957).

65. (a) H. P. Kelly, Phys. Rev. 152, 62 (1966); (b) E.S. Chang, R. T. Pu and T. P. Das, Phys. Rev. 174, 16 (1968); (c) ibid. 182, 84 (1969); (d) C. Matsubara, N. C. Datta, T. Ishihara and T. P. Das, Phys. Rev. A1, 561 (1970); (e) J. A. Miller and H. P. Kevy, Phys. Rev. A 5, 516 (1972).

66. M. B. Doran, J. Phys. B 7, 558 (1974).

67. (a) S. N. Ray, T. Lee and T. P. Das, Phys. Rev. A 9, 93 (1974); (b) M. Vajed-Samii, S. N. Ray and T. P. Das, Phys. Rev. B 12, 4591 (1975).

68. J. D. Lyons, R. T. Pu and T. P. Das, Phys. Rev. 178, 103 (1969).

69. (a) R. K. Nesbet, Phys. Rev. A 2, 661 (1970); (b) ibid. A 2, 1208 (1970).

70. S. Hameed and H. M. Foley, Phys. Rev. A 6, 1399 (1972).

71. S. Garpman, I. Lindgren, J. Lindgren and J. Morrison, Phys. Rev. 11, 758 (1975).

72. T. P. Das (Private discussion).

73. (a) H. P. Kelly, Phys. Rev. 173, 142 (1968); (b) H. F. Schaefer, III, R. A. Klemm, and F. E. Harris, Phys. Rev. 176, 49 (1968); (c) ibid. 180, 55 (1969); (d) S. Larsson,

Phys. Rev. A 2, 1248 (1970); (e) S. N. Ray, T. Lee and T. P. Das, Phys. Rev. 8, 1748 (1973); (f) J. E. Rodgers and T. P. Das, Phys. Rev. A 12, 353 (1975); (g) I. Lindgren, At. Phys. 4, 747 (1975); (h) S. Garpman, I. Lindgren, J. Lindgren and J. Morrison, Z. Physik A 276, 167 (1976).

74. (a) R. M. Sternheimer, Phys. Rev. 164, 10 (1967); (b) R. M. Sternheimer and R. F. Peierls, Phys. Rev. A 3, 837 (1971); (c) R. M. Sternheimer and R. F. Peierls, Phys. Rev. A 4, 1722 (1971); (d) R. M. Sternheimer, Phys. Rev. A 6, 1702 (1972); (e) L. Armstrong, Jr. "Theory of the Hyperfine Structure of free Atoms" (John Wiley, New York, 1971). For a compilation of Sternheimer R factors till 1971.

75. D.V.G.L. Narasimha Rao, J. Sci. Industr. Res. 24, 220 (1965). For a brief account of early estimates of $(1-\gamma_\infty)$ based on magnetic resonance experiments.

76. (a) C. A. Lee, B. P. Fabricand, R. O. Carlson, and I. I. Ralei, Phys. Rev. 91, 1395 (1953); (b) ibid. 91, 209 (1953); (c) Professor P. Kusch (Private communication to R. M. Sternheimer in ref. 7g).

77. (a) V. Jaccarino and J. G. King, Phys. Rev. 83, 471 (1951); (b) ibid. 91, 209 (1953).

78. R. V. Pound, Phys. Rev. 79, 685 (1950).

79. M. H. Cohen and F. Reif, Solid St. Phys. 5, 321 (1957).

80. (a) R. Bersohn, J. Chem. Phys. 20, 1505 (1952); (b) G. M. Volkoff, H. E. Petch and D.W.L. Smelie, Can. J. Phys. 30, 270 (1952); (c) G. M. Volkoff, ibid. 31, 820 (1953).

81. (a) J. Van Kranendonk, Physica 20, 781 (1954); (b) T.P. Das, D. K. Roy and S. K. Ghosh Roy, Phys. Rev. 104, 156 (1956).

82. (a) K. Yoshida and T. Moriya, J. Phys. Soc. Japan 11, 33 (1956); (b) J. Kondo and J. Yamashida, J. Phys. Chem. Solids, 10, 245 (1959).

83. H. Kawamura, E. Otsuka and K. Ishiwatari, J. Phys. Soc. Japan 11, 1064 (1956).

84. E. Otsuka and H. Kawamura, J. Phys. Soc. Japan 12, 1071 (1957).

85. R. Bersohn, J. Chem. Phys. 29, 326 (1958).

86. R. F. Kiddle and W. G. Proctor, Phys. Rev. 104, 932 (1956).

87. K. A. Valiev, Soviet Phys. - JETP 11, 883 (1959).

88. E. G. Wikner, W. E. Blumberg and E. L. Hahn, Phys. Rev. 118, 631 (1960).

89. G. Burns, Phys. Rev. 123, 1634 (1961).

90. T. P. Das and B. G. Dick, Phys. Rev. 127, 1063 (1962).

91. W. D. Wilson and M. Blume, J. Phys. Chem. Solids, 29, 1167 (1968).

92. M. Raymond, Phys. Rev. B 3, 3697 (1971).

93. R. R. Sharma, Phys. Rev. Lett. 25, 1622 (1970).

94. H. Lew and G. Wessel, Phys. Rev. 90, 1 (1953).

95. T. P. Das and E. L. Hahn, Solid St. Phys. Supplement 1 (1958).

96. R. R. Hewit, Phys. Rev. 121, 45 (1961).

97. R. G. Barnes, S. L. Segel, and W. H. Jones, Jr., J. Appl. Phys. 533, 296 (1962).

98. (a) D.V.G.L. Narasimha Rao and A. Narasimhamurthy, Phys. Rev. 132, 961 (1963); (b) P. Raj and V. Amirthalingam, Phys. Rev. 146, 590 (1966).

99. A. Narath, Phys. Rev. 140, A552 (1965).

100. Y. S. Liu, J. Chem. Phys. 62, 2727 (1975).

101. D. M. Current, J. Mag. Resonance 20, 259 (1975).

102. R. W. Hewit and B. F. Williams, Phys. Rev. 129, 1188 (1963).

103. H. K. Collan, M. Krusius and G. R. Pickett, Phys. Rev. B 1, 2888 (1970).

104. M. Krussius and G. R. Picket, Solid St. Comm. 9, 1917 (1971).

105. K. Murakawa, Phys. Rev. 100, 1369 (1955).

106. E. H. Hygh and T. P. Das, Phys. Rev. 143, 452 (1966).

107. (a) D. A. Cornell, Phys. Rev. 153, 208 (1967);

(b) F. A. Rossini, E. Geissler, E. M. Dickson, and W. D. Knight, Adv. Phys. 16, 287 (1967); (c) F. A. Rossini and W. D. Knight, Phys. Rev. 178, 641 (1968); (d) W. W. Warren, Jr. and W. G. Clark, Phys. Rev. 177, 600 (1969).

108. N. C. Haldar, J. Mag. Resonance 22, 33 (1976).

109. K. K. Rao and C.R.K. Murthy, Ind. J. Pure & Appl. Phys. 7, 320 (1969).

110. A. L. Kerlin and W. G. Clark, Phys. Rev. B 12, 3533 (1975).

111. T. F. Feuchtwang, "Paramagnetic Resonance" (Edited by W. Low, Academic, New York, 1963) Vol. II, pp 749.

112. P. H. Zimmermann and R. Valentin, Phys. Rev. B 12, 3519 (1975).

113. A. Kastler, Experientia 8, 7 (1952).

114. A. Al'tshular, Soviet Phys. -JETP 1, 37 (1955).

115. (a) R. G. Shulman, B. J. Wyluda and P. W. Anderson, Phys. Rev. 107, 953 (1957); (b) J. L. Marsh, Ph.D. Thesis, Rensselaer Polytechnic Institute, 1966.

116. E. Otsuka, J. Phys. Soc. Japan 13, 1155 (1958).

117. Y. Fukai, J. Phys. Soc. Japan 19, 175 (1964).

118. E. F. Taylor and N. Bloembergen, Phys. Rev. 113, 431 (1959).

119. (a) D. I. Bolef and M. Menes, Phys. Rev. 114, 1441 (1959); (b) D. I. Bolef, "Physical Acoustics" (Edited by W.P. Mason, Academic, New York, 1966), Vol. 4A, Chap III.

120. J. L. Marsh and P. A. Casabella, Phys. Rev. 150, 546 (1966).

121. D. Ikenbery and T. P. Das, Phys. Rev. 184, 989 (1969).

122. (a) W. G. Proctor and W. H. Tantilla, Phys. Rev. 101, 1757, (1956); (b) W. G. Proctor and W. Robinson, ibid. 104, 1344 (1956).

123. D. A. Jennings, W. H. Tantilla, and O. Krauss, Phys. Rev. 109, 1059 (1958).

124. G. L. Antokoloskii, V. M. Sarnatskii and V. A. Shutilov, Soviet Phys. - Acoustics 17, 115 (1971).

125. J. R. Anderson and J. S. Karra, Phys. Rev. B 5, 4334 (1972).

126. T. Kanashiro, J. Phys. Soc. Japan 32, 1270 (1972).

127. T. Kanashiro, T. Ohno and M. Satoh, J. Phys. Soc. Japan 38, 1293 (1975).

128. (a) R. K. Sundfors, Phys. Rev. 177, 1221 (1969); (b) ibid. 10, 4244 (1974).

129. R. K. Sundfors and R. K. Tsui, Phys. Rev. B 12, 790 (1975).

130. R. K. Sundfors, T. H. Wang, D. I. Bolef, P. A. Fedders, and D. G. Westlake, Phys. Rev. B 12, 26 (1975).

131. G. Burns, Phys. Rev. 124, 524 (1961).

132. R. Ingalls, Phys. Rev. 188, 1045 (1969).

133. N. N. Greenwood and T. C. Gibbs, "Mossbauer Spectroscopy" (Chapman-Hill, London, 1971) pp 99.

134. (a) R. R. Sharma, Phys. Rev. Lett. 26, 563 (1971); (b) R. R. Sharma and Bung Ning Teng, ibid. 27, 679 (1971); (c) R. R. Sharma, Phys. Rev. B 6, 4310 (1972).

135. V. G. Bhide and M. S. Hegde, Phys. Rev. B 5, 3488 (1972).

136. A. K. Sharma and R. R. Sharma, Phys. Rev. B 10, 3792 (1974).

137. E. Karlsson, E. Matthias and K. Siegbahn, "Perturbed Angular Correlations" (North-Holland, Amsterdam, 1964).

138. H. J. Behred and D. Budnick, Z. Physik, 168, 155 (1962).

139. T. P. Das, Phys. Scripta 11, 121 (1975).

140. R. S. Raghavan, E. N. Kaufmann, and P. Raghavan, Phys. Rev. Lett. 34, 1280 (1975).

141. I. Lindgren and A. Rosen, "Case Studies in Atomic Physics" (Edited by M. R. C. McDowell and E. W. McDaniel, North-Holland, 1964).

142. (a) M. Bucka (Private communication to Dr. R. M. Sternheimer in ref. 75a); (b) J. Ney, Z. Physik 196, 53 (1966); (c) W. Fischer, H. Huhnerman, and K.J. Kollath, Z. Physik 194, 417 (1966); (d) ibid. 200, 158 (1967); (e) M. Elbel and H. Wilhelm, Ann. Physik 18, 42 (1966).

143. (a) K. Murakawa and T. Kamei, Phys. Rev. 105, 671 (1957); (b) K. Murakawa, ibid. 110, 393 (1958); (c) J. Phys. Soc. Japan 16, 2533 (1961); (d) ibid. 17, 891 (1962).

144. (a) W. J. Childs, Phys. Rev. A 2, 316 (1970); (b) Atomic Phys. 4, 731 (1975).

145. (a) M. Bucka, H. Kopfermann, M. Rasiwala and H. A. Schussler, Z. Physik 176, 45 (1963); (b) H. A. Schussler, ibid. 132, 289 (1965); (c) G. Zu Putlitz and A. Schenck, ibid. 183, 428 (1965); (d) U. Knohl, G. Zu Putlitz and A. Schenck, ibid. 208, 364 (1968); (e) F. Feiertag and G. Zu Putlitz, ibid 208, 447 (1968); (f) H. Bucka, G. Zu Putlitz and R. Rabold, ibid. 213, 101 (1968); (g) G. Zu Putlitz, Atomic Physics 1, 227 (1969); (h) D. Feiertag, A. Sahm and G. Zu Putlitz, Z. Physik 255, 93 (1972); (i) D. Feiertag and G. Zu Putlitz, ibid. 261, 1 (1963); (j) G. Belin and S. Svanberg, Phys. Scripta 4, 269 (1971); (k) S. Svanberg, ibid. 4, 275 (1971); (l) S. Rydberg and S. Svanberg, ibid. 5, 209 (1972).

146. H. P. Povel, Nucl. Phys. A 217, 573 (1973).

147. S. Buttgenback and R. Dicke, Z. Physik A 275, 197 (1975).

148. (a) R. L. Mossbauer, R. G. Barnes, E. Kankleit and J. M. Poindexter, Phys. Rev. 136, 175 (1964); (b) M. H. Cohen, Phys. Rev. 134, A 94 (1964); (c) S. Hufner, M. Kalvius, P. Kienle, W. Wiedemann, and H. Eicher, Z. Physik 175, 416 (1963); (d) ibid. 182, 499 (1965); (e) H. H. Wickman and I. Nowik, Phys. Rev. 142,115 (1966).

149. B. D. Dunlap, G. M. Kalvius and G. K. Shenoy, Phys. Rev. Lett. 26, 1085 (1971).

150. (a) T. C. Wang, Phys. Rev. 99, 566 (1955); (b) R. J. Mahler, L. W. James, and W. H. Tantilla, Phys. Rev. Lett. 16, 259 (1966); (c) Dinesh and J. A. S. Smith, Paper presented in Second International Symposium on Nuclear Quadrupole Resonance Spectroscopy, Viareggio, Italy (1973); (d) W. Dankwort, J. Ferch and H. Gebauer, Z. Physik 267, 229 (1974); (e) L. S. Goodman, H. Diamond and H.E. Stanten, Phys. Rev. A 11, 499 (1975).

151. J. Blok and D. A. Shirley, Phys. Rev. 143, 278 (1966).

152. J. Pelzl, S. Hufner and S. Scheller, Z. Physik 231, 377 (1970).

153. J. Pelzl, Z. Physik 251, 13 (1972).

154. (a) T. Novakov and J. M. Hollander, Phys. Rev. Lett. 21, 1133 (1968); (b) Bull. Am. Phys. Soc. 14, 524 (1969).

155. R. P. Gupta and S. K. Sen, Phys. Rev. A 8, 1169 (1973).

156. (a) J. C. Slater, Phys. Rev. 81, 385 (1951); (b) R. Gaspar, Acta Phys. Acad. Sci. Hung. 3, 263 (1954); (c) W. Kohn and L. J. Sham, Phys. Rev. 140, A1733 (1965); (d) I. Lindgren, Phys. Lett. 19, 382 (1965); Arkiv Fysik 31, 59 (1966); (e) R. D. Cowan, A. C. Larson, D. Liberman, J. B. Mann, and J. Waber, Phys. Rev. 144, 5 (1966); (f) J. C. Slater, T. M. Wilson and J. H. Wood, Phys. Rev. 179, 28 (1969).

157. (a) J. C. Slater, "Solid State and Molecular Theory" (John-Wiley, New York, 1974) and references therein; (b) T. L. Loucks "Augmented Plane Wave Method" (Benjamin, New York, 1967).

158. K.M.S. Saxena and P. T. Narasimhan, J. Chem. Phys. 42, 4304 (1965); Int. J. Quant. Chem. I, 731 (1967).

159. F. Herman and F. Skillman "Atomic Structure Calculations" (Prentice-Hall, Englewood, Cliffs., N.J., 1963).

160. G. Malli and S. Fraga, Theoret. Chim. Acta. 5, 275 (1966); 5, 285 (1966).

161. R. M. Sternheimer, Phys. Rev. A 1, 321 (1970).

162. E.A.C. Lucken, "Nuclear Quadrupole Coupling Constants" (Academic, New York, 1969), Chap. 5.

163. E. Paschalis and A. Weiss, Theoret. Chim. Acta 13, 381 (1969).

164. R. E. Watson, Phys. Rev. 111, 1108 (1958).

165. L. Pauling, "The Nature of Chemical Bond" (Cornell, N.Y., 1960) p. 514.

166. See for example in C. Kittel "Introduction to Solid State Physics" (John-Wiley, New York, 1968), p. 105.

167. D. R. Hartree "The Calculation of Atomic Structure", (John Wiley, New York, 1957), Chap. 4.

168. H. Margenau and G. M. Murphy, "The Mathematics of Physics and Chemistry " (D. Van Nostrand, New York, 1947), p. 500.

169. F. D. Feiock and W. R. Johnson, Phys. Rev. 187, 39 (1969).

170. E. Clementi and A. D. McLean, Phys. Rev. 133, A419 (1964).

171. (a) J. Yamashita and M. Kojima, J. Phys. Soc. Japan 7, 261 (1952); (b) J. Yamashita, J. Phys. Soc. Japan 7, 284 (1952); (c) J. Yamashita and M. Asano, J. Phys. Soc. Japan 31, 980 (1970).

172. (a) T. Fukamachi and S. Hosoya, J. Phys. Soc. Japan 31, 980 (1970); (b) Y. Tsuchiya, S. Noguchi, T. Fukamachi and S. Hosoya, J. Phys. Soc. Japan 39, 1586 (1975).

173. R. M. Sternheimer, Phys. Rev. 159, 226 (1967).

174. S. N. Ray, T. Lee, T.P. Das, R. M. Sternheimer, R.P. Gupta and S. K. Sen, Phys. Rev. 11, 1804 (1975).

175. R. M. Sternheimer, Phys. Rev. 130, 1423 (1963).

176. E. Clementi, IBM J. Res. Develop. 9, 2 (1965).

177. P. C. Sood and D. A. Hutcheon, Nucl. Phys. A96, 159 (1967).

178. P. C. Patnaik, M. D. Thompson and T. P. Das, Bull. Am. Phys. Soc. 21, 240 (1976).

179. J. C. Parikh, Phys. Lett. B 25, 181 (1967).

180. F. A. Garev, S. P. Ivanova and V. V. Pashkevich, Sov. J. Nucl. Phys. 11, 667 (1970).

181. (a) A. Nakada and Y. Touzuka, J. Phys. Soc. Japan, 32, 1 (1972); (b) E. Eichler, N. R. Johnson, R. D. Sayer, D. C. Hensley, and L. L. Riedinger, Phys. Rev. Lett. 30, 568 (1973); (c) R. de Swiniarski, G. Bagieu, A. J. Cole, P. Gaillard, A. Guichard, J.Y. Grossiord, M. Gusakov, and J. R. Pizzi, J. Phys. (France), 35, 25 (1974); (d) H. Rebel, G. W. Schweimer, J. Specht, G. Schatz, R. Lohken, D. Habs, G. Hauser, and H. Klewe-Nebenios, Phys. Rev. Lett. 26, 1190 (1971).

182. (a) B. Elbeck, M. Kregar and P. Vedelsby, Nucl. Phys. 86, 385 (1966); (b) K. A. Erb, J. E. Holdel, I. Y. Lee, J. X. Saladin, and T. K. Saylor, Phys. Rev. Lett. 29, 1010 (1972); (c) C. E. Bemis Jr., F. K. McGowan, J.L.C. Ford,Jr., W.T. Milner, P. H. Stelson and R. L. Robinson, Phys. Rev. C 8, 1934 (1973); (d) P. Kleinheinz, R. F. Casten, and B. Nilsson, Nucl. Phys. A 203, 539 (1973).

183. (a) J.R.P. Angel, P.G.H. Sandars and G.K. Woodgate, J. Chem. Phys. 47, 1552 (1967); (b) M. A. Player and P.G.H. Sandars, J. Phys. B 3, 1620 (1970).

184. A. D. Buckingham, J. Chem. Phys. 30, 1580 (1959).

185. P.G.H. Sandars and A. J. Stewart, Atomic Physics, 3, 429 (1973).

186. P.G.H. Sandars (Private communication to R.M. Sternheimer, cited in reference 13).

187. J. F. Herbst, R. E. Watson, and J. W. Wikins, Phys. Rev. B 13, 1439 (1976).

APPENDIX

LISTING OF THE MAIN COMPUTER PROGRAM TO GENERATE THE ZEROTH ORDER FREE AND CRYSTAL ION WAVE FUNCTIONS

```
C     HARTREE-FOCK-SLATER SELF-CONSISTENT ATOMIC FIELD PROGRAM
C      ORIGINALLY  WRITTEN BY SHERWOOD SKILLMAN
C      RCA LABORATORIES, PRINCETON, NEW JERSEY, SPRING 1961
C      MODIFIED BY FRANK HERMAN, SUMMER 1961
C      FURTHER MODIFIED BY RICHARD KORTUM,  LOCKHEED RESEARCH
C       LABORATORIES, PALO ALTO, CALIFORNIA,  SUMMER 1962
C     ITERATION NUMBER,MEASURE OF SELF-CONSISTENCY,AND ATOMIC NUMBER Z
C     ARE ALWAYS PRINTED ON-LINE.
C      MODIFIED BY K D SEA FOR 7044/1401 COMPUTER SYSTEM
C      TO GENERATE HFS WAVE FUNCTIONS FOR FREE AND CRYSTAL IONS
C     OUTPUT TAPE B-5 CONTAINS SELF-CONSISTENT ATOMIC POTENTIAL,
C      ENERGY EIGENVALUES, AND RADIAL WAVE FUNCTIONS
C      SUCCESSIVE SOLUTIONS SEPARATED BY END OF FILE
C     Z = ATOMIC NUMBER.  ION = IONICITY.  ZZZ = ION+1
C     IF KEY = 0   NORMALIZED NUMERICAL ATOMIC POTENTIAL IS READ IN
C      FOR EVERY 4TH MESH POINT FROM 1 TO 437.
C     IF KEY = 1     NUMERICAL ATOMIC POTENTIAL IS TO BE READ IN.
C     IF KEY = 2   EXTRAPOLATE FOR STARTING POTENTIAL
C     IPRATT IS THE NUMBER OF CONSECUTIVE ITERATIONS TO USE THE PRATT
C      IMPROVEMENT SCHEME FOLLOWING EACH APPLICATION OF THE ARITHMETIC
C      AVERAGE SCHEME.
C     MAXIT = MAXIMUM NO. OF ITERATIONS UNLESS MAXIT IS READ AS 0 ,
C      IN WHICH CASE MAXIT IS SET TO 20.
C     NOCOPY =0, B-5 IS COPIED TO A-3. NOCOPY = 1, B-5 IS NOT COPIED.
C     KUT = 1, THE CUTOFF POTENTIAL IS -2(ION+1)/R.
C     KUT = 0, NO CUTOFF POTENTIAL IS IMPOSED.
      DIMENSION X(521),RSCORE(521),RUINL1(521), RU2(521), RU(521),
     1 NNLZ(17),R(521),RSVALE(521),RUFNL1(521), RU3(521), XI(521),
     2 NNNL(17),V(521),RSATOM(521),RUINL2(521),XNUM(521), XJ(521),
     3 NKKK(17),EE(17),RUEXCH(521),RUFNL2(521),DENM(521),
     4SNL(17,521),SNLC(521),A(4,5)
      COMMON V,SNLC, R, RSCORE,RSVALE,RU,RUEXCH,XI,XJ,    RSATOM,  SNL,
     1RUINL1,RUFNL1,RUINL2,RUFNL2,RU2,RU3,NNLZ,NNNL,NKKK,EE,A
      COMMON KUT,MAXIT,IPRATT,NOCOPY,KEY,TOL,THRESH,MESH
      EQUIVALENCE (RSCORE,XNUM),(RSVALE,DENM)  ,(CC,RSATOM)
      DIMENSION ACF(20)
      CALL FLUN(32000)
      EXPF(X)=EXP(X)
      ABSF(X)=ABS(X)
      SQRTF(X)=SQRT(X)
```

```
      XMINCF(M,N)=AMINC(M,N)
    1 FORMAT(F8.5,9F7.5)
    2 FORMAT (I4,  3E14.7,I4,  E14.7)
    3 FORMAT(F5.1,3I4)
    4 FORMAT(9F8.8)
    5 FORMAT(6H WWW= F4.0,6H ZZZ= F4.0,6H   Z= F4.0,11H   NCORES= I4,
     1 11H   NVALES= I4,11H   NCSFVS= I4/25H CONTROL CARDS INCORRECT. )
    6 FORMAT(6F9.2,F10.3)
    7 FORMAT(I4,F5.1,F12.4)
    8 FORMAT(I7,F7.0,  E14.7,  2(I6,F9.3))
    9 FORMAT(6(I5,  E14.7))
   10 FORMAT(  E15.7,  4E14.7)
   11 FORMAT(10H  NCARDS= I4, 10H  NCARDS= I4)
  100 FORMAT(I4,2F9.6,5I4)
  102 FORMAT(2F4.0,2F7.3)
  103 FORMAT(6H ZZ1= F4.0,8H   ZZ2= F4.0,10H   BETA1= F7.3,
     1 10H   BETA2= F7.3)
  203 FORMAT(8H   KEY = I4)
  908 FORMAT  (6H  ITER,7X,1HZ,4X5HDELTA,7X,30HI(DEL)  X(DEL)  I(CUT)  X
     1(CUT)  )
 2002 FORMAT(I4,  3E14.7,I4,  E14.7,8X,1HZ,I3,I4)
 2003 FORMAT(54.0,3I4,56X,1HZ,I3,I4)
 2010 FORMAT(  E14.7,  4E14.7,1X,1HZ,I3,I4)
 2011 FORMAT (  E15.7,57X,1HZ,I3,I4)
 9000 FORMAT (72H
     1                                    )
   15 CONTINUE
C     READ HEADING CARD.
      READ 9000
      PRINT 9000
      READ 8000,ANAME
        READ 741,RADIUS,RATIO,ALFA,IWAT,ITAPE
  741     FORMAT(3F10.4,2I4)
  742   FORMAT(1X,*WAT RAD IN A.U=*,E14.7,*RATIO=*,E14.7,*ST-ENGTH OF
     1SLATER EXCH=*,E14.7 , *IWAT(1 FOR WATSON)=*,I4,* ITAPE=*,I4)
 8000 FORMAT(A6)
      WRITE (4,8001) ANAME
 8001 FORMAT(18H CALCULATIONS FOR ,A6,31H ( USING H-F-S WAVE FUNCTIONS )
     /)
C     READ CONTROL CARDS AND INPUT POTENTIALS. CALCULATE TRIAL POTENTIAL
```

```
      READ 100,KEY,TOL,THRESH,MESH,IPRINT,MAXIT,KUT
      PRINT 100,KEY,TOL,THRESH,MESH,IPRINT,MAXIT,KUT
      NCARDS=90
      PRINT 203,KEY
      IF(MAXIT) 104,104,105
  104 MAXIT=20
  105 CONTINUE
  107 NBLOCK =(MESH)/40
C     CONSTRUCT X MESH AND R MESH
      I=1
      X(1)=0.0
      R(1)=0.0
      DELTAX=0.0025
      DO 25 J=1,NBLOCK
      DO 24 K=1,40
      I=I+1
   24 X(I)=X(I-1)+DELTAX
   25 DELTAX=DELTAX+DELTAX
      IF(KEY-1)1203,208,14
   14 READ 10,(RU2(N),N=1,441)
      READ 10,(RU3(N),N=1,441)
      ZE2=-RU2(1)/2.0
      ZE3=-RU3(1)/2.0
      GO TO 205
C     READ IN ATOMIC POTENTIAL
 1203 READ 1,(RU2(N),N=1,437,4)
      GO TO 205
  208 READ 10,(RU3(N),N=1,441)
      ZE3=-RU3(1)/2.0
  205 READ 3,Z,NCORES,NVALES,ION
      IF (Z) 1000,15  ,206
  206 IZ=Z
      NCSPVS=NCORES+NVALES
      C=0.88534138/Z**(1.0/3.0)
      WRITE (4,8003) C
 8003 FORMAT(1H ,E14.7)
      WRITE (4,8004) NCSPVS
 8004 FORMAT(1H ,I3)
      THOION=ION+ION
         IF(IWAT.NE.1)  GO TO 716
```

```
        RADICN=RADIUS/0.529
      THXICN=THCICN*RATIC
        PRINT 742,RADICN,RATIC,ALFA,IWAT,ITAPE
  716     CONTINUE
      ZZZ=ICN+1
      THCZZZ = ZZZ+ZZZ
      DO 224 I=2,MESH
  224 R(I)=C*X(I)
  21C READ 7,(NNLZ(I),WWNL(I),EE(I),I=1,NCSPVS)
      READ 8C6C,(ACR(J),J=1,NCSPVS)
 8C6C     FORMAT(1X,2CA2)
      WWW=C.C
      DO 112 I=1,NCSPVS
  112 WWW=WWW+WWNL(I)
      IF(ABSF(Z+1.C-WWW-ZZZ)-0.CC1) 114,113,113
  113 PRINT 5,WWW,ZZZ,Z,NCCRES,NVALES,NCSPVS
  114 CONTINUE
      IF (KEY-1) 2C4,2C7,16
C     CONSTRUCT ATOMIC POTENTIAL
   16   IF(ABSF(ZE3-ZE2-Z+ZE3)-0.001) 18,18,1818
 1818 PRINT 1817,Z,ZE2,ZE3
 1817 FORMAT (27HCSTARTING POTENTIALS AND Z=,F4.0,9H IN ERROR,2F4.C)
   18 DO 21 I=1,441
      RL(I)=RU3(I)+RU3(I)-RU2(I)
   21 CONTINUE
      GO TC 211
  2C4 THCZ=Z+Z
      DO 11C I=1,437,4
  11C RL(I)=-RU2(I)+THCZ
      RL(441)=RL(437)
      RL(445)=RL(437)
      M=5
      DO111 I=1,437,4
      M=M-1
      IF(M) 11CC,1103,1101
 11CC RL(I+1)=(22.C*RU(I)+11.0*RU(I+4)-RU(I+8))/32.0
      RL(I+2)=(1C.C*RU(I)+15.0*RU(I+4)-RU(I+8))/24.0
      RL(I+3)=( 6.C*RU(I)+27.0*RU(I+4)-RU(I+8))/32.0
      M=5
      GO TC 111
```

```
1101 RU(I+1)=(21.0*RU(I)+14.0*RU(I+4)-3.0*RU(I+8))/32.0
     RU(I+2)=( 3.0*RU(I)+ 6.0*RU(I+4)-    RU(I+8))/ 8.0
     RU(I+3)=( 5.0*RU(I)+30.0*RU(I+4)-3.0*RU(I+8))/32.0
 111 CONTINUE
     GO TO 211
 207 IF(ABSF(ZE3-Z)-0.001)  215,215,220
 215 DO 213 I=1,441
     RU(I)=RU3(I)
 213 CONTINUE
     GO TO 211
 220 ZOZ=Z/ZE3
     DO 223 I=1,441
     RU(I)=RU3(I)*ZOZ
 223 CONTINUE
 211 V(1)=-9.9E35
     M=XMINOF(441,MESH)
     IF(KLT) 1212,1260,1212
1212 DO 1213 I= 1,M
1213 V(I)= RU(I)/R(I)
     IF(MESH-M)1214,1214,1216
1214 DO 1215 I=442, MESH
1215 V(I)=-THOICK/R(I)
1216 LIMIT=M
     ICUT= MESH
     KC=MESH
     GO TO 268
1260 CONTINUE
     ICUT=0
     DO 26 I=2,M
     IF (ICUT) 261,261,263
 261  IF( THOZZZ+RU(I)) 264,264,262
 262 ICUT =I
 263 V(I)=-THOZZZ/R(I)
     GO TO 26
 264 V(I)=RU(I)/R(I)
  26 CONTINUE
     IF(ICUT) 265,265,266
 265  ICUT=M
 266 LIMIT=ICUT
     IF(MESH-M) 268,268,267
```

```
  267 CONTINUE
      DO 115 I=442,MESH
  115 V(I)=-TWO222/R(I)
  268 CONTINUE
      DELTA =10CCCCO.
      NITER=C
      NONMCN =3
C     START ITERATION
      PRINT 908
      IPRSW=C
   27 MCARDS=90
      IF(MAXIT-NITER) 405,28,28
  405 CONTINUE
      PRINT 45C
       DC 5C4 I=1,MESH
 5C4   RL(I)=RU(I)/TWOZ
      DO 41C I=1,MESH,5
      PRINT 451,I,X(I),RU3(I),RUINL1(I),RUFNL1(I),RUINL2(I),RUFNL2(I),RU
     /(I)
  41C CONTINUE
  45C FORMAT (4CH1I,X,RU3,RUINL1,RUFNL1,RUINL2,RUFNL2,RU    )
  451 FORMAT (I8,F10.4,  6E16.7)
      GO TC 205
   28 DO 29 I=1,MESH
         RU3(I)=        C.0
      RSCORE(I)=C.C
   29 RSVALE(I)=C.C
C     SOLVE SCHROEDINGER EQUATION FOR EACH STATE IN TURN. ALSO CALCULATE
C           CORE AND VALENCE CHARGE DENSITY.
      DO 35 M=1,NCSPVS
      E=EE(M)
       NN=NNL2(M)/100
       LAM =NNL2(M)/10 -10*NN
       XL= LAM
       CALL SCHEQ(Z,E,LAM,NN,KKK,MESH,C,THRESH)
      IF(M-NCORES)30,30,32
   30 DO 31 I=1,KKK
         RU3(I)=WWNL(M)*SNLC(I)**2
   31    RSCORE(I)=RSCORE(I)+RU3(I)
      GO TC 34
```

```
   32 DO 33 I=1,KKK
   33 RSVALE(I)=RSVALE(I)+WWNL(N)*SNLC(I)**2
   34 DO 201 I=1,KKK
  201 SNL(N,I)=SNLC(I)
      NKKK(N)=KKK
      MCARDS=MCARDS+2+((KKK-1)/40)*8
   35 EE(N)=E
C     CALCULATE TOTAL CHARGE DENSITY AND ATOMIC EXCHANGE POTENTIAL
      DO 37 I=1,MESH
   36 RSATOM(I)=RSCORE(I)+RSVALE(I)
   37  RUEXCH(I)=-6.*ALFA*((3.0*R(I)*RSATOM(I))/315.82734)**(1.0/3.0)
C     CALCULATE ATOMIC COULOMB POTENTIAL
      A1=0.0
      ASUM=0.0
      B1=0.0
      BSUM=0.0
      H=0.0025*0
      I=1
      XI(1)=0.0
      XJ(1)=0.0
      DO 39 J=1,NBLOCK
      DO 38 K=1,40
      I=I+1
      A2=RSATOM(I)/2.0
      A1=A1+A2
      B2=RSATOM(I)/(2.0*R(I))
      B1=B1+B2
      XI(I)=ASUM+A1*H
      XJ(I)=BSUM+B1*H
      A1=A1+A2
   38 B1=B1+B2
      ASUM=XI(I)
      BSUM=XJ(I)
      A1=A2
      B1=B2
   39 H=H+H
   40 CONTINUE
   41 DO 44 I=1,MESH
      XI(I)=-2.0*2+2.0*(XI(I)+R(I)*(XJ(MESH)-XJ(I)))
      XJ(I)=XI(I)+RUEXCH(I)
```

```
   44 CONTINUE
        IF(IWAT.NE.1)GO TO 717
          DO 714   I=2,MESH
             IF(R(I).GE.RADICN)  GO TO 715
           XJ(I)=XJ(I)+(TWXICN*R(I))/RADICN
             GO TO 714
  715       XJ(I)=XJ(I)+TWXICN
  714         CONTINUE
  717       CONTINUE
   74 DO 75  I=1,MESH
      RLINL1(I)=RLINL2(I)
      RLFNL1(I)=RLFNL2(I)
      RLINL2(I)=RL(I)
   75 RLFNL2(I)=XJ(I)
   76 NITER=NITER+1
      PDELTA =DELTA
      DELTA =0.0
      DO 48  I=1,LIMIT
   45 SNLO(I)=RL(I)-XJ(I)
   46 XI(I)=ABSF(SNLO(I))
      IF (XI(I)-DELTA)48,48,47
   47 DELTA=XI(I)
      IDELTA=I
   48 CONTINUE
      PRINT 8,NITER,Z,DELTA,IDELTA,X(IDELTA),ICUT,X(ICUT)
C     TEST SELF-CONSISTENCY OF ATOMIC POTENTIAL.
   50 IF(DELTA-TOL) 58,51,51
C     IF SCF CRITERION NOT SATISFIED, CALCULATE NEXT TRIAL POTENTIAL.
   51   PART=0.7
          IF(IWAT.NE.1) PART=0.5
        PART1=1.-PART
        IF(IPRSW) 80,80,82
   80 DO 81  I=2,LIMIT
   81   RU(I)=PART*RU(I)+PART1*XJ(I)
      IF (MESH-LIMIT)  280,280,270
  270 RUZM=XJ(MESH)
      RATIO =(RUZM-RU(LIMIT))/(RUZM-XJ(LIMIT))
      DO 271  I=LIMIT,MESH
  271 RL(I)=RUZM-RATIO*(RUZM-XJ(I))
      LIMIT =MESH
```

```
  280 IPRSW=IPRATT
      GO TO 87
   82 CONTINUE
  282 IF(NCNMCN) 80,80,183
  183 IF(PDELTA-DELTA)184,184,185
C       IF DELTA IS NOT MONOTONIC DECREASING FOUR TIMES, BYPASS
C         PRATT IMPROVEMENT SCHEME
  184 NONMCN =NCNMCN-1
      IF(NCNMCN)80,80,185
  185 ALPH=0.5
C       PRATT IMPROVEMENT SCHEME
      DO 849 I=2,ICUT
      XNUM(I)=RUINL1(I)*RUFNL2(I)-RUINL2(I)*RUFNL1(I)
      DENM(I)=RUFNL2(I)-RUFNL1(I)-RUINL2(I)+RUINL1(I)
  182 IF(ABSF(DENM(I)/RUINL2(I))-0.0001) 83,83,84
   83 CONTINUE
  832 ALPH=0.5
      GO TO 846
   84   ALPH=(XNUM(I)/DENM(I)-RUFNL2(I))/SNLO(I)
      IF(ALPH) 841,845,842
  841 ALPH=0.0
      GO TO 846
  842 IF(0.5-ALPH) 843,845,845
  843 ALPH=0.5
  845 CONTINUE
  846 XI(I)=ALPH
  849 CONTINUE
      IPRSW=IPRSW-1
      IF(KLT) 1873,1849,1873
 1849 CONTINUE
      IC=ICUT+20
      IC1=ICUT+1
      ADEL=XI(ICUT)/20.
      DO 873 I=IC1,IC
      XI(I)=XI(I-1)-ADEL
  873 XJ(I)=XI(I)
 1873 CONTINUE
      XJ(1)=0.5
      XJ(2)=XI(2)
      ASUM=XI(2)+XI(3)+XI(4)+XI(5)
```

```
      DO 874 I=3,ICUT
      XJ(I)=ASUM*C.2
  874 ASUM=ASUM-XI(I-2)+XI(I+3)
      IF(KLT) 1875,1874,1875
 1874 CONTINUE
      IC1=IC+1
      DO 875 I=IC1,MESH
      XJ(I)=C.C
  875 RU(I)=RUFAL2(I)
 1875 CONTINUE
      DO 876 I=2,IC
  876 RU(I)= RUFAL2(I)+XJ(I)*SALC(I)
   87 CONTINUE
      IF(KLT) 287C,187C,2870
 287C ICLT=MESH
      LIMIT=MESH
      DO 2871 I=2,MESH
      VLAST= V(I)
      V(I)=RU(I)/R(I)
 2871 XI(I)=V(I)-VLAST
      GO TO 1861
 187C CONTINUE
      ICLT =C
      DO 86 I=2,MESH
      VLAST=V(I)
      IF(ICLT) 851,851,853
  851 IF(TWOZZZ+RL(I)) 854,854,852
  852 ICLT=I
  853 V(I)=-TWOZZZ/R(I)
      GO TO 86
  854 V(I)=RU(I)/R(I)
   86 XI(I)=V(I)-VLAST
 1861 CONTINUE
      XI(1)=0.0
C     NEXT TRIAL EIGENVALUES P
      NCARDS=90
      DO 55 M=1,NCSPVS
      K=(NKKK(M)-1)/40
      H=C.CC25*C
      ASUM=C.0
```

```
      A1=C.C
      I=1
      DO 54 J=1,K
      DO 53 L=1,4C
      I=I+1
      A2=X[(I)*SNL(M,I)**2
   53 A1=A1+A2*H
      ASLM=ASLM+A1-(A2/2.0)*H
      H=H+H
   54 A1=(A2/2.C)*H
      EE(M)=EE(M)+ASLM
   55 NCARDS=NCARDS+8*K+2
      GO TO 27
C     RESULTS TRANSFERRED FROM INTERNAL MEMORY TO OUTPUT TAPE(S).
C     OUTPUT
C       COM
   58 CONTINUE
  58C PRINT 11,NCARDS,NCARDS
      PRINT 719 ,(R(I),I=1,MESH)
        PRINT 719, ( RSATCN(I),I=1,MESH )
C       PRINT 719,     (RU3(I),I=1,MESH)
  719   FORMAT(1X,10E12.5)
      NC=1
      PRINT 2CC3,Z,NCORES,NVALES,ION,IZ,NC
      DO 583 I=1,441
      IF(THICN+RUINL2(I)) 583,583,581
  581 DO 582 M=1,441
  582 RUINL2(M)=-THICN
      GO TO 584
  583 CONTINUE
  584 CONTINUE
      DO 588 MIN =1,440,5
      MAX=MIN+4
        NC=NC+1
  588 CONTINUE
      NC=NC+1
      DO 55 M=1,NCSPVS
      NLZ=NNLZ(M)
      KKK=NKKK(M)
      XL=NLZ/10-3C*(NLZ/100)
```

```
      ELEC=WHNL(M)
      MBLOCK=KKK/4C
      LP=XL+1.C
C     COMPLT
      DO 591 I=1,4
      A(I,1)=1.C
      A(I,2)=R(I+1)
      A(I,3)=R(I+1)*R(I+1)
      A(I,4)=R(I+1)*A(I,3)
  591 A(I,5)=SNL (M,I+1)/R(I+1)**LF
      CALL CRCSYM (4)
      NC=NC+1
      PRINT 2C02,ALZ,XL,EE(M),WHNL(M),KKK,A(1,5),IZ,NC
      WRITE (4,8CC5) ACR(M),IELEC,XL,MBLOCK,EE(M)
 8CC5  FORMAT(1H ,A2,1H(,I2,1H),F4.C,I3,E14.7)
      K1=KKK-1
      DO 598 MIN=1,K1,5
      NC=NC+1
      MAX= MIN+4
C        PRINT WAVE FUN BY REMOVING IT
  598 CONTINUE
      NC=NC+1
C        PRINT WAVE FUN BY REMOVING IT
      DELTAX=.CC25
      JJ=1
      JJ1=1
      DO 8C59 J=1,MBLOCK
      JJ=JJ+4C
      IF(J-1) 8C5C,8C51,8C50
 8C51 NEW=41
      GO TO 8C52
 8C5C NEW=44
 8C52   WRITE (4,8C53) NEW,DELTAX,X(JJ1)
 8C53 FORMAT(1H ,I3,2F5.4)
      DELTAX=DELTAX+DELTAX
      IF(J-1) 8C55,8C54,8C55
 8C54 WRITE (4,8C56) (SNL(M,I),I=1,JJ)
 8C56 FORMAT(1H ,5E14.7)
      GO TO 8C58
 8C55 WRITE (4,8C56) ((SNL(M,I),I=JJ1,JJ2,2),SNL(M,JJ3))
```

```
      WRITE (4,8C56) (SNL(P,I),I=JJ4,JJ)
      JJJ=JJJ-6
      JJ2=JJJ
      JJ3=JJJ+1
      JJ4=JJJ+2
C55   CONTINUE
 55   CONTINUE
      IF(KEY-1)  958,960,965
 958  KEY=1
 960  DO 961 I=1,NESH
 961  RU3(I)=RU(I)
      ZE3=Z
      GO TO 2C5
 965  DO 966 I=1,NESH
      RU2(I)=RU3(I)
 966  RU3(I)=RU(I)
      ZE2=ZE3
      ZE3=Z
      GO TO 2C5
 1CCC CONTINUE
      STOP
 2C05 END
```

LISTING OF THE MAIN COMPUTER PROGRAM
TO CALCULATE γ_∞ AND R FACTORS

```
      DIMENSION XRI(13),XLWPU(4),C(4),MENTRY(13),AORBIT(17),NELECT(17),X
     /LWLN(17),MCREG(17),GUNC(13,47),KENTRY(13),LENTRY(13),DELXR(13),DEL
     /XRR(13),GAMAIN(17,4),RR(17,4),ORBITP(17,4),NEXITA(17),ENERGY(17)
      DIMENSION WPU(13,47),XR(13,47),WUN(16,12,44),FUNC(13,47),A(4,5)
      COMMON WPU,XR,WUN,FUNC,A
      COMMON ENERGY
        DIMENSION SRDSUM(17,4),SRESUM(17,4)
      CALL FLUN(32000)
        RR1=0.0
          CALL FLCV( 32000)
        ITAPE=4
        GM1=0.0
C READ NCATOM, THE NUMBER OF THE ATOM/ION TO BE TREATED IN ONE RUN
      REWIND 4
      READ 500,NCATOM
  500 FORMAT(I3)
C
C  THIS DO-LOOP PERFORMS THE CALCULATION OF ALL THE NOATOM ATOMS ONE BY O
C
      DO 7 NATOM=1,NOATOM
C
C  READ AND PRINT THE NAME OF THE ATOM/ION BEING TAKEN FOR THE CALCULATIO
C
      READ (ITAPE,8001)
 8001 FORMAT(1X,35H                                    )
      PRINT 9000
 9000 FORMAT(//)
      PRINT 8001
      PRINT 9001
 9001 FORMAT(125H ************************************************************
     /************************************************************
     /****)
      PRINT 9001
C
C  READ Z, THE SCALE FACTOR USED IN DEFINING THE VARIABLE -XR- AS XR=Z*R
C  H-F-S CALCULATIONS.
C
      READ (ITAPE,8003) Z
 8003 FORMAT(1H ,E14.7)
      ZZ=(0.88534138/Z)**3
C
C  READ NOORB, THE TOTAL NUMBER OF THE ORBITALS IN THE ATOM UNDER CONSIDE
C
      READ (ITAPE,8004) NOORB
C       JTAPE=3
C        WRITE (JTAPE,8004) NOORB
C          PRINT 8004,NOORB
 8004 FORMAT(1H ,I3)
C
C  THIS DO-LOOP DOES THE CALCULATIONS FOR THE VARIOUS ORBITALS ONE BY ONE
```

```
C
CC        WHEN DOING CALCULATIONS  SHIFT 781 TO 789  AFTER 850 . REMOVE
CC          NCRBVA=3
C             THE FOLLOWING CARD
      DO 5 NORB=1,NCORE
C
CC  READ AORBIT, THE ORBITAL SPECTRASCOPIC DESIGNATION
CC  READ NELECT, THE NUMBER OF THE ELECTRONS IN THE ORBITAL
CC  READ XLWUN, THE L VALUE FOR THE ORBITAL
CC  READ NOREG, THE NUMBER OF THE REGIONS USED IN THE TABULAR REPRESENTATI
CC  THE UNPERTURBED WAVE FUNCTION.
C
       READ (ITAPE,8005) AORBIT(NCRE),NELECT(NCRB),XLWUN(NCRB),NOREG(NORB
     1),ENERGY(NCRE)
C        WRITE (JTAPE,8005) AORBIT(NCRB),NELECT(NORB),XLWUN(NORB),
CC     1NOREG(NCRB),ENERGY(NCRB)
CC       PRINT 8005,              AORBIT(NCRB),NELECT(NORB),XLWUN(NORB),
C      1NOREG(NORB),ENERGY(NCRB)
 8005  FORMAT(1H ,A2,1H(,I2,1H),F4.0,I3,E14.7)
       NOREG=NCREG(NCRB)
C
CC  IN THIS DO-LOOP WE READ REGIONWISE, FIRST, NENTRY(NORG), THE NUMBER OF
CC  ,DELXR(NORG), THE INCREMENT IN THE XR VALUES AND XRI(NORG), THE STARTI
CC  OF XR. AFTER THIS WE READ ALL THE NENTRY(NORG) ENTRIES OF WUN(NORG,J),
CC  RY(NORG) ,THE UNPERTURBED WAVE FUNCTION OF THE ORBITAL
C
       DO 5 NORG=1,NOREG
       READ (ITAPE,8053) NENTRY(NORG),DELXR(NORG),XRI(NORG)
 8053  FORMAT(1H ,I3,2F9.4)
       NENTRY=NENTRY(NORG)
       READ (ITAPE,8056) (WUN(NORB,NORG,J),J=1,NENTRY)
C      IF(NORG-1) 51,51,52
C51      WRITE (JTAPE,8056) (WUN(NORB,NORG,J) ,J=1,40)
CC       PRINT 8056,              (WUN(NORB,NORG,J) ,J=1,40)
C          GO TO 53
C52      WRITE (JTAPE,8056)       (WUN(NORB,NORG,J),J=4,43)
CC       PRINT 8056,              (WUN(NORB,NORG,J),J=4,43)
C53        CONTINUE
 8056  FORMAT(1H ,5E14.7)
C
CC  WITH THE HELP OF XRI(NORG) AND DELXR(NORG) WE NOW GENERATE THE XR MESH
CC  REGION UNDER CONSIDERATION (NORG-TH REGION)
C
       DELXR(NORG)=2*DELXR(NORG)
       XR(NORG,1)=XRI(NORG)*Z
       DO 5 J=2,NENTRY
  5    XR(NORG,J)=XR(NORG,J-1)+DELXR(NORG)
C              NOREG=NCREG(NCRBVA)
CC       DO 55   NORG=1,NOREG
C         IF(NORG-1) 56,56,57
```

```
C56       WRITE(JTAPE,8056)        (XR(NORG,J),J=1,40)
C            PRINT 8056,           (XR(NORG,J),J=1,40)
C              GO TO 55
C57       WRITE (JTAPE,8056) (XR(NORG,J),J=4,43)
C      PRINT 8056,               (XR(NORG,J),J=4,43)
C55         CONTINUE
      READ 2224,NCAL
 2224 FORMAT(I2)
      GO TO (2226,2225,2225),NCAL
 2225 READ 999,NCRBVA
 999  FORMAT(I2)
      LO=0
      NOREG=NCREG(NCRBVA)
      FUNC(1,1)=C.C
      DO 1CC4 NCRG=1,NCREG
      NENTRY=MENTRY(NCRG)
      IF(NCRG-1) 9994,9995,9994
 9995 J1=2
      GO TO 9996
 9994 J1=1
 9996 DO 1004 J=J1,NENTRY
 1004 FUNC(NCRG,J)=(WUN(NCRBVA,NCRG,J)**2)/(XR(NCRG,J)**3)
      CALL INTEGR (EXPVA,NCREG,MENTRY,LO,DELXR)
      PRINT 1011,EXPVA
 1011 FORMAT(//68H THE EXPECTATION VALUE (WUN*(1/(R**3))*WUN) FOR THE VA
     /LENCE ORBITAL=,E14.7)
 2226 SURRAD=0.C
      SURANG=0.C
       SMETCT=0.C
       SMDICT=0.C
       SREANG=0.C
      SRDANG=0.C
      SRERAD=0.C
        SRDRAD=C.C
      R-SUM=0.0
      R1=0.0
      SUGRAD=0.0
      SUGANG=0.C
      DO 77 NCRB=1,NOORB
      NOREG=NCREG(NCRB)
      EZERC=ABS(ENERGY(NORB))
      LWUN=XLWUN(NCRB)
C
C  PRINT THE ORBITAL SPECIFICATIONS
C
      PRINT 111,ACRBIT(NORB),NELECT(NORB),LWUN
 111  FORMAT(//9H ORBITAL ,A2,1H(,I2,6H)  L= ,I2)
      PRINT 9002
 9002 FORMAT(22H ----------------------)
      PRINT 9002
```

```
C
C -LESS AND THEY ARE GIVEN ARBITRILLY.
C
      READ 4,NEXITA(NCRB),NCRGM,JM
C     WRITE(JTAPE,4) NEXITA(NCRB),NCRGM,JM
C     PRINT 4,       NEXITA(NCRB),NCRGM,JM
 4    FORMAT(I2,2I3)
      NEX=NEXITA(NCRB)
C
C  IF THERE IS NO EXITATION TO BE CONSIDERED, SKIP TO THE NEXT ORBITAL
C
      IF(NEX) 5C1,7CC,5C1
 7CC  PRINT 7C1
 7C1  FORMAT(//14H NO EXCITATION//)
      NEXITA(NCRB)=1
      RR(NCRB,1)=C.C
      GAMAIN(NCRB,1)=C.C
      GO TO 77
 5C1  CONTINUE
      FUNC(1,1)=C.C
      DO 1CC3 NCRG=1,NCREG
      NENTRY=MENTRY(NCRG)
      IF(NCRG-1) 9991,9992,9991
 9992 J1=2
      GO TO 9993
 9991 J1=1
 9993 DO 1CC3 J=J1,NENTRY
 1CC3 FUNC(NCRG,J)=(WUN(NCRB,NCRG,J)**2)/(XR(NCRG,J)**3)
      CALL INTEGR (EXPWUN,NCREG,MENTRY,LO,DELXR)
      PRINT 1CI2,EXPWUN
 1C12 FORMAT(//61H THE EXPECTATION VALUE (WUN*(1/(R**3))*WUN) FOR THIS O
     /RBITAL=,E14.7)
      DO 1CC5 I=1,4
      A(I,1)=1.C
      A(I,2)=XR(1,I+1)
      A(I,3)=A(I,2)**2
      A(I,4)=A(I,2)**3
 1CC5 A(I,5)=WUN(NCRB,1,I+1)/(XR(1,I+1)**(LWUN+1))
      CALL SIMULT (4)
      AZERO=A(1,5)
      PRINT 1CC9,AZERO
 1CC9 FORMAT(//16H THE CONSTANT A=,E14.7//)
C
CC READ XLWPU, THE L VALUES AND C, THE C-(LWUN,LWPU) VALUES FOR ALL THE N
CC EXITATIONS IN THE ORBITAL
C
      READ 6,(ORBITP(NCRB,NEXIT),XLWPU(NEXIT),C(NEXIT),NEXIT=1,NEX)
C     WRITE(JTAPE,6)(ORBITP(NCRB,NEXIT),XLWPU(NEXIT),C(NEXIT),NEXIT=1,
CC   1 NEX)
C     PRINT 6,       (ORBITP(NCRB,NEXIT),XLWPU(NEXIT),C(NEXIT),NEXIT=1,
```

```
C     1 NEX)
  6    FORMAT(4(A2,2F8.5))
C
C THIS DO-LOOP PERFORMS THE CALCULATIONS FOR ALL THE EXITATIONS IN THE O
C ONE BY ONE.
C
      DO 777 NEXIT=1,NEX
      LWPU=XLWPU(NEXIT)
      PRINT 222,ACRBIT(NCRB),LWUN,ORBITP(NCRB,NEXIT),LWPU
      RR(NCRB,NEXIT)=0.0
       SRDSLM(NCRB,NEXIT)=0.0
          SRESUM(NCRB,NEXIT)=0.0
C     WRITE (JTAPE,222) ACRBIT(NCRB),LWUN,ORBITP(NCRB,NEXIT),LWPU
  222 FORMAT(//16H THE EXCITATION ,A2,3H(L=,I2,5H) TO ,A2,3H(L=,I2,1H)//
     /)
      DLWUWP=(LWPL*(LWPU+1)-LWUN*(LWUN+1))
      IF(DLWUWP) 9,8,9
    9 PRINT 221
  221 FORMAT(29H THIS IS A ANGULAR EXITATION //)
      EXTEST=0.0
      GO TO 16
    8 PRINT 220
  220 FORMAT(28H THIS IS A RADIAL EXITATION //)
      EXTEST=1.0
   16 CALL PURWAV(LWPU,LWUN,EXPWUN,NORGM,JM,NOREG,MENTRY,NORB,DELXR,ZZ,
     1AZERO)
C
C
      IF(DLWUWP) 1041,1040,1041
 1040 DO 11 NORG=1,NOREG
      NENTRY=MENTRY(NORG)
      DO 11 J=1,NENTRY
   11 FUNC(NORG,J)=WUN(NORB,NORG,J)*WPU(NORG,J)
      CALL INTEGR (OLAP,NOREG,MENTRY,LO,DELXR)
      PRINT 9011,OLAP
 9011 FORMAT(  31H THE OVERLAP INTEGRAL IS      =,E14.7)
      DO 12 NORG=1,NOREG
      NENTRY=MENTRY(NORG)
      DO 12 J=1,NENTRY
   12 WPL(NORG,J)=WPU(NORG,J)-OLAP*WUN(NORB,NORG,J)
C
C LET US NOW CHECK THE ORTHOGONALITY BETWEEN WPU AND WUN.
C
      DO 9008 NORG=1,NOREG
      NENTRY=MENTRY(NORG)
      DO 9008 I=1,NENTRY
 9008 FUNC(NORG,I)=WUN(NORB,NORG,I)*WPU(NORG,I)
      CALL INTEGR (OLAP,NOREG,MENTRY,LO,DELXR)
      PRINT 9009,OLAP
 9009 FORMAT(  31H THE OVERLAP INTEGRAL IS NOW  =,E14.7)
```

```
C
CC  NOW PRINT THE PURTURBED WAVE FUNCTION WHICH IS ORTHOGONAL TO THE UNPUR
C   ONE
C
 1041 PRINT 333
  333 FORMAT(//5CH THE PURTURBED WAVE FUNCTION FOR THE EXCITATION IS//)
 1C1C FORMAT(1H ,9E14.7)
C
CC  NOW EVALUATE THE INTEGRAL (WPU*(R**2)*WUN) REQUIRED TO CALCULATE GAMA-
C
      GO TO (2228,2227,2228),NCAL
 2227 GAMAIN(NCRB,NEXIT)=0.0
      GO TO 2223
 2228 DO 15 NCRG=1,NOREG
      NENTRY=MENTRY(NCRG)
      DO 15 J=1,NENTRY
   15 FUNC(NORG,J)=WUN(NCRB,NCRG,J)*WPU(NORG,J)*(XR(NORG,J)**2)
      CALL INTEGR (GAMA,NCREG,MENTRY,LO,DELXR)
      GAMAIN(NCRB,NEXIT)=C(NEXIT)*GAMA
      GM1=GM1+GAMAIN(NCRB,NEXIT)
      IF(NCAL-1) 2223,2222,2223
 2222 RR(NCRB,NEXIT)=0.0
      GO TO 1111
 2223 IF(NCRB-NCREVA) 6666,6661,6666
 6661 RR(NCRB,NEXIT)=0.0
 6666  CONTINUE
      READ 670,NGEN
C     NGEN GIVES TOTAL NO OF DIFFERENT CONTRIBUTIONS TO BE CALCULATED
  670   FORMAT(1X,I3)
  671   FORMAT(1X,I3,F8.5)
      DO 672 NTIME=1,NGEN
      READ 671,L,C(NTIME)
      IF(NTIME-1) 673,673,674
  673   NOREG=NCREG(NCRB)
      NOREGV=NCREG(NCREVA)
      NOR5=NCRB
      NOR6=NCRBVA
      GO TO  675
  674   NO1=NOREG(NORE)
      NO2=NCREG(NCRBVA)
      NOREG=MINO(NO1,NO2)
      NCR5=NCRBVA
      NOR6=NCRB
        NOREGV=NCREG
  675  IF(NTIME.EQ.1.AND.L.EQ.0) GO TO 672
      DO 870 NORGR=1,NCREG
       NENTRY=MENTRY(NCRGR)
      IF(NCRGR-NCREG) 886,887,887
  887 NENTRY=NENTRY-2
      GO TO 868
```

```
      IF(NCRGR-1) 868,869,868
869   JR1=1
      KO=0
      GO TO 867
868   JR1=5
867   DO 884 JR=JR1,NENTRY
      IF(JR-3) 896,895,895
895   KO=2
896   FINT1=0.0
      FINT2=0.0
      IF(JR-1) 885,876,885
885   DO 871 NCRG=1,NCRGR
871   KENTRY(NCRG)=NENTRY(NCRG)
      KENTRY(NCRGR)=JR+2
      IF(JR-NENTRY+1) 872,873,873
873   IF(NCRGR-NCREG) 890,872,872
890   WPL(NCRGR,NENTRY+1)=(WPU(NCRGR+1,4)+WPU(NCRGR+1,5))*0.5
      WUN(NCRB,NCRGR,NENTRY+1)=(WUN(NCRB,NCRGR+1,4)+WUN(NCRB,NCRGR+1,5))
     /*(0.5)
      WUN(NCRBVA,NCRGR,NENTRY+1)=(WUN(NCRBVA,NCRGR+1,4)+WUN(NCRBVA,
     1NCRGR+1,5))*(0.5)
      XR(NCRGR,NENTRY+1)=(XR(NCRGR+1,4)+XR(NCRGR+1,5))*(0.5)
      WPL(NCRGR,NENTRY+2)=WPU(NCRGR+1,5)
      WUN(NCRB,NCRGR,NENTRY+2)=WUN(NCRB,NCRGR+1,5)
      WUN(NCRBVA,NCRGR,NENTRY+2)=WUN(NCRBVA,NCRGR+1,5)
      XR(NCRGR,NENTRY+2)=XR(NCRGR+1,5)
872   DO 874 NCRG=1,NCRGR
      NJ=KENTRY(NCRG)
      DO 874 J=1,NJ
      IF(L.LT.1) GO TO 478
      FUNC(NCRG,J)=WUN(NCRB,NCRG,J)*WPU(NCRG,J)*(XR(NCRG,J)**L)
      GO TO 874
478   FUNC(NCRG,J)=WUN(NCRB,NCRG,J)*WPU(NCRG,J)
874         CONTINUE
      CALL INTEGR (FINT1,NCRGR,KENTRY,LO,DELXR)
      IF(JR-NENTRY+2) 876,875,875
875   IF(NCRGR-NCREG) 750,884,750
750   NORGS=NCRGR+1
      N=NORGS-1
      NORGL=NCREG-NCRGS+1
      IF(JR-NENTRY+1) 994,994,993
994   JRR=3
      GO TO 877
993   JRR=4
      GO TO 877
876   NORGS=NCRGR
      N=NORGS-1
      NORGL=NCREG-NORGS+1
      JRR=JR
877   DO 878 NN=1,NCRGL
```

```
  878   LENTRY(NN)=MENTRY(NN)
        LENTRY(1)=MENTRY(NCRGS)-JRR+1+KO
        DO 881 NN=1,NCRGL
        N=N+1
        DELXRR(NN)=DELXR(N)
        NJ=LENTRY(NN)
        IF(NN-1) 883,882,883
  882   J=JRR-1-KC
        GO TO 892
  883   J=C
  892   DO 881 JJ=1,NJ
        J=J+1
  881     FUNC(NN,JJ)=WUN(NCRS,N,J)*WPU(N,J)/(XR(N,J)**(L+1))
        CALL INTEGR (FINT2,NCRGL,LENTRY,KO,DELXRR)
        IF(JR-NENTRY+1) 884,991,884
  991   F1=(WPU(NCRGR,JR)*WUN(NCRS,NCRGR,JR))/((XR(NORGR,JR)**(L+1)))
        F2=(WPU(NCRGR,JR+2)*WUN(NCRS,NORGR,JR+2))/((XR(NORGR,JR+2)**(L+1))
       1)
        FINT2=FINT2-((F1+F2)*DELXR(NCRGR)*(1./2.))
  884     GUNC(NCRGR,JR)=(FINT1+FINT2*(XR(NORGR,JR)**(2*L+1)))
        GUNC(NCRGR+1,1)=GUNC(NCRGR,NENTRY-6)
        GUNC(NORGR+1,2)=GUNC(NCRGR,NENTRY-4)
        GUNC(NORGR+1,3)=GUNC(NCRGR,NENTRY-2)
        GUNC(NCRGR+1,4)=GUNC(NCRGR,NENTRY)
  870   CONTINUE
        GUNC(NOREG,NENTRY+1)=GUNC(NCREG,NENTRY)
        GUNC(NOREG,NENTRY+2)=GUNC(NCREG,NENTRY)
C
        IF(NCREG-NCREGV) 1007,1008,1008
  1007  GLIMIT=GUNC(NCREG,NENTRY)
        NORG1=NCREG+1
        DO 1006 NCRG=NORG1,NCREGV
        NENTRY=MENTRY(NORG)
        DO 1006 J=1,NENTRY
  1006  GUNC(NCRG,J)=GLIMIT
  1008  PRINT 998
  998   FORMAT(//41H THE GENERAL QUADRUPOLE POLARIZABILITY IS//)
        FUNC(1,1)=0.0
        DO 891 NORG=1,NCREGV
        NENTRY=MENTRY(NORG)
        IF(NCRG-1) 996,997,996
  997   J1=2
        GO TO 995
  996   J1=1
  995   DO 891 J=J1,NENTRY
  891     FUNC(NORG,J)=GUNC(NORG,J)*(WUN(NOREVA,NORG,J)*WUN(NOR6,NORG,J))/
       1(XR(NCRG,J)**(L+1))
        R=0.0
        CALL INTEGR (R,NCREGV,MENTRY,LO,DELXR)
        R1=R*C(NTIME)/EXPVA
```

```
      RTSUM=RTSUM+R1
C
      IF(NTIME.EQ.1) SRDSUM(NCRB,NEXIT)=SRDSUM(NORB,NEXIT)+R1
      IF(NTIME.GT.1) SRESUM(NCRB,NEXIT)=SRESUM(NORB,NEXIT)+R1
      RDSUM=SRDSUM(NCRB,NEXIT)
       RESUM=SRESUM(NCRB,NEXIT)
      PRINT 676,NTIME,L,C(NTIME),R1    ,RDSUM,RESUM,RR(NORB,NEXIT)
      RR(NCRB,NEXIT)=SRDSUM(NCRB,NEXIT)+SRESUM(NORB,NEXIT)
  672   CONTINUE
  676  FORMAT(1X,*NTIME=*,I3,*L =*,I3,*COEF=*,F8.5,*R FOR THIS=*,E14.7,
     1*R-DIRECT=*,E14.7,*R-EXCH=*,E14.7,*R-TOTAL=*,E14.7)
      PRINT 1CC2
 1CC2 FORMAT(//28H THE RATIC GAMA(R)/GAMAIN IS//)
      DO 1CCO NCRG=1,NCREGV
      NENTRY=MENTRY(NORG)
      DO 1CC1 J=1,NENTRY
 1CC1       GUNC(NCRG,J)=GUNC(NCRG,J)/GAMA
 1CCO    CONTINUE
 1111     PRINT 444,RR(NCRE,NEXIT),GAMA,GAMAIN(NORB,NEXIT)
          NCREG=NCREG(NCRE)
             NCRB1= 11
          IF(NCRB.NE.11 )       GO TO 324
        WRITE ( 3,321)  (NCREG,NCRB1,       (MENTRY(NORG),NORG=1,NOREG))
        PUNCH 321,      (NCREG,NCRB1,       (MENTRY(NORG),NORG=1,NOREG))
        PRINT 321,      (NCREG,NCRB1,       (MENTRY(NORG),NORG=1,NOREG))
          DO 322 NCRG=1,NCREG
        NENTRY=MENTRY(NCRG)
        WRITE(3,323) (WUN(NCRB1,NCRG,I),I=1,NENTRY)
        PRINT 323 ,     (WUN(NCRB1,NCRG,I),I=1,NENTRY)
          WRITE(3,323) (WPU(NCRG,I),I=1,NENTRY)
        PUNCH 323 ,     (WUN(NCRB1,NCRG,I),I=1,NENTRY)
        PRINT 323,       (WPU(NCRG,I),I=1,NENTRY)
        PUNCH 323,       (WPU(NCRG,I),I=1,NENTRY)
          WRITE (3,323)  ( XR(NCRG,I),I=1,NENTRY)
        PUNCH 323,         ( XR(NCRG,I),I=1,NENTRY)
        PRINT 323,         ( XR(NCRG,I),I=1,NENTRY)
  322     CONTINUE
          REWIND    3
  321       FORMAT(1X,12I4)
  323       FORMAT(1X,5E14.7)
  324       CONTINUE
  444  FORMAT(//22X21HSTERNHEIMER R-FACTOR=,E14.7//4X39HTHE EXPECTATION V
     /ALUE (WPU*(R**2)*WUN)=,E14.7//29X14HGAMA-INFINITY=,E14.7//)
       RR1=RR1+RR(NCRB,NEXIT)
        PRINT 677, GM1,RR1
  677   FORMAT(1X,*SUM OF GAMMA-INFINITY=*,E14.7,*SUM OF R-FACTOR=*,
     1E14.7,* TELL THIS EXCITATION.*)
       IF(EXIST) 1C22,1021,1022
 1C21 SURANG=SURANG+RR(NCRB,NEXIT)
      SUGANG=SUGANG+GAMAIN(NCRB,NEXIT)
```

```
      SRDANG=SRDANG+SRDSUM(NCRB,NEXIT)
      SREANG=SREANG+SRESUM(NCRB,NEXIT)
      GO TO 777
 1C22 SURRAD=SURRAD+RR(NCRB,NEXIT)
      SUGRAD=SUGRAD+GAMAIN(NCRB,NEXIT)
      SRDRAD=SRDRAD+SRDSUM(NCRB,NEXIT)
      SRERAD=SRERAD+SRESUM(NCRB,NEXIT)
  777 CONTINUE
   77 CONTINUE
      SURTOT=SURANG+SURRAD
      SUGTOT=SUGANG+SUGRAD
      SMETOT= SREANG+SRERAD
      SMDTOT=SRDANG+SRDRAD
      PRINT 9000
      PRINT 8001
      PRINT 1013
      PRINT 1013
 1013 FORMAT(55H **********************************************************)
      PRINT 9000
      PRINT 1014
 1014 FORMAT(1X,113H**********************************************************
     1**********************************************************)
C
      PRINT 1015
 1015 FORMAT(1X,113H*                  *                        *
     1   *                    *                    *                    *)
      PRINT 1016
 1016 FORMAT(1X,113H*LAPR-ORBITAL*  PERTURBED ORBITAL   * GAMMA-INFINITY
     1   *      R-DIRECT      *     R-EXCHANGE     *      R-TOTAL      *)
      PRINT 1015
      PRINT 1014
      DO 1019 NCRB=1,NCORE
      NEX=NEXITA(NCRB)
      PRINT 1015
      DO 1018 NEXIT=1,NEX
 1018  PRINT 1017,ACRBIT(NCRB),ORBITP(NORB,NEXIT),GAMAIN(NORB,NEXIT),
     1SRDSUM(NORB,NEXIT),SRESUM(NCRB,NEXIT),RR(NORB,NEXIT)
 1017 FORMAT(1X,1H*,5X,A2,5X,1H*,10X,A2,10X,1H*,2X,F14.7,2X,1H*,2X,F14.7
     1,2X,1H*,2X,F14.7,2X,1H*,2X,F14.7,2X,1H*)
      PRINT 1015
 1019 PRINT 1014
      PRINT 9000
      PRINT 1020,SUGANG,SRDANG,SREANG,SURANG
 1020  FORMAT(2X,'TOTAL(ANGULAR)..................*',1H*,
     12X,F14.7,2X,1H*,2X,F14.7,2X,1H*,2X,F14.7,2X,1H*,2X,F14.7,2X,1H*)
      PRINT 1023,SUGRAD,SRDRAD,SRERAD,SURRAD
 1023  FORMAT(2X,'TOTAL( RADIAL)..................*',1H*,
     12X,F14.7,2X,1H*,2X,F14.7,2X,1H*,2X,F14.7,2X,1H*,2X,F14.7,2X,1H*)
      PRINT 1024,SUGTOT,SMDTOT,SMETOT,SURTOT
 1024  FORMAT(2X,'TOTAL(  GRAND)..................*',1H*,
```

```
     12X,F14.7,2X,1H*,2X,F14.7,2X,1H*,2X,F14.7,2X,1H*,2X,F14.7,2X,1H*)
 7    CONTINUE
 2230 CONTINUE
      STOP
      END
      SUBROUTINE FORWAV(LWPU,LWUN,EXPWUN,N,J,NCREG,MENTRY,NORB,DELXR,ZZ,
     1AZERO)
C
      SUBROUTINE INTEGR (FUNCI,NCREG,JENTRY,KC,DELXR)
C
C THIS SUBROUTINE EVALUATES THE INTEGRALS FUNCI OF THE INTEGRANDS FUNC G
C VARIOUS MESH POINTS. THE METHOD OF FINITE DIFFERENCES IS USED. THE INT
C IS PERFORMED THROUGH ADJCENT INTERVALS AND THE FOURTH DIFFERENCES INCL
C
      DIMENSION JENTRY(13),DELXR(13)
      DIMENSION WPL(13,47),XR(13,47),WUN(16,12,44),FUNC(13,47),A(4,5)
      COMMON WPL,XR,WUN,FUNC,A
      FUNCI=0.0
      DO 31 NCRG=1,NCREG
      FUNCI1=0.0
      FUNCI2=0.0
      FUNCI3=0.0
      NENTRY=JENTRY(NCRG)
      IF(NCRG-1) 17,16,17
 16   IF(KC) 17,35,17
 35   K=1
      L=1
      Q=2.
      KK=0
      GO TO 18
 17   K=3
      L=2
      Q=1.
      KK=1
 18   FUNCI1=FUNC(NCRG,K)+FUNC(NCRG,K+1)
      IF(NENTRY-4) 32,30,32
 32   IF(KK) 37,37,40
 40   IF(NENTRY-6) 22,22,37
 37   J=K+1
 20   FUNCI1=FUNCI1+FUNC(NCRG,J)+FUNC(NCRG,J+1)
      J=J+1
      IF(J-NENTRY+3) 20,20,22
 22   FUNCI2=FUNC(NCRG,L+3)+(Q-2.)*FUNC(NCRG,L+2)+(1.-2.*Q)*FUNC(NCRG,L+
     /1)+Q*FUNC(NCRG,L)
      IF(NENTRY-5) 33,30,33
 33   IF(KK) 38,38,41
 41   IF(NENTRY-6) 26,26,38
 38   J=L+1
 24   FUNCI2=FUNCI2+FUNC(NCRG,J+3)-FUNC(NCRG,J+2)-FUNC(NCRG,J+1)+FUNC(NC
     /RG,J)
```

```
      J=J+1
      IF(J-NENTRY+4) 24,24,26
   26 FUNCI3=FUNC(NORG,6)+(Q-4.)*FUNC(NORG,5)+(6.-4.*Q)*FUNC(NORG,4)+(6.
     /*Q-4.)*FUNC(NORG,3)+(1.-4.*Q)*FUNC(NORG,2)+Q*FUNC(NORG,1)
      IF(NENTRY-6) 34,30,34
   34 J=2
   28 FUNCI3=FUNCI3+FUNC(NORG,J+5)-3.*FUNC(NORG,J+4)+2.*FUNC(NORG,J+3)+2
     /.*FUNC(NORG,J+2)-3.*FUNC(NORG,J+1)+FUNC(NORG,J)
      J=J+1
      IF(J-NENTRY+5) 28,28,30
   30 FUNCI1=FUNCI1*(DELXR(NORG))*(1./2.)
      FUNCI2=FUNCI2*(DELXR(NORG))*(-1./24.)
      FUNCI3=FUNCI3*(DELXR(NORG))*(11./1440.)
      FUNCI=FUNCI+FUNCI1+FUNCI2+FUNCI3
   31 CONTINUE
      RETURN
      END
      SUBROUTINE SIMULT (M)
C
CC  SIMULTANEOUS EQUATION SOLVER
CC      SOLVE M SIMULTANEOUS EQUATIONS BY THE METHOD OF CROUT
C
      DIMENSION WPL(13,47),XR(13,47),WUN(16,12,44),FUNC(13,47),A(4,5)
      COMMON WPL,XR,WUN,FUNC,A
      ABSF(X)=ABS(X)
      N=M+1
      I1=1
    1 I3=I1
      SUM=ABSF(A(I1,I1))
      DO3I=I1,M
      IF(SUM-ABSF(A(I,I1)))2,3,3
    2 I3=I
      SUM=ABSF(A(I,I1))
    3 CONTINUE
      IF(I3-I1)4,6,4
    4 DO 5J=I,N
      SUM=-A(I1,J)
      A(I1,J)=A(I3,J)
    5 A(I3,J)=SUM
    6 I3=I1+1
      DO7I=I3,M
    7 A(I,I1)=A(I,I1)/A(I1,I1)
   14 J2=I1-1
      I3=I1+1
      IF(J2)8,11,8
    8 DO9J=I3,N
      DO9I=1,J2
    9 A(I,J)=A(I1,J)-A(I1,I)*A(I,J)
      IF(I1-M)11,15,11
   11 J2=I1
```